Summer 1989

Mathematical Models of Prevascular Tumor Growth by Diffusion

Sophia A. Maggelakis
Old Dominion University

MATHEMATICAL MODELS OF PREVASCULAR TUMOR GROWTH BY DIFFUSION

by

Sophia A. Maggelakis

B.S., May 1980, Old Dominion University, Norfolk, VA

M.S., December 1982, Old Dominion University, Norfolk, VA

A Dissertation Submitted to the Faculty of Old Dominion University
in Partial Fulfilment of the Requirements for the Degree of

DOCTOR OF PHILOSOPHY
in
COMPUTATIONAL AND APPLIED MATHEMATICS

August, 1989

Approved by:

J. Adam (Director)

Στούς αγαπημένους μου γονείς,

και στον Ανδρέα

ABSTRACT

Mathematical Models of Prevascular Tumor Growth by Diffusion

Sophia A. Maggelakis

Old Dominion University, 1989

Director: Dr. John A. Adam

A study of several complementary mathematical models that describe the early, prevascular stages of solid tumor growth by diffusion under various simplifying assumptions is presented. The advantage of these models is that their degree of complexity is relatively low, which ensures fairly straightforward comparisons with experimental or clinical data (as it becomes available), yet they are mathematically sophisticated enough to capture the main biological phenomena of interest.

The tumor growth and cell proliferation rate are assumed to depend on the local concentrations of nutrients and inhibitory factors. The effects of geometry and spatially non-uniform inhibitor production and non-uniform nutrient consumption on the prevascular tissue growth are examined. The concentrations of nutrients and growth inhibitor are governed by diffusion processes, and thus the equations are of diffusion type in spherically symmetric geometries. Since a key characteristic of cancerous diseases is uncontrolled growth, the sensitivity of a model to the nature of different mitotic control functions is examined and the stability of

subsequent tissue growth is discussed. A limiting size for the stable tissue growth is provided, and in related models the time-evolution of the tissue prior to that limiting state is described via a growth (integro-differential) equation for the different phases of tumor growth; the kernel of which depends on the solutions of the spherically symmetric diffusion equations for the concentration of nutrient and growth inhibitor within the tumor. Conditions on the existence and uniqueness of solutions to two classes of non-linear time-independent diffusion equations, which arise in tumor growth models, are also examined.

A detailed study of theoretical models of the type constructed here provides useful insight into the basic biological mechanisms of tumor growth, and therefore may offer possibilities for optimization of cancer therapy (e.g. chemo-or radiotherapy).

Acknowledgements

I am grateful to many individuals who have contributed during the process of this research. I could never adequately acknowledge each and every one of them, however, it is my pleasure to sincerely thank the following.

I am indebted to all Mathematics faculty for their professional encouragement, constructive feedback, and cooperation. In particular, I wish to thank Professor John Tweed, Chairman, for his support, consideration, and courteous remarks when most needed.

I am deeply grateful to my advisor, Professor John Adam, for his guidance, understanding, and confidence in me. His support and enthusiasm in our work made this research project a very pleasant endeavour.

I express my appreciation to the members of my committee, Professor John Heinbockel, Dr. Philip Wohl, and Dr. Lloyd Wolfinbarger for their constructive criticism and respected comments. I especially like to express my gratitude to Dr. Heinbockel who has always been more than willing to help me and answer my questions, and who has offered me many valuable suggestions. His enthusiasm in Mathematics and his teaching charisma have inspired me a great deal. My gratitude must be extended to Dr. Wohl who has advised me throughout my years as a graduate student.

My special thanks to all my fellow graduate students for becoming my friends and sharing the good and difficult times that I went through. It is a pleasure to

acknowledge Barbara Jeffrey for the excellent typing of this manuscript and for being a good friend.

Above all, I owe more than words can describe to my husband, Andreas, for his untiring support, devotion, and understanding. His continuing encouragement, and faith in me contributed considerably in making this work possible.

TABLE OF CONTENTS

LIST OF TABLES

Chapter 3

LIST OF FIGURES

Chapter 2

Chapter 3

Chapter 4

Chapter 5

Chapter 1

Introduction

Cancer has proved to be one of the deadliest diseases of our times. Cancer types can be classified as either "fluid like" or "solid like". In the former, the cancer cells float in a body fluid (e.g. leukemias), while in the latter, they form a solid tumor mass (e.g. carcinomas). Tumors are groups of abnormally proliferating cells that can arise in any part of the body. They can invade their surrounding tissues and spread from their site of origin by reaching the bloodstream (malignant tumors), or they can remain strictly local growths (non-malignant tumors).

An approach to studying the biology of human tumors and tumors in animals is to develop models which have many of their characteristics. Mathematical models, while put to a secondary role, can provide information and understanding that can be used to gain insight into the nature of the growth processes of tumors.

Depending upon the configuration of cell growth, cell populations may be considered as either two-dimensional or three-dimensional. Three-dimensional multicellular spheroids are spherical masses of cells that are supplied with oxygen

and nutrients by diffusion from the surrounding growth medium. Multicellular spheroids are more sensitive than single-cell or monolayer cultures to changes in culture environment. Since the growth pattern of multicellular spheroids shows many of the characteristics of the growth development of solid tumors in vivo, an approach to studying the biology of tumors is to culture cancer cells in the form of a three-dimensional multicellular spheroid. A significant attempt has been made over several years to use these spheroids in studying cell cycle state, the interrelationships with metabolism, and the response of tumor cells to cancer treatment with drugs and/or radiation (Sutherland & Durand, 1976).

By the time a tumor has grown to a detectable size, the cancer cells and their local environments have often become heterogeneous. Heterogeneous cell populations are a considerable problem in solid tumor therapy. This cellular heterogeneity in solid tumors may be similar, on a microenvironmental level, to cellular heterogeneity in spheroids. Hence, since it is easier to investigate systematically multicellular spheroids, studies on spheroids can be of great practical importance (Vaupel et al., 1981; Poste & Greig, 1983). Multicellular spheroids, therefore, can be useful models in vitro for studying tumor growth characteristics. (For a summary of the relevant experimental data on such spheroids see Appendix III).

Furthermore, the resistance of solid tumors to certain therapeutic techniques, with particular reference to chemotherapy and radiotherapy can be studied by using diffusion models of multicellular spheroids. It was shown by King et al. (1986) that multiregion models can often reproduce clinical measurements ac-

curately. Therefore, they may serve as predictors for establishing new oxygen levels through the intake of pure oxygen under atmospheric or hyperbaric conditions. They also point out that solutions to the time dependent version of the models may give an estimate of the time period that is required to sufficiently oxygenate tumors before therapy begins. A detailed study, concerning this point, of a moving boundary value problem has been made by Arve and Liapis (1988) (see also Liapis et al., 1982). They model oxygen concentrations in idealized tumors in one-dimensional slab geometry, and they are interested to determine optimum radiation dosages for radiotherapy by coupling theoretical results from time-dependent diffusion models with tumor oxygen radiosensitivity data.

Almost all transplanted tumors in animals and spontaneous tumors in man pass through an early prevascular (avascular) stage in which the pint-size tumor colony grows in three dimensions (Folkman & Greenspan, 1975). A tumor in the prevascular stage of growth lacks its own network of blood vessels for supplying nutrients and removing wastes. Thus, the transfer of nutrients and wastes has to be accomplished by simple diffusion through its host. It has been found (McElwain et al., 1979) that models of prevascular growth are valid up to the "dormant" phase of avascular nodules (1-2 mm in diameter), which may last for several months. When the tumor growth is near this dormant state, the cancer cells release a diffusable chemical substance called Tumor Angiogenesis Factor (TAF). The concentration of TAF rises and stimulates the nearby capillaries that grow toward and eventually penetrate the tumor. The tumor then becomes vas-

cularized, and it no longer has to depend solely on diffusion processes for oxygen, nutrient and waste transport. A rapid growth ensues because fresh nutrients flow in and wastes are quickly removed, and the tumor is no longer limited to a dormant state. When the diameter of the vascularized tumor reaches 1-3 cm (Folkman, 1974), the growth rate slows down again and a gompertzian curve now describes the growth of the tumor. The exponential growth therefore is not preserved indefinitely. This description has been shown to be excellent for a wide variety of mouse, rat and rabbit tumors by Laird (1965). The vascularized tumor destroys the neighboring tissue, and it can spread cells that are capable of setting up secondary tumors elsewhere in the body (metastasis). Also, the abnormal growth of blood vessels may play a role in the development of many diseases other than solid cancers (e.g. the joint degeneration occurring in rheumatoid arthritis and the eye damage frequently suffered by diabetes patients, and by premature infants who are exposed to high concentrations of oxygen because of their immature lungs (Folkman & Klagsbrun, 1987)).

A number of mathematical models that describe the early stages of tumor growth exist in the literature. The spatial distribution of oxygen and other nutrients diffusing into a spherical tumor from its periphery has been studied by Burton (1966). Using this concept he derived a criterion for the onset of necrosis in tumors. Detailed models were developed by Greenspan (1972, 1974) and Wette et al. (1974a,b) in which both the nutrients and waste products of metabolism were identified as growth parameters. Deakin (1975) reconstructed Burton's model by

assuming that the consumption rate of nutrient (oxygen) is a piecewise linear function of the nutrient concentration, and showed that this can lead to growth inhibition. McElwain & Ponzo (1977) extended these ideas by incorporating the effects of nonuniformity of oxygen consumption on the growth rate of a solid tumor.

Experiments have shown that there exists an inner layer of viable cells within the tumor in which mitosis is almost non-existent (Greenspan, 1972). A chemical (growth inhibitor) appears to be produced somewhere within the tumor which inhibits mitosis of cancer cells without causing their death. However, the nature or the source of this growth inhibitor remains controversial. This source may be the metabolic wastes from living cells, the necrotic debris, an inadequate supply of nutrients, or combination of all these and possibly other mechanisms. The basic mechanism in the model developed by Glass (1973) is that of tissue size regulation via negative feedback from the tissue itself. The agents of negative feedback ("chalones") are mitotic inhibitors produced by the tissues, and it has been suggested that a breakdown in the normal functioning of the chalone mechanism may be responsible for limitless tissue growth in at least some types of cancer (Bullough, 1965). Strong supporting evidence for this hypothesis comes from a study of tumor growth by Bullough & Deol (1971). Glass's model provides a limiting size for stable tissue growth, without describing the time evolution of the tissue prior to that limiting state. Shymko & Glass (1976) consider diffusion of nutrients and growth stimulating and inhibiting factors (produced uniformly in the tissue)

to explain growth in tissues. Adam (1986, 1987a, 1987b) extended these ideas to take account of non-uniform production of growth inhibitor throughout the tissue for a variety of geometrical configurations. It should be noted that growth inhibition occurs in areas other than solid cancers (e.g. wounds of any kind, wherein the mechanisms inhibiting cell proliferation are suspended in damaged tissue until the normal tissue structure has been regained).

The purpose of the study presented here is to further develop existing models of tumor growth by diffusion in order to test them with experimental and clinical data (as it becomes available) so that eventually the major internal processes involved in tumor growth may be inferred. The models discussed pertain primarily to the prevascular stage of tissue growth.

In Chapter 2, a mathematical model of tumor growth by diffusion is constructed in which the effects of non-uniform inhibitor production on one-dimensional tissue growth are examined. A parameter is used to measure the degree of nonuniformity of the inhibitor production rate, and growth patterns are presented for several values of this parameter. The advantage of such a model is that it is analytically tractable, and at the same time it incorporates the essential physics for a fully three-dimensional model so it can serve as a precursor to the more realistic model presented in Chapter 3.

Relatively simple multiregion type models can have practical use as the in vivo measurements of oxygen tension profiles within human tumors, reported by Gatenby et al. (1985), suggest. Patterns of necrosis were often seen with a necrotic

core surrounded by a region of viable cells. Non-uniform oxygen distribution was demonstrated within tumors of many patients, where the concentration of oxygen was highest at the periphery of the tumor and lowest in its center. Thus, in order to construct a realistic model, the following features should be incorporated: the existence of necrosis, non-uniform nutrient consumption and associated non-uniform cell proliferation, possible non-uniform inhibitor production, and geometrical constraints. Since these features are not mutually exclusive, they are not all necessarily appropriate in one model. However, it would be profitable to have a model that combined all the features mentioned so that some of them could be "turned" on or off as it becomes necessary when compared with known results. The mathematical model proposed in Chapter 3 is an example of such a model. A detailed discussion of the computations is presented in that Chapter in order to provide a basis for future comparison with experimental data as it becomes available. This is of especial interest in the light of recent developments in models of multicellular spheroids (King et al., 1988; Sutherland, 1988), and with the resurgence of interest in tumor angiogenesis factors (Folkman & Klagsbrun, 1987).

Two mathematical models for the control of the growth of a tumor by diffusion of mitotic inhibitor are presented in Chapter 4. The inhibitor production rate is taken to be uniform in a necrotic core for the first model and in the region of living cells for the second model. Regions of stable and unstable growth are determined, and conclusions are drawn about the limiting peripheral widths of stable tissue

growth for both models. Comparisons of the results from each model indicate that the models are sensitive to the source distributions of inhibitor production.

Chapter 5 is more theoretical in nature. It studies the existence and uniqueness of solutions to two classes of nonlinear time-independent diffusion equations for arbitrary oxygen consumption rates.

Concluding remarks and discussion of results, from all the different models examined, are presented in Chapter 6.

Mathematical models of the type suggested above are of considerable value, because they may indicate the degree of sensitivity of the models to particular physical mechanisms. These models together with the earlier mentioned studies of boundary value problems by Arve and Liapis (1988) and the time-independent analyses by King et al. (1986, 1988) and Schultz & King (1986) are approaches complementary to one another. It is hoped that they will provide a firm theoretical base from which a deeper understanding of tumor growth and tumor characteristics will arise. If the results obtained from the proposed models can be compared and contrasted with observations of tissue growth in vitro, then it may be possible to identify which simplifications are appropriate, and which are not, and subsequently to develop more sophisticated models. Such models are needed to design and interpret experiments and to supply knowledge to areas of application within the biological and medical sciences.

Chapter 2

The Effects of Non-uniform Inhibitor Production on One-dimensional Tissue Growth

In this chapter, a model is studied in which the effects of non-uniform inhibitor production on the growth rate of one-dimensional tissue are examined with a parameter b used to measure the degree of this nonuniformity. The source of the growth inhibitor is assumed to be the necrotic debris which is accumulated as a result of inadequate nourishment for every cell in the "interior" of the culture.

The advantage of a one-dimensional model is that it incorporates the essential physics necessary for a fully three-dimensional model, and at the same time it remains analytically tractable. It therefore represents a precursor to more realistic models, and as such is a useful probe or calibration device with which to compare the results from more sophisticated models.

2.1 The Growth Equation

The growth of cell population is governed by a conservation of mass or cell volume. Following Greenspan (1972), we may write the conservation of mass or cell volume (growth equation) as follows:

$$A = B + C - D - E \tag{2.1.1}$$

where

A = total volume of living cells at any time t ;

B = initial volume of living cells at time $t = 0$;

C = total volume of cells produced in time $t \geq 0$;

D = total volume of necrotic debris at time t ;

E = total volume of cells lost in the necrotic core in time $t \geq 0$.

We consider the growth of a cell culture in a small tube with a small constant cross sectional area, α, and the three interfacial heights $z_0(t), z_g(t), z_i(t)$ to separate the cell culture from the ambient medium, dividing from nondividing cells, and living from dead cells respectively (see Fig 2.1). The rate of cell proliferation $S(\sigma, \beta)$ (volume created per unit volume of viable cells) is a function of the nutrient consumption $\sigma(z,t)$ and inhibitor production $\beta(z,t)$ such that

$$S(\sigma,\beta) = \begin{cases} s, & \text{a constant, for } \sigma > \sigma_i, \quad \beta < \beta_i \\ 0, & \text{otherwise;} \end{cases} \tag{2.1.2}$$

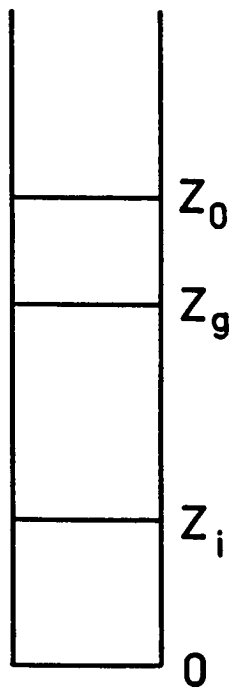

Figure 2.1. A three-layer cell culture consisting of the necrotic region $(0 \leq z \leq z_i)$, the region of viable cells (no mitosis) $(z_i \leq z \leq z_g)$ and the region of proliferating cells $(z_g \leq z \leq z_0)$.

where σ_i is the critical nutrient concentration below which the cells die, and β_i is the critical inhibitor concentration above which mitosis is inhibited. It is assumed that the column of necrotic debris loses cell volume by diffusion of waste material outward at a rate proportional to its volume with λ the proportionality constant.

It follows that the individual terms of equation (2.1.1) are

$$\begin{aligned} A &= \alpha(z_0(t) - z_i(t)); \\ B &= \alpha z_0(0); \\ C &= \int_0^t dt \left\{ \alpha \int_{\max(z_g, z_i)}^{z_0} S(\sigma, \beta) dz \right\} = s\alpha \int_o^t [z_0 - \max(z_g, z_i)]\, dt; \\ D &= \alpha z_i(t); \\ E &= \int_0^t dt \{\lambda \alpha z_i(t)\}; \end{aligned}$$

so that equation (2.1.1) can be written

$$\begin{aligned} z_0(t) - z_i(t) = z_0(0) &+ s\int_0^t [z_0(t) - \max(z_g(t), z_i(t))]dt \\ &- z_i(t) - \lambda \int_0^t z_i(t)dt \end{aligned} \tag{2.1.3}$$

or in time-differentiated form

$$\frac{dz_0}{dt} = s[z_0(t) - \max(z_g(t), z_i(t))] - \lambda z_i(t) \tag{2.1.4}$$

with the initial conditions

$$z_0(0) = h_0,$$

$$z_i(0) = z_g(0) = 0.$$

We need to find the relationships between $z_i(t), z_g(t)$, and $z_0(t)$, and to accomplish this we must solve the diffusion equations for the uniform nutrient consumption σ and inhibitor production β.

2.2 The Diffusion Equations

Since the time scale for growth is large compared with a typical diffusion time, it is assumed that the culture is in a state of diffusive equilibrium at all times (further justification for this assumption may be found in Shymko and Glass (1976), see also Chapter 4).

This part of our model does not differ from that of Greenspan (1974), so we merely note his results here. Thus, we find from the nutrient diffusion equation for σ

$$\frac{d^2\sigma}{dz^2} = \begin{cases} \dfrac{A}{k}, & z_i \leq z \leq z_0 \\ 0, & \text{elsewhere} \end{cases} \tag{2.2.1}$$

that

$$\left.\begin{aligned} \sigma(z) &= \sigma_\infty, && z \geq z_0 \\ \sigma(z) &= \frac{A}{2k}(z^2 - z_0^2) + \frac{A}{k} z_i (z_0 - z) + \sigma_\infty, && z_0 \geq z \geq z_i \\ \sigma(z) &= \sigma_i, && z_i \geq z \geq 0 \end{aligned}\right\} \tag{2.2.2}$$

and

$$z_0 - z_i = \left[\frac{2k}{A}(\sigma_\infty - \sigma_i)\right]^{\frac{1}{2}} = h_c \tag{2.2.3}$$

with σ_∞ being the nutrient concentration in the ambient medium, A the constant rate of nutrient consumption, k the diffusivity constant, and h_c the critical height of the cell culture. When the culture reaches this critical height h_c, the cells at the bottom of the vial ($z = 0$) start to die.

However, in distinction to Greenspan (1974), it is assumed that the chemical inhibitor is produced at a non-uniform rate throughout the necrotic region. The diffusion equation for the inhibitor concentration β is

$$\frac{d^2\beta}{dz^2} = \begin{cases} -\dfrac{P}{K}\left(1 - \dfrac{bz}{z_i}\right), & z \leq z_i, \quad 0 \leq \beta \leq 1 \\ 0, & z \geq z_i \end{cases} \tag{2.2.4}$$

subject to the conditions that

(i) $\dfrac{d\beta}{dz} = 0$ at $z = 0$

(i.e. there is no inhibitor flux through the tube),

(ii) $\beta = 0$ at $z = z_0$

(i.e. the contaminant is removed from the ambient fluid),

(iii) β and $\frac{d\beta}{dz}$ are continuous at $z = z_i$.

The parameter b is used to measure the degree of nonuniformity of the inhibitor production rate, P is the inhibitor production rate, and K is the diffusivity constant.

The solution to this system is

$$\left.\begin{aligned} \beta(z) &= 0, && z \geq z_0 \\ \beta(z) &= \frac{P}{K} z_i (z_0 - z)\left(1 - \frac{b}{2}\right), && z_i \leq z \leq z_0 \\ \beta(z) &= -\frac{P}{K}\left[\frac{z^2}{2} - z_i\left(z_0 - \frac{z_i}{2}\right) - \frac{b}{6z_i}\left(z^3 + z_i^2(2z_i - 3z_0)\right)\right], && z \leq z_i \end{aligned}\right\} \tag{2.2.5}$$

Figure 2.2 shows the change of the inhibitor concentration β as the parameter b takes on different values. When mitotic inhibition is effective the inhibitor concentration β is greater than the critical concentration β_i in the layer $z_i \leq z \leq z_g$. This is determined by

$$\beta_i = \frac{P}{K} z_i (z_0 - z_g)(1 - \frac{b}{2}). \tag{2.2.6}$$

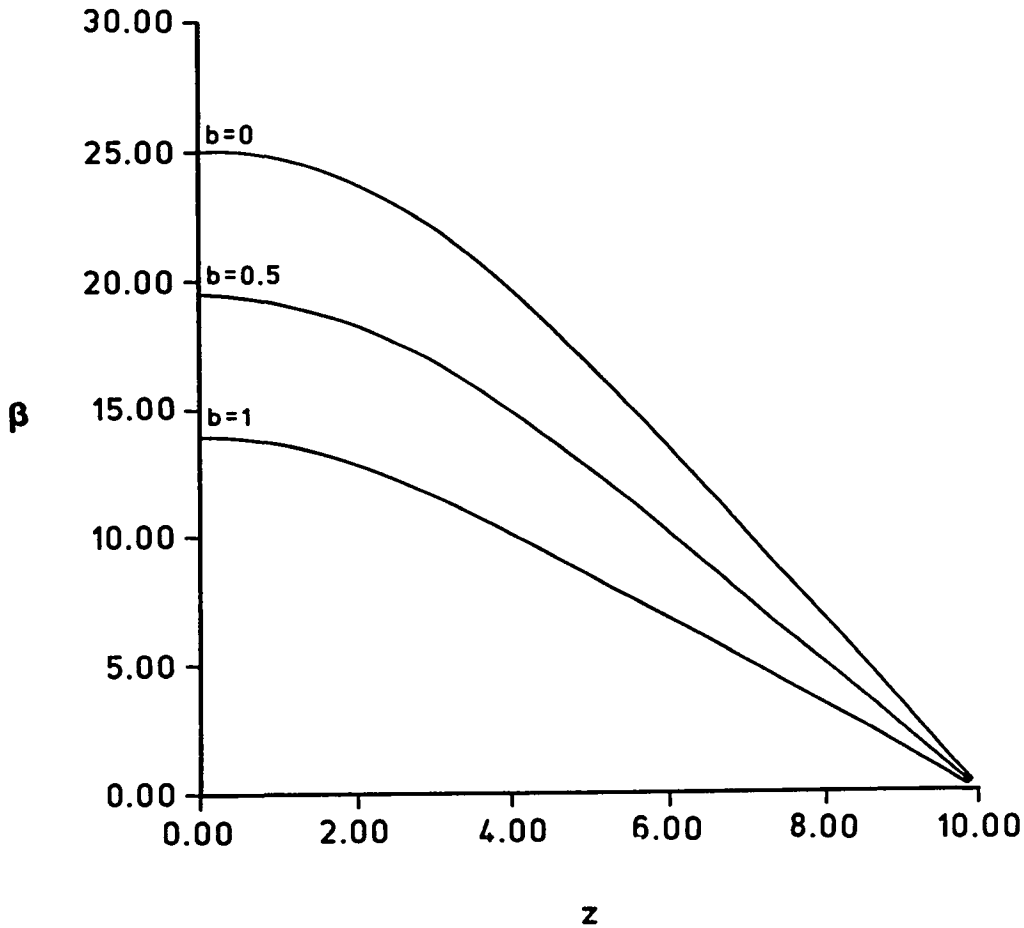

Figure 2.2. The inhibitor concentration β as a function of the axial distance z for different values of the parameter b (i.e. $b = 0$, $b = 0.5$, $b = 1$).

Note that inhibition is first evident when $z_g = z_i$ and

$$\beta_i = \frac{P}{K} z_i (z_0 - z_i)(1 - \frac{b}{2}). \tag{2.2.7}$$

2.3 The Growth of Cell Population

The growth of cell population occurs in three distinct stages:

Stage 1: All cells are alive and proliferating so that a period of exponential growth exists until the onset of necrosis. There is no necrosis or inhibition yet in this stage so that

$$z_g(t) = z_i(t) = 0,$$

and $z_0(t)$ satisfies the condition

$$\frac{h_0}{h_c} \leq \frac{z_0(t)}{h_c} \leq 1.$$

The conservation law (2.1.4) becomes

$$\frac{dz_0}{dt} = s z_0(t) \tag{2.3.1}$$

with the initial condition

$$z_0(0) = h_0. \tag{2.3.2}$$

Thus,

$$z_0(t) = h_0 e^{st} \tag{2.3.3}$$

which is valid for times $0 \leq t \leq t_1$ up until $h_0 = h_c$ i.e.

$$z_0(t_1) = h_c = h_0 e^{st_1} . \tag{2.3.4}$$

Hence, the cell culture reaches the critical height h_c at

$$t_1 = \frac{1}{s} \ln \left(\frac{h_c}{h_0} \right) . \tag{2.3.5}$$

The growth will, therefore, be exponential for times in

$$0 \leq t \leq \frac{1}{s} \ln \left(\frac{h_c}{h_0} \right) . \tag{2.3.6}$$

Stage 2: (Onset of necrosis). The proliferation rate at the bottom of the vial ($z = 0$) begins to slow down and cells begin to die. During this stage, the culture has two-layer structure. In the outer layer, the cells grow exponentially. Inside this region a necrotic layer forms so that a period of growth retardation exists, due to cell death, which lasts from the onset of necrosis until $\beta = \beta_i$ at the necrotic interface $z = z_i$. The volume of the necrotic debris begins to increase as does the concentration of the inhibitor β. As the growth rate slows down, it can lead to a steady or dormant state in which the volume loss due to necrosis is balanced by the volume gained due to cell division. Hence, under certain conditions, inhibition is not necessary for the existence of a dormant state. If the steady state is not

reached, however, a third stage is initiated. The conservation law (2.1.4) in this second stage becomes

$$\frac{dz_0}{dt} = sz_0(t) - (s+\lambda)z_i(t) \tag{2.3.7}$$

with

$$z_0 - z_i = h_c\,,$$

and the differential equation to be solved is

$$\frac{d}{dt}\left[z_0(t) - \frac{s+\lambda}{\lambda}h_c\right] = -\lambda\left[z_0(t) - \frac{(s+\lambda)h_c}{\lambda}\right] \tag{2.3.8}$$

with solution given by

$$\frac{z_0(t)}{h_c} = \frac{s+\lambda}{\lambda} + \left(1 - \frac{s+\lambda}{\lambda}\right)e^{-\lambda(t-t_1)} \tag{2.3.9}$$

or

$$\frac{z_0(t)}{h_c} = 1 + \frac{1}{\gamma} - \frac{1}{\gamma}e^{-\lambda(t-t_1)}\,, \tag{2.3.10}$$

where $\gamma = \dfrac{\lambda}{s}$. Also, note that

$$z_g(t) = z_i(t) = z_0(t) - h_c. \tag{2.3.11}$$

The inhibitor is produced non-uniformly in the necrotic region and $z_g(t) > z_i(t)$ after $\beta = \beta_i$ at $z = z_i$. Thus, inhibition is first evident when $z_g = z_i$ and from (2.2.7) and (2.3.11) we find that

$$\frac{z_i}{h_c} = \frac{Q^2}{2-b} = z_{g(t)} \tag{2.3.12}$$

at the onset of necrosis, where the dimensionless parameter Q is given by

$$Q^2 = \frac{\beta_i K A}{(\sigma_\infty - \sigma_i) k P}. \tag{2.3.13}$$

Q^2 is therefore a measure of the competing effects of nutrient consumption/ diffusion and inhibitor production/diffusion. As mentioned earlier, under certain conditions either a steady state is attained or a third stage is initiated. These cutoff conditions depend critically on the dimensionless parameters Q, b and γ (see below). As $z_g(t)$ moves ahead of $z_i(t)$, the following inequality holds,

$$\frac{z_i}{h_c} \leq \frac{Q^2}{2-b}. \tag{2.3.14}$$

Therefore,

$$\frac{z_0}{h_c} = \frac{z_i}{h_c} + 1 \leq 1 + \frac{Q^2}{2-b}. \tag{2.3.15}$$

If necrosis balances growth in this stage then (2.3.7) becomes

$$\frac{dz_0}{dt} = 0 = (s+\lambda)h_c - \lambda z_0(t)\,. \tag{2.3.16}$$

Consider

$$\frac{dz_0}{dt} \to 0^+\,,$$

i.e.

$$(s+\lambda)h_c - \lambda z_0 = \varepsilon > 0$$

or

$$\frac{z_0}{h_c} = \frac{(s+\lambda)}{\lambda} - \frac{\varepsilon}{\lambda h_c}\,. \tag{2.3.17}$$

Clearly, in approach to equilibrium,

$$\frac{z_0}{h_c} \leq \frac{s+\lambda}{\lambda} = 1 + \frac{1}{\gamma}\,. \tag{2.3.18}$$

Since $z_0(t_1) = h_c$, the range of z_0 for this stage is

$$1 \leq \frac{z_0(t)}{h_c} \leq \min\left\{1 + \frac{1}{\gamma},\ \ 1 + \frac{Q^2}{2-b}\right\}\,. \tag{2.3.19}$$

Thus, if

$$1+\frac{Q^2}{2-b} \geq 1+\frac{1}{\gamma}, \tag{2.3.20}$$

equilibrium has been reached at time t in $t_1 \leq t < \infty$ and the development is completed in this stage. Otherwise

$$1+\frac{Q^2}{2-b} < 1+\frac{1}{\gamma}, \tag{2.3.21}$$

and a further stage of growth ensues. To find the time t_2, when the inhibitor β reaches the critical value β_i, consider equation (2.3.10) for $t = t_2$, i.e.

$$1+\frac{Q^2}{2-b} = 1+\frac{1}{\gamma}-\frac{1}{\gamma}e^{-\lambda(t_2-t_1)}, \tag{2.3.22}$$

or equivalently

$$t_2 = t_1 - \frac{1}{\lambda}\ln\left(1-\frac{Q^2\gamma}{2-b}\right). \tag{2.3.23}$$

Thus, at time t_2 given by (2.3.23) inhibition will start, and growth retardation due to cell death will last for times in the interval

$$t_1 \leq t \leq t_2 = t_1 - \frac{1}{\lambda}\ln\left(1-\frac{Q^2\gamma}{2-b}\right). \tag{2.3.24}$$

Stage 3: This is a period of retarded growth due to death of cells and chemical inhibition of mitosis which begins when $\beta = \beta_i$ at the necrotic interface $z_i(t)$ and lasts until the dormant steady state is achieved. During this stage, the cell culture has a three layer structure. In the outer layer, the growth of cells is normal as in stage 1. Inside this layer, the rate of cell proliferation is below normal, due to inhibition of mitosis, and consists of viable cells only. In the innermost layer there is accumulation of necrotic debris.

The conservation law now is

$$\frac{dz_0}{dt} = s\{z_0(t) - z_g(t)\} - \lambda z_i(t)\,. \tag{2.3.25}$$

From equations (2.2.3), (2.2.7), and (2.3.13) we obtain

$$z_g(t) = z_0(t) - \frac{2K\beta_i}{Pz_i(2-b)} = z_i(t) + h_c - \frac{Q^2h_c^2}{z_i(2-b)}\,. \tag{2.3.26}$$

Thus, the differential equation (2.3.25) becomes

$$(z_0 - h_c)\frac{dz_0}{dt} = \frac{2Ks\beta_i}{P(2-b)} - \lambda(z_0 - h_c)^2\,. \tag{2.3.27}$$

By making the following transformations

$$u = z_0 - h_c$$

and

$$v = u^2 - \frac{2Ks\beta_i}{\lambda P(2-b)},$$

the differential equation (2.3.27) is reduced to

$$\frac{dv}{dt} = -\lambda v$$

with solution

$$v = De^{-2\lambda(t-t_2)}$$

and hence

$$u = \left[De^{-2\lambda(t-t_2)} + \frac{2Ks\beta_i}{\lambda P(2-b)}\right]^{1/2}.$$

Thus,

$$z_0(t) = h_c + \left[De^{-2\lambda(t-t_2)} + \frac{2Ks\beta_i}{\lambda P(2-b)}\right]^{1/2} \qquad (2.3.28)$$

where

$$D = \left\{(z_0 - h_c)^2 - \frac{2Ks\beta_i}{\lambda P(2-b)}\right\}\Big|_{t=t_2}.$$

So

$$\frac{D}{h_c^2} = \left\{ \left(\frac{z_0}{h_c} - 1 \right)^2 - \frac{2Ks\beta_i}{\lambda P(2-b)h_c^2} \right\} \Big|_{t=t_2} .$$

From stage 2, at $t = t_2$,

$$\frac{z_0}{h_c} - 1 = \frac{1}{\gamma} - \frac{1}{\gamma} e^{-\lambda(t_2 - t_1)}$$

and for $\frac{Q^2}{2-b} < \frac{1}{\gamma}$,

$$t_2 - t_1 = -\frac{1}{\lambda} \ln \left(1 - \frac{Q^2 \gamma}{2-b} \right) .$$

Therefore,

$$\frac{z_0}{h_c} - 1 = \frac{1}{\gamma} - \frac{1}{\gamma} \left(1 - \frac{Q^2 \gamma}{2-b} \right) = \frac{Q^2}{2-b}$$

and

$$\frac{D}{h_c^2} = \left\{ \frac{Q^4}{(2-b)^2} - \frac{2Ks\beta_i}{\lambda P(2-b)h_c^2} \right\}$$

which by using equation (2.3.13) yields

$$\frac{D}{h_c^2} = \left\{ \frac{Q^4}{(2-b)^2} - \frac{Q^2}{\gamma(2-b)} \right\} = \frac{Q^2}{(2-b)\gamma} \left[\frac{\gamma Q^2}{2-b} - 1 \right].$$

Hence, (2.3.28) becomes

$$\frac{z_0(t)}{h_c} = 1 + \left\{ \frac{Q^2}{(2-b)\gamma} \left[\frac{\gamma Q^2}{2-b} - 1 \right] e^{-2\lambda(t-t_2)} + \frac{1}{\gamma} \frac{Q^2}{(2-b)} \right\}^{1/2}$$

and the solution to the differential equation (2.3.27) is

$$\frac{z_0(t)}{h_c} = 1 + \frac{Q}{\sqrt{\gamma(2-b)}} \left[1 - \left(1 - \frac{Q^2\gamma}{2-b} \right) e^{-2\lambda(t-t_2)} \right]^{1/2}. \tag{2.3.29}$$

for $t_2 \leq t < \infty$. As $t \to t_2$ and $t \to \infty$ in (2.3.29) we get the range of $z_0(t)$

$$1 + \frac{Q^2}{2-b} \leq \frac{z_0(t)}{h_c} \leq 1 + \frac{Q}{\sqrt{\gamma(2-b)}}. \tag{2.3.30}$$

Also, we have

$$z_i(t) = z_0(t) - h_c \tag{2.3.31}$$

and hence from (2.3.26)

$$z_g(t) = z_i(t) + h_c - \frac{Q^2 h_c^2}{z_i(2-b)}. \tag{2.3.32}$$

Figure 2.3 shows the full culture growth as a function of time. The three stages of growth development (exponential, inhibited (quasi- linear), and steady state) are graphically illustrated in this figure for $Q = 1.5$, $\gamma = 0.5$, and different values of b. As b increases, the concentration of inhibitor decreases (see Fig. 2.2). Hence, the mitotically active region grows due to the lack of enough inhibitor, and this causes the cell culture to grow.

The results from this model indicate that there is a significant difference between the growth pattern predicted by the Greenspan model and that predicted by the present model for the same values of Q and γ. For example, as the nonuniformity parameter b is varied from zero (uniform production) to unity (maximum nonuniformity of inhibitor production) there results a relative increase of 22% in the asymptotic steady state outer "radius" z_0, and a relative increase of 39% for the corresponding inner necrotic core size z_i. Interestingly the model predicts little change in the "radius" separating the viable cell region from the proliferating cell region, indicating that the limiting size of the culture is determined primarily in this model by the nature of the inhibitor production in the necrotic core. Simply put, the change in z_i induces a corresponding change in z_0.

The above simple yet significant range of deviation over the uniform model merits a further more sophisticated study of a spherically symmetric growth model incorporating non-uniform nutrient consumption and non-uniform inhibitor production rates, which is studied in the next chapter. Indeed, this present analytically tractable one-dimensional model, while simplistic, is physically suggestive

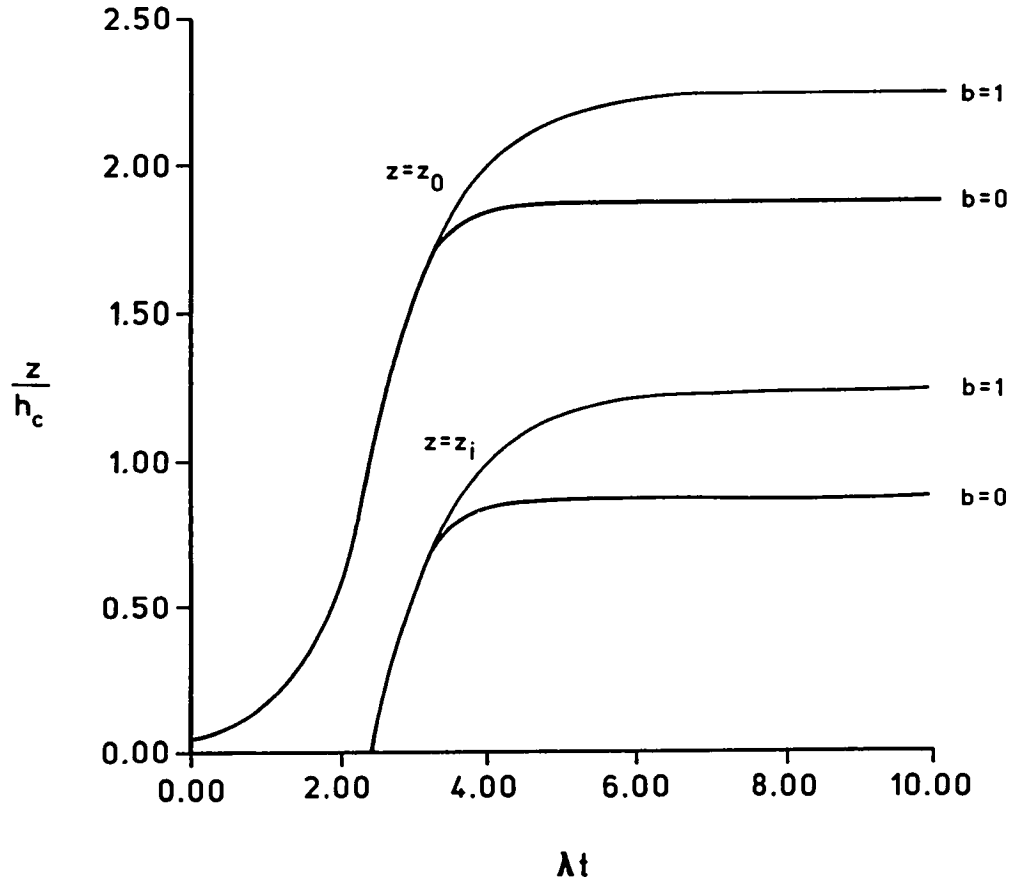

Figure 2.3. The full growth pattern of the cell culture as a function of time. The three stages of growth development for the outer "radius" z_0 and the inner "radius" z_i are illustrated.

of the type of variations that may occur in more realistic geometries. Any future comparisons with clinical or experimental data (King et al., 1986; Freyer et al., 1984) will naturally require the three dimensional diffusion equations and the corresponding integro-differential equation for the outer tumor radius to be solved which is accomplished in Chapter 3.

Chapter 3

Diffusion Regulated Growth Characteristics of a Spherical Prevascular Carcinoma

This chapter proposes a model in which the effects of non-uniform nutrient consumption and non-uniform inhibitor production on the growth rate of a spherically symmetric multicellular spheroid are examined. The source of the growth inhibitor is assumed to be the necrotic debris which is a result of insufficient nutrient being available for every cell of the spheroid. Due to the combined effects of non-uniform nutrient consumption and non-uniform inhibitor production, a four-layer structure in the dormant steady state is predicted, and successive stages of growth are examined. The three-dimensional spherically symmetric diffusion equations for the nutrient consumption and inhibitor production with the corresponding integro-differential equation for the outer radius of the tumor have been solved for each stage of growth.

3.1 Assumptions of the Model

The basic assumptions necessary to construct this model are discussed in detail by Greenspan (1972) and McElwain & Ponzo (1977). Only the most important of these assumptions are restated here:

(i) The solid tumor is a sphere and is spherically symmetric at all times such that the concentrations of nutrient $\sigma(r)$ and the growth inhibitor $\beta(r)$ depend only on the radial distance, r, from the center of the sphere.

(ii) The transport of nutrient and growth inhibitor that regulate the prevascular development of a tumor is governed by diffusion processes.

(iii) The nutrient is consumed by living cells only, and the tumor cells die when the concentration of nutrient falls below a critical value σ_i.

(iv) The growth inhibitor, which is produced within the tumor, inhibits cell mitosis. This inhibition of mitosis occurs when the local concentration of the growth inhibitor exceeds a critical value β_i.

(v) Since the time-scale for growth is large compared with a typical diffusion time, the tumor is in a state of diffusive equilibrium at all times.

3.2 The Growth Equation

The time-development of a spherically symmetric multicellular spheroid is determined by an integro-differential equation (Greenspan, 1972; McElwain & Ponzo,

1977). The conservation of mass or cell volume is described by equation (2.1.1). Here, we denote by $R_0(t), \hat{R}(t), R_g(t)$ and $R_i(t)$ the outer radius of the spheroid, the radius at which the concentration of nutrient $\sigma(r) = \hat{\sigma}$ (the critical concentration), the radius at which the concentration of inhibitor $\beta(r) = \beta_i$, and the radius of the necrotic core respectively. The individual terms of the growth equation (2.1.1) now become

$$\begin{aligned} A &= \frac{4}{3}\pi[R_0^3(t) - R_i^3(t)]; \\ B &= \frac{4}{3}\pi R_0^3(0); \\ C &= 4\pi \int_0^t dt \int_{\max(R_i(t),R_g(t))}^{R_0(t)} S(\sigma,\beta) r^2 dr; \\ D &= \frac{4}{3}\pi R_i^3(t); \\ E &= \frac{4}{3}\pi \int_0^t 3\lambda R_i^3(t) dt \end{aligned}$$

so that equation (2.1.1) can be written as

$$R_0^3(t) = R_0^3(0) + 3\int_0^t dt \int_{\max(R_i,R_g)}^{R_0} S(\sigma,\beta) r^2 dr - 3\lambda \int_0^t R_i^3(t) dt$$

or in time-differentiated form

$$R_0^2 \frac{dR_0}{dt} = \int_{\max(R_i,R_g)}^{R_0} S(\sigma,\beta) r^2 dr - \lambda R_i^3 \qquad (3.2.1)$$

where λ is the proportionality constant for the volume loss term.

The functional form of the proliferation rate $S(\sigma,\beta)$ is stated in terms of the Heaviside unit step function $H(x)$ so that

$$\begin{aligned} S(\sigma(r),\beta(r)) &= s\left\{\frac{\sigma(r)}{\hat{\sigma}}[H(\sigma(r)-\sigma_i)-H(\sigma(r)-\hat{\sigma})]+\right. \\ &+ \left. H(\sigma(r)-\hat{\sigma})\right\}\{H(\beta_i-\beta(r))\} \qquad (3.2.2) \\ &= sS_\sigma(\sigma(r))S_\beta(\beta(r)) \end{aligned}$$

with s being the normal proliferation rate of cells, i.e. when $\beta < \beta_i$ and $\sigma(r) > \hat{\sigma}$ for a discontinuous inhibitor switch mechanism. This proliferation rate, $S(\sigma,\beta)$, is obtained from the solutions of the time independent diffusion equations for $\sigma(r)$ and $\beta(r)$.

3.3 Mathematical Analysis of the Model

As in McElwain and Ponzo (1977), it happens that the growth of a multicellular spheroid proceeds in several stages. Figures 3.1a and 3.1b show schematically the sequence of stages in the growth of the spheroid. These successive stages of growth are examined below:

Phase I. All cells obtain sufficient nutrient, i.e. $\sigma(r) > \hat{\sigma}$ holds everywhere, and mitosis proceeds normally. It is assumed that all cells consume nutrient at

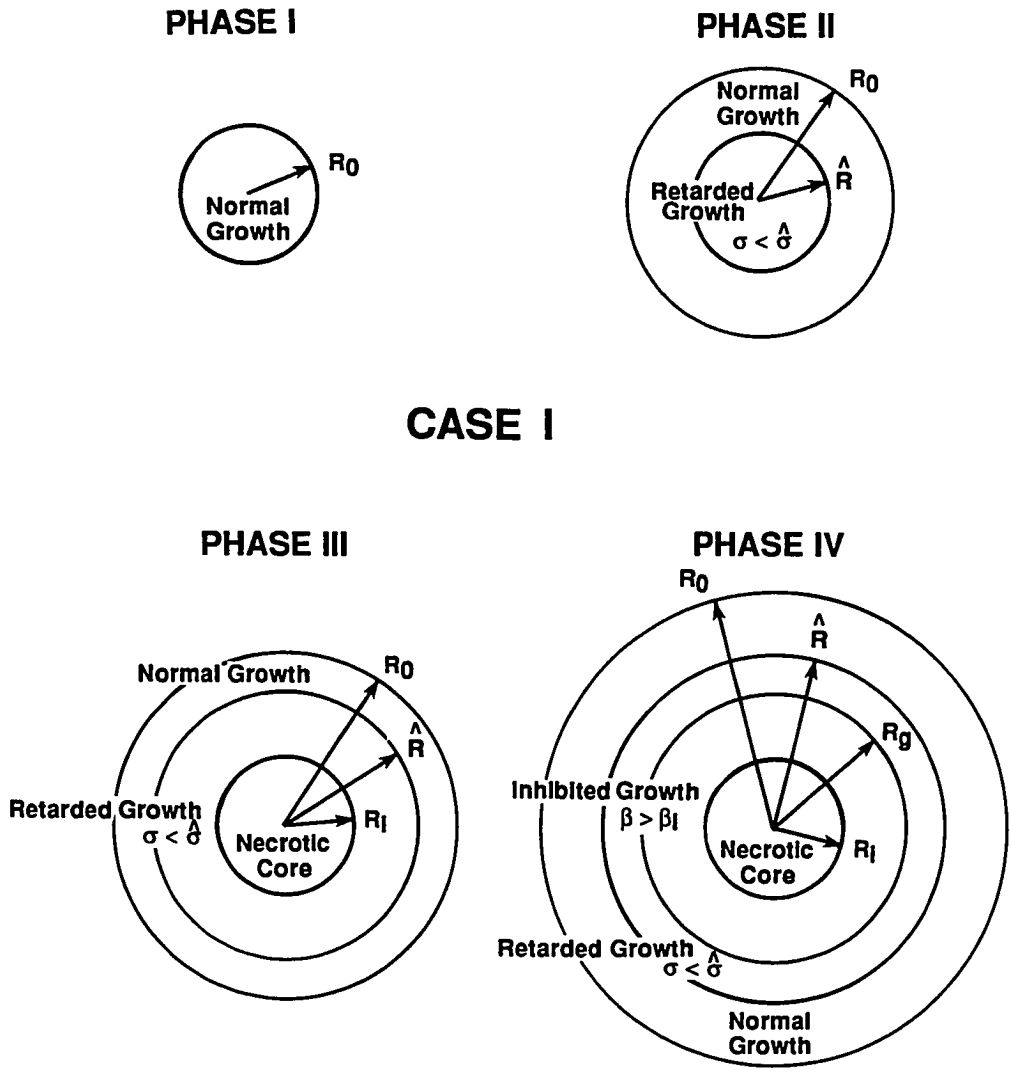

Figure 3.1a. The sequence of stages in the growth of a spheroid for case I of phase IV of the growth development.

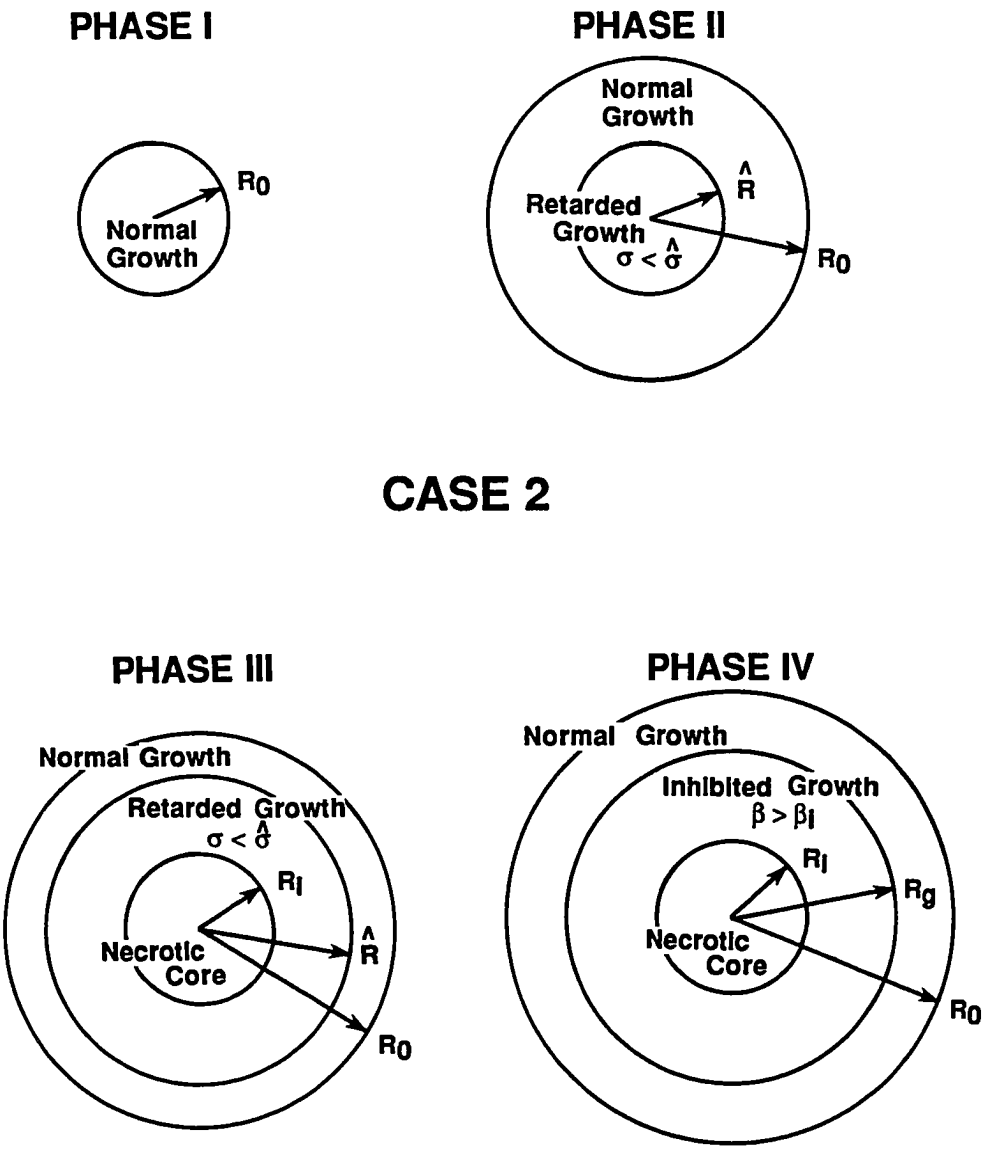

Figure 3.1b. The sequence of stages in the growth of a spheroid for case II of phase IV of the growth development.

a uniform rate, and so the tumor grows at an exponential rate until the nutrient concentration at the center of the nodule drops to the critical value $\hat{\sigma}$ (i.e. until $\sigma(r) = \hat{\sigma}$ at $r = 0$). The appropriate diffusion equation is

$$\frac{k}{r^2}\frac{d}{dr}\left[r^2\frac{d\sigma}{dr}\right] = A\,, \qquad 0 \le r \le R_0 \tag{3.3.1}$$
$$\beta(r) = 0 \ \text{ for all } \ r$$

with the boundary conditions:

(i) $\sigma(r)$ bounded at the origin ($r = 0$),

(ii) $\sigma(r) = \sigma_\infty$ and $\beta(r) = 0$ at $r = R_0$ (inhibitor removed at the boundary),

where k is the diffusion coefficient of the nutrient, $\sigma(r)$, in the nodule, A is the normal nutrient consumption rate, and σ_∞ is the external nutrient concentration ($r \ge R_0$).

The solution to this system is

$$\sigma(r) = \sigma_\infty + \frac{A}{6k}(r^2 - R_0^2) \ , \ 0 \le r \le R_0\,. \tag{3.3.2}$$

The growth equation during this phase is given by

$$\frac{4\pi}{3}\frac{dR_0^3}{dt} = 4\pi\int_0^{R_0} r^2 S(\sigma,\beta)dr\,. \tag{3.3.3}$$

From (3.2.2),

$$S(\sigma,\beta) = s \text{ for } \sigma(r) > \hat{\sigma}$$

Thus, (3.3.3) becomes

$$\frac{dR_0^3}{dt} = sR_0^3 . \tag{3.3.4}$$

By integrating (3.3.4) and introducing a scaled time τ as $\tau = st$ and a scaled radius ξ as $\xi = BR_0$, where $B = (A/k\hat{\sigma})^{1/2}$, we get

$$\xi(\tau) = \xi(0)e^{\tau/3} . \tag{3.3.5}$$

This exponential phase continues until $\sigma(r) = \hat{\sigma}$ at $r = 0$. The corresponding outer radius ξ_c of the nodule, which is the scaled outer radius when the nutrient $\sigma(r)$ has reached this critical value $\hat{\sigma}$, is given by

$$\xi_c = \left[6\left(\frac{\sigma_\infty}{\hat{\sigma}} - 1\right)\right]^{\frac{1}{2}} . \tag{3.3.6}$$

Phase II. In this phase, $\sigma(r) < \hat{\sigma}$ in the central region of the tumor, and the cell proliferation rate decreases in that region. The overall growth rate begins to

slow down due to the insufficient nutrient concentration, and a two layer structure constitutes the nodule. The outer layer consists of cells with normal proliferation rate as in Phase I. Inside this, a layer of viable cells exists with proliferation rate below normal. The diffusion equation for this phase is

$$\frac{k}{r^2}\frac{d}{dr}\left[r^2\frac{d\sigma}{dr}\right] = \begin{cases} A\dfrac{\sigma(r)}{\hat{\sigma}}, & 0 \le r \le \hat{R} \\ A, & \hat{R} \le r \le R_0 \end{cases} \tag{3.3.7}$$

$$\beta(r) = 0 \text{ for all } r$$

with the boundary conditions:

(i) $\sigma(r)$ bounded at the origin,

(ii) $\sigma(r) = \hat{\sigma}$, at $r = \hat{R}$,

(iii) $\sigma(r), \dfrac{d\sigma}{dr}$ are continuous at $r = \hat{R}$,

(iv) $\sigma(r) = \sigma_\infty$ at $r = R_0$.

To solve

$$\frac{k}{r^2}\frac{d}{dr}\left[r^2\frac{d\sigma}{dr}\right] = A\frac{\sigma(r)}{\hat{\sigma}} \quad , \quad 0 \le r \le \hat{R},$$

let $r\sigma(r) = y(r)$ to get

$$\frac{d^2y}{dr^2} - My(r) = 0,$$

whose solution is given by

$$y(r) = C_1 \cosh \sqrt{M} r + C_2 \sinh \sqrt{M} r \quad , \quad 0 \leq r \leq \hat{R}$$

with $M = \dfrac{A}{k\hat{\sigma}}$. Thus,

$$\sigma(r) = \frac{C_1}{r} \cosh \sqrt{M} r + \frac{C_2}{r} \sinh \sqrt{M} r$$

and the solution to system (3.3.7) is

$$\sigma(r) = \frac{\hat{\sigma}\hat{R} \sinh Br}{r \sinh B\hat{R}} \quad , \quad 0 \leq r \leq \hat{R} \tag{3.3.8}$$

and

$$\begin{aligned} \sigma(r) &= \sigma_\infty + \frac{A}{6k}(r^2 - R_0^2) \\ &+ [\hat{\sigma} - \sigma_\infty - \frac{A}{6k}(\hat{R}^2 - R_0^2)] \left[\frac{\hat{R}(r - R_0)}{r(\hat{R} - R_0)}\right] , \quad \hat{R} \leq r \leq R_0 . \end{aligned} \tag{3.3.9}$$

Continuity of $\dfrac{d\sigma}{dr}$ at $r = \hat{R}$ yields the expression

$$\frac{\sigma_\infty}{\hat{\sigma}} - 1 = \frac{1}{6}(\xi^2 - \rho^2) + \left[\rho(\rho \coth \rho - 1) - \frac{\rho^3}{3}\right] \left[\frac{1}{\rho} - \frac{1}{\xi}\right] , \tag{3.3.10}$$

where $\rho = B\hat{R}$. The growth equation for this phase becomes

$$\frac{4\pi}{3}\frac{dR_0^3}{dt} = 4\pi\left[\int_0^{\hat{R}} r^2 S(\sigma,\beta)dr + \int_{\hat{R}}^{R_0} r^2 S(\sigma,\beta)dr\right]. \qquad (3.3.11)$$

From (3.2.2),

$$S(\sigma,\beta) = \begin{cases} s, & \sigma(r) > \hat{\sigma} \\ s\dfrac{\sigma(r)}{\hat{\sigma}}, & \sigma_i < \sigma(r) < \hat{\sigma} \end{cases}.$$

Hence, (3.3.11) takes the form

$$\frac{dR_0^3}{dt} = 3s\int_0^{\hat{R}} r^2\frac{\sigma(r)}{\hat{\sigma}}dr + s(R_0^3 - \hat{R}^3). \qquad (3.3.12)$$

Integration of (3.3.12) with $\sigma(r)$ given by (3.3.8) and transformation into dimensionless variables gives

$$\xi^2\frac{d\xi}{d\tau} = \frac{1}{3}(\xi^3 - \rho^3) + \rho(\rho\coth\rho - 1)$$

which, by using equation (3.3.10), can be rewritten as

$$\xi^2\frac{d\xi}{d\tau} = \frac{1}{3}\xi^3 + \left[\frac{\sigma_\infty}{\hat{\sigma}} - 1 - \frac{1}{6}(\xi^2 - \rho^2)\right]\left[\frac{\rho\xi}{\xi - \rho}\right]. \qquad (3.3.13)$$

This phase continues until $\sigma(r) = \sigma_i$ at the center ($r = 0$) of the tumor, marking

the onset of necrosis (inhibitor production commences at the next stage), and this occurs when $\rho = \rho_c$, where ρ_c can be obtained from

$$\frac{\sigma_i}{\hat{\sigma}} = \frac{\rho_c}{\sinh \rho_c}. \tag{3.3.14}$$

The corresponding outer radius ξ_c of the nodule, which is the scaled outer radius when necrosis starts, is given by (3.3.10) with $\rho = \rho_c$.

The solution to the integro-differential equation (3.3.13) is obtained by numerical integration using a fourth order Runge- Kutta procedure. The value of ρ is needed for a given value of ξ at each step of the method, so that equation (3.3.10) must be solved numerically for ρ several times during each step. The results are stated in Section 3.4.

Phase III. This is a further period of retarded growth. There are two possibities here:

(i) The tumor may reach a dormant steady state with a three layer structure: In the outer shell ($\hat{R} \leq r \leq R_0$), there is normal nutrient consumption and mitosis. In the middle region ($R_i \leq r \leq \hat{R}$, $\sigma_i < \sigma(r) < \hat{\sigma}$), consumption of nutrient and mitosis still occur but at a reduced level. In the inner region ($r \leq R_i$, $\sigma(r) = \sigma_i$), necrotic debris exists and no nutrient consumption occurs. In this steady state, inhibitor is produced (non-uniformly) in $r \leq R_i$ but the concentration $\beta(r)$ need not exceed the critical value β_i, since volume loss due to necrosis balances the volume gain due to mitotic activity outside the necrotic core. This is, in effect the model by McElwain and Ponzo (1977), exhibiting, however, the early stages of inhibitor production.

(ii) The growth is retarded by necrosis volume loss and nutrient consumption decrease but not enough to yield a steady state. Under these circumstances the model enters a fourth stage.

The diffusion of nutrient and growth inhibitor are governed by the equations

$$\frac{k}{r^2}\frac{d}{dr}\left[r^2\frac{d\sigma}{dr}\right] = \begin{cases} 0, & 0 \le r \le R_i \\ A\dfrac{\sigma(r)}{\hat{\sigma}}, & R_i \le r \le \hat{R} \\ A, & \hat{R} \le r \le R_0 \end{cases} \tag{3.3.15}$$

and

$$\frac{K}{r^2}\frac{d}{dr}\left[r^2\frac{d\beta}{dr}\right] = \begin{cases} 0, & r \ge R_i \\ -P\left(1-\dfrac{br}{R_i}\right), & 0 \le r \le R_i \end{cases} \tag{3.3.16}$$

where K is the diffusion coefficient for the growth inhibitor, P is the inhibitor production rate and b is a parameter which measures the degree of non-uniformity for the inhibitor production rate. These equations are subject to the conditions that

(i) $\sigma(r), \beta(r)$ are bounded at the origin $(r = 0)$,

(ii) $\sigma(r), \dfrac{d\sigma}{dr}, \beta$, and $\dfrac{d\beta}{dr}$ are continuous across all interfaces,

(iii) $\sigma(r) = \sigma_i, \beta(r) = \beta_i$, and $\dfrac{d\sigma}{dr} = 0$ at $r = R_i$,

(iv) $\sigma(r) = \hat{\sigma}$ at $r = \hat{R}$,

(v) $\sigma(r) = \sigma_\infty$ and $\beta(r) = 0$ at $r = R_0$.

The solutions to these systems are:

$$\sigma(r) = \sigma_i\,, \qquad 0 \le r \le R_i$$

$$\sigma(r) = \frac{\sigma_i}{Br}[\sinh B(r - R_i) + BR_i \cosh B(r - R_i)]\,, \quad R_i \le r \le \hat{R} \tag{3.3.17}$$

$$\sigma(r) = \sigma_\infty + \frac{A}{6k}(r^2 - R_0^2) + \left[\hat{\sigma} - \sigma_\infty - \frac{A}{6k}(\hat{R}^2 - R_0^2)\right] \frac{\hat{R}}{r} \frac{r - R_0}{\hat{R} - R_0}\,, \qquad \hat{R} \le r \le R_0$$

and

$$\beta(r) = \frac{P}{3K} R_i^3 \left(\frac{3}{2R_i} - \frac{r^2}{2R_i^3} - \frac{1}{R_0}\right) + \frac{Pb}{4K} R_i \left(\frac{r^3}{3R_i^2} - \frac{4R_i}{3} + \frac{R_i^2}{R_0}\right)\,, \qquad 0 \le r \le R_i \tag{3.3.18}$$

$$\beta(r) = \left(\frac{P}{3K} R_i^3 - \frac{Pb}{4K} R_i^3\right) \left(\frac{1}{r} - \frac{1}{R_0}\right)\,, \quad R_i \le r \le R_0\,.$$

Application of the conditions at $r = \hat{R}$, and the use of the non-dimensional variables ξ, ρ, and $\eta = BR_i$ results in the following system of equations:

$$\frac{\hat{\sigma}}{\sigma_i} = \frac{1}{\rho}[\sinh(\rho - \eta) + \eta \cosh(\rho - \eta)] \tag{3.3.19}$$

and

$$\frac{\sigma_\infty}{\hat{\sigma}} - 1 = \frac{1}{6}(\xi^2 - \rho^2) + \left(G\rho - \frac{\rho^3}{3}\right)\left(\frac{1}{\rho} - \frac{1}{\xi}\right) \qquad (3.3.20)$$

with

$$G = \frac{\sigma_i}{\hat{\sigma}}[\cosh(\rho - \eta) + \eta \sinh(\rho - \eta)] - 1 .$$

The growth in this phase is described by

$$\begin{aligned} \frac{4\pi}{3}\frac{dR_0^3}{dt} &= 4\pi\left[\int_0^{R_i} r^2 S(\sigma,\beta)dr + \int_{R_i}^{\hat{R}} r^2 S(\sigma,\beta)dr \right. \\ &+ \left. \int_{\hat{R}}^{R_0} r^2 S(\sigma,\beta)dr\right] - 3\lambda\left(\frac{4\pi}{3}\right)R_i^3 , \end{aligned}$$

where $3\lambda\left(\frac{4\pi}{3}\right)R_i^3$ is the volume loss in viable dormant state to balance the volume gain due to mitosis in the viable region of the tumor. Again from (3.2.2),

$$S_\sigma(\sigma,\beta) = \begin{cases} 0, & \sigma < \sigma_i \\ \dfrac{\sigma(r)}{\hat{\sigma}}, & \sigma_i < \sigma(r) < \hat{\sigma} \\ 1, & \hat{\sigma} < \sigma(r) , \end{cases}$$

and

$$S_\beta(\sigma,\beta) = \begin{cases} 1\,, & \beta(r) < \beta_i \\ 0\,, & \beta(r) > \beta_i \end{cases}$$

so that

$$S(\sigma,\beta) = \begin{cases} 0\,, & 0 \le r \le R_i \\ s\dfrac{\sigma(r)}{\hat{\sigma}}\,, & R_i \le r \le \hat{R} \\ s\,, & \hat{R} \le r \le R_0\,. \end{cases} \tag{3.3.21}$$

The growth equation for this phase then is

$$\frac{dR_0^3}{dt} = s(R_0^3(t) - \hat{R}^3(t)) + 3s\int_{R_i}^{\hat{R}} r^2\frac{\sigma(r)}{\hat{\sigma}}dr - 3\lambda R_i^3(t)\,. \tag{3.3.22}$$

Using equation (3.3.17) and integrating, the growth equation (3.3.22) in dimensionless form becomes

$$\begin{aligned} \xi^2\frac{d\xi}{d\tau} &= \frac{1}{3}(\xi^3 - \rho^3) + \frac{\sigma_i}{\hat{\sigma}}\rho[\cosh(\rho-\eta) + \eta\sinh(\rho-\eta)] \\ &- \frac{\sigma_i}{\hat{\sigma}}[\sinh(\rho-\eta) + \eta\cosh(\rho-\eta)] - \gamma\eta^3 \end{aligned} \tag{3.3.23}$$

where

$$\gamma = \frac{\lambda}{s}\,.$$

A simpler expression for the growth equation can be obtained by using equations (3.3.19 and 3.3.20) to get

$$\xi^2 \frac{d\xi}{d\tau} = \frac{1}{3}\xi^3 + \left[\frac{\sigma_\infty}{\hat{\sigma}} - 1 - \frac{1}{6}\left(\xi^2 - \rho^2\right)\right] \frac{\rho\xi}{\xi - \rho} - \gamma\eta^3 . \tag{3.3.24}$$

This phase continues until $\beta(r) = \beta_i$ at $r = R_i$ (inhibition of mitosis occurs in phase IV). Inhibition is then first evident when $\beta(r) = \beta_i$, and equation (3.3.18) for $(0 \leq r \leq R_i)$ becomes

$$\beta_i = \frac{Pk\hat{\sigma}\eta^2}{3KA}\left(1 - \frac{\eta}{\xi}\right)\left(1 - \frac{3b}{4}\right) . \tag{3.3.25}$$

Let

$$Q^2 = \frac{\beta_i KA}{\hat{\sigma}kP}$$

then (3.3.25) takes the form

$$Q^2 = \frac{\eta^2}{3}\left(1 - \frac{\eta}{\xi}\right)\left(1 - \frac{3b}{4}\right) . \tag{3.3.26}$$

The parameter Q is therefore a measure of the competing effects of nutrient consumption/diffusion and inhibitor production/diffusion. As mentioned earlier, under certain conditions a steady state is reached or a fourth stage is initiated. These cutoff conditions depend critically on the parameters Q, b, and γ.

The growth equation (3.3.24) is solved numerically using a fourth order Runge-Kutta procedure. The values of ρ and η are needed for a given value of ξ at each step of the method, so that the system of equations (3.3.19, 3.3.20) must be solved numerically for ρ and η several times during each step. The results are stated in Section 3.4.

Phase IV. This is a period of retarded growth due to necrosis volume loss, nutrient consumption decrease, and chemical inhibition of mitosis beginning when $\beta(r) = \beta_i$ at $r = R_i$. There are two cases to be considered in this stage of growth (if it occurs):

Case I: We assume that $R_g < \hat{R}$ and that the chemically inhibited cells, since they are not dead, continue to consume some nutrient. The rate of growth decreases further and the tumor eventually reaches a steady state with a four layer structure. In the outer region $(\hat{R} < r < R_0)$, the growth is exponential. Inside this, there is a region $(R_g < r < \hat{R})$ of retarded growth of cells (due to insufficient nutrient $(\sigma_i < \sigma(r) < \hat{\sigma})$. Adjacent to this region, there is a layer $(R_i < r < R_g)$ of viable cells with proliferation rate below normal due to inhibition of mitosis. In the innermost region $(0 < r < R_i)$, there is accumulation of necrotic debris. The diffusion equations that govern this case are

$$\frac{k}{r^2}\frac{d}{dr}\left[r^2\frac{d\sigma}{dr}\right] = \begin{cases} 0, & 0 \le r \le R_i \\ \delta^2 A\dfrac{\sigma(r)}{\hat{\sigma}}, & R_i \le r \le R_g \\ A\dfrac{\sigma(r)}{\hat{\sigma}}, & R_g \le r \le \hat{R} \\ A, & \hat{R} \le r \le R_0 \end{cases} \tag{3.3.27}$$

and

$$\frac{K}{r^2}\frac{d}{dr}\left[r^2\frac{d\beta}{dr}\right] = \begin{cases} 0, & r \ge R_i \\ -P\left(1-\dfrac{br}{R_i}\right), & 0 \le r \le R_i \end{cases} \tag{3.3.28}$$

with the associated boundary conditions

(i) $\sigma(r)$, $\beta(r)$ bounded at the origin $(r = 0)$,

(ii) $\sigma(r) = \sigma_i$, $\dfrac{d\sigma}{dr} = 0$ at $r = R_i$,

(iii) $\beta(r) = \beta_i$ at $r = R_g$,

(iv) $\sigma(r) = \hat{\sigma}$ at $r = \hat{R}$,

(v) $\sigma(r) = \sigma_\infty$, $\beta(r) = 0$ at $r = R_o$,

(vi) $\sigma(r)$, $\beta(r)$, $\dfrac{d\sigma}{dr}$ and $\dfrac{d\beta}{dr}$ are continuous across all interfaces.

A parameter $\delta^2(0 < \delta < 1)$ is introduced to measure the effect (if any) of non-zero inhibitor concentration $\beta(r)$ on the nutrient consumption rate. Solving the systems above we obtain

$$\sigma(r) = \sigma_i\,, \qquad 0 \le r \le R_i$$

$$\sigma(r) = \frac{\sigma_i}{\delta B r}[\sinh \delta B(r - R_i) + \delta B R_i \cosh \delta B(r - R_i)], \quad R_i \le r \le R_g$$

$$\sigma(r) = \frac{\hat{\sigma}\hat{R}\delta B \sinh B(r - R_g) + \mu\sigma_i \sinh B(\hat{R} - r)}{r\delta B \sinh B(\hat{R} - R_g)}, \qquad R_g \le r \le \hat{R} \tag{3.3.29}$$

$$\sigma(r) = \sigma_\infty + \frac{A}{6k}(r^2 - R_0^2) + \left[\hat{\sigma} - \sigma_\infty - \frac{A}{6k}(\hat{R}^2 - R_0^2)\right]\frac{\hat{R}}{r}\frac{r - R_0}{\hat{R} - R_0}, \qquad \hat{R} \le r \le R_0$$

where

$$\mu = \sinh \delta B(R_g - R_i) + \delta B R_i \cosh \delta B(R_g - R_i)$$

and

$$\beta(r) = \frac{P}{3K}R_i^3\left(\frac{3}{2R_i} - \frac{r^2}{2R_i^3} - \frac{1}{R_0}\right) + \frac{Pb}{4K}R_i\left(\frac{r^3}{3R_i^2} - \frac{4R_i}{3} + \frac{R_i^2}{R_0}\right), \qquad 0 \le r \le R_i \tag{3.3.30}$$

$$\beta(r) = \left(-\frac{Pb}{4K}R_i^3 + \frac{P}{3K}R_i^3\right)\left(\frac{1}{r} - \frac{1}{R_0}\right), \quad R_i \le r \le R_0\,.$$

Application of the conditions $\beta(r) = \beta_i$ at $r = R_g$, $\dfrac{d\sigma}{dr}$ continuous at $r = R_g$, and $\dfrac{d\sigma}{dr}$ continuous at $r = \hat{R}$ results into the following three equations (note $\varsigma = BR_g$)

$$Q^2 = \eta^3\left(\frac{b}{4} - \frac{1}{3}\right)\left(\frac{1}{\xi} - \frac{1}{\varsigma}\right)$$

$$\begin{aligned}\frac{\hat{\sigma}}{\sigma_i} &= \frac{1}{\rho}\sinh(\rho-\varsigma)[\cosh\delta(\varsigma-\eta)+\delta\eta\sinh\delta(\varsigma-\eta)] \\ &+ \frac{1}{\delta\rho}\sinh(\rho-\varsigma)\coth(\rho-\varsigma)[\sinh\delta(\varsigma-\eta)+\delta\eta\cosh\delta(\varsigma-\eta)]\end{aligned}$$

$$\begin{aligned}\frac{\sigma_\infty}{\hat{\sigma}}-1 &= -\frac{\xi-\rho}{\xi}\left[1+\frac{\rho^2}{3}\right]+\frac{1}{6}(\xi^2-\rho^2)+\frac{\rho(\xi-\rho)}{\xi}\coth(\rho-\varsigma) \\ &- \frac{\sigma_i(\xi-\rho)}{\hat{\sigma}\delta\xi}\operatorname{csch}(\rho-\varsigma)[\sinh\delta(\varsigma-\eta)+\delta\eta\cosh\delta(\varsigma-\eta)]\end{aligned} \tag{3.3.31}$$

respectively. The growth equation now is

$$\begin{aligned}\frac{4\pi}{3}\frac{dR_0^3}{dt} &= 4\pi\left[\int_0^{R_i} r^2S(\sigma,\beta)dr+\int_{R_i}^{R_g} r^2S(\sigma,\beta)dr+\int_{R_g}^{\hat{R}} r^2S(\sigma,\beta)dr+\right. \\ &+ \left.\int_{\hat{R}}^{R_0} r^2S(\sigma,\beta)dr\right]-3\lambda\left(\frac{4\pi}{3}\right)R_i^3\,.\end{aligned}$$

From (3.2.2), the proliferation rate for this phase of growth becomes

$$S(\sigma,\beta)=\begin{cases}0, & 0\le r\le R_i\\ 0, & R_i\le r\le R_g\\ s\dfrac{\sigma(r)}{\hat{\sigma}}, & R_g\le r\le\hat{R}\\ s, & \hat{R}\le r\le R_0\,.\end{cases} \tag{3.3.32}$$

Hence, the growth equation takes the form

$$\frac{dR_0^3}{dt}=s(R_0^3(t)-\hat{R}^3(t))+\frac{3s}{\hat{\sigma}}\int_{R_g}^{\hat{R}} r^2\sigma(r)dr-3\lambda R_i^3(t)\,. \tag{3.3.33}$$

By integrating (3.3.33), after substituting $\sigma(r)$ from (3.3.29), and using the non-dimensional variables $\xi, \rho, \varsigma, \eta$, a dimensionless form of the growth equation can be obtained

$$\begin{aligned} \xi^2 \frac{d\xi}{d\tau} &= \frac{1}{3}(\xi^3 - \rho^3) + \rho[\rho \coth(\rho - \varsigma) - \varsigma \operatorname{csch}(\rho - \varsigma) - 1] \\ &+ \frac{\sigma_i}{\hat{\sigma}\delta}[\varsigma \coth(\rho - \varsigma) - \rho \operatorname{csch}(\rho - \varsigma) + 1][\sinh \delta(\varsigma - \eta) \\ &+ \eta\delta \cosh \delta(\varsigma - \eta)] - \gamma\eta^3 . \end{aligned} \tag{3.3.34}$$

This growth equation is solved numerically as in the previous phases. The values of ρ, ς, and η are required for a given value of ξ at each step of the method, so that the system of equations (3.3.31) must be solved numerically for ρ, ς and η several times during each step. The results are stated in Section 3.4.

At this point some further analysis is of interest. The radius R_g, of the mitotically inactive region, may move out and "pass" the radius $\hat{R}$, of the region with retarded cell growth, converting outer shell material into regions of inhibited growth, which is Case II of this phase.

Case II: It is now supposed that $R_g > \hat{R}$, which may never be realized, and the tumor consists of a three layer structure. An inner shell $(0 < r < R_i)$ which is the necrotic core, a middle shell $(R_i < r < R_g)$ of mitotically inactive cells, and the outer shell $(R_g < r < R_0)$ in which the growth of cells is normal. The diffusion of the nutrient $\sigma(r)$ is described by

$$\frac{k}{r^2}\frac{d}{dr}\left[r^2\frac{d\sigma}{dr}\right] = \begin{cases} 0, & 0 \le r \le R_i \\ \delta^2 A\dfrac{\sigma(r)}{\hat{\sigma}}, & R_i \le r \le R_g \\ A, & R_g \le r \le R_o \end{cases} \tag{3.3.35}$$

while the diffusion of inhibitor $\beta(r)$ is described by (3.3.28). The solution to system (3.3.28) is the same as in case I, and the solution to system (3.3.35) is given by

$$\sigma(r) = \sigma_i\,, \qquad 0 \le r \le R_i$$

$$\sigma(r) = \frac{\sigma_i}{\delta B r}[\sinh\delta B(r-R_i) + \delta B R_i \cosh\delta B(r-R_i)]\,, \quad R_i \le r \le R_g$$

$$\begin{aligned} \sigma(r) = {} & \frac{A}{6k}\left[r^2 + \frac{R_g R_0}{r(R_0-R_g)}(R_0^2-R_g^2) + \frac{R_g^3-R_0^3}{R_0-R_g}\right] \\ & -\frac{R_0}{r(R_0-R_g)}[\sigma_\infty R_g - \sigma_i R_i\cosh\delta B(R_g-R_i)] \\ & +\frac{\sigma_i\sinh\delta B(R_g-R_i)}{r\delta B(R_0-R_g)}[R_0-r] \\ & +\frac{1}{R_0-R_g}[\sigma_\infty R_0 - \sigma_i R_i\cosh\delta B(R_g-R_i)], \qquad R_g \le r \le R_0 \end{aligned} \tag{3.3.36}$$

The conditions $\beta(r) = \beta_i$ at $r = R_g$ and $\dfrac{d\sigma}{dr}$ continuous at $r = R_g$ give the following system of equations

$$Q^2 = \eta^3\left(\frac{b}{4}-\frac{1}{3}\right)\left(\frac{1}{\xi}-\frac{1}{\varsigma}\right)$$

$$\frac{\sigma_\infty\xi}{\varsigma(\xi-\varsigma)} = \frac{\sigma_i}{\varsigma}[\cosh\delta(\varsigma-\eta) + \delta\eta\sinh\delta(\varsigma-\eta)] +$$

$$+ \quad \frac{\hat{\sigma}}{6(\xi-\varsigma)}\left[\frac{\xi^3}{\varsigma}-\xi\varsigma\right]-\frac{\hat{\sigma}\varsigma}{3}$$
$$+ \quad \frac{\sigma_i}{\delta\varsigma^2}\left[\frac{\xi}{\xi-\varsigma}-1\right][\sinh\delta(\varsigma-\eta)$$
$$+ \quad \delta\eta\cosh\delta(\varsigma-\eta)] \qquad (3.3.37)$$

The proliferation rate for this case is

$$S(\sigma,\beta)=\begin{cases} 0, & 0\le r\le R_i \\ 0, & R_i\le r\le R_g \\ s, & R_g\le r\le R_0 \end{cases}$$

and the appropriate growth equation in dimensionless form becomes

$$\xi^2\frac{d\xi}{d\tau}=\frac{1}{3}\left(\xi^3-\varsigma^3\right)-\gamma\eta^3 \qquad (3.3.38)$$

Again, a numerical solution to this differential equation is obtained. To find the values of ς and η for a given value of ξ, which are needed in the attempt to obtain the above solution, the system of equations (3.3.37) is solved numerically for ς and η several times during each step of the Runge-Kutta method. The results of these solutions are stated in the following section. This phase lasts until the dormant steady state is reached. The dimensionless parameters Q, b, and γ control the rapidity at which this steady state is attained.

3.4 The Results of the Model

The model studied in this chapter is deterministic in that the evolution of a multicellular spheroid from an initial form is determined by an integro-differential equation, the kernel of which depends on the solutions of the spherically symmetric diffusion equations for the concentration of nutrient and growth inhibitor within the tumor. The radial dependence induced by spherical symmetry introduces considerable simplifications in the analysis while retaining the basic physics and appropriate geometric figures.

The general behavior of the system is subject to the values that $\frac{\sigma_\infty}{\hat{\sigma}}$, $\frac{\sigma_i}{\hat{\sigma}}$ and the parameters γ, Q, b, and δ take. The data used for these parameters is taken from Greenspan (1972) and McElwain and Ponzo (1977) models. A complete history of model tumor growth, by prescribing several values of each parameter follows below.

1. The parameter $\gamma = \frac{\lambda}{s}$:

Description of variables:

λ is the proportionality constant for the volume loss.

s is the normal proliferation rate of cells, i.e. when $\sigma(r) > \hat{\sigma}$ and $\beta(r) = 0$, or $\beta(r) < \beta_i$ for a discontinuous switch mechanism.

Table 3.1 lists the values for the scaled radii at critical stages of the tumor growth for various values of the parameter γ.

TABLE 3.1

$b = 0.4$, $Q = 0.8$ and $\delta = 0.5$

γ	$\sigma_\infty/\hat{\sigma}$	$\sigma_i/\hat{\sigma}$	ξ	ρ	ς	η	End of
0.2	1.41	0.1	1.56	0.00	0.00	0.00	Phase I
	1.41	0.1	4.94	4.50	0.00	0.00	Phase II
	1.41	0.1	6.39	5.97	0.00	2.41	Phase III
	1.41	0.1	12.82	12.59	12.01	8.04	Phase IV (case I)
	8	10^{-6}	6.48	0.00	0.00	0.00	Phase I
	8	10^{-6}	20.50	17.40	0.00	0.00	Phase II
	8	10^{-6}	21.98	18.84	0.00	2.71	Phase III
	8	10^{-6}	39.53	38.82	38.72	17.27	Phase IV (case I)
0.5	1.41	0.1	1.56	0.00	0.00	0.00	Phase I
	1.41	0.1	4.94	4.50	0.00	0.00	Phase II
	1.41	0.1	6.34	5.92	0.00	2.35	Phase III
	1.41	0.1	10.77	10.45	9.44	5.94	Phase IV (case I)
	8	10^{-6}	6.48	0.00	0.00	0.00	Phase I
	8	10^{-6}	20.50	17.40	0.00	0.00	Phase II
	8	10^{-6}	21.98	18.84	0.00	2.71	Phase III
	8	10^{-6}	37.31	36.28	36.13	14.62	Phase IV (case I)
0.9	1.41	0.1	1.56	0.00	0.00	0.00	Phase I
	1.41	0.1	4.94	4.50	0.00	0.00	Phase II
	1.41	0.1	6.28	5.85	0.00	2.28	Phase III
	1.41	0.1	9.46	9.09	7.57	4.71	Phase IV (case I)
	8	10^{-6}	6.48	0.00	0.00	0.00	Phase I
	8	10^{-6}	20.50	17.40	0.00	0.00	Phase II
	8	10^{-6}	21.97	18.84	0.00	2.71	Phase III
	8	10^{-6}	36.03	34.67	34.46	19.92	Phase IV (case I)
0.25	5.68	0.1	5.30	0.00	0.00	0.00	Phase I
	5.68	0.1	7.49	4.50	0.00	0.00	Phase II
	5.68	0.1	8.06	4.01	0.00	2.80	Phase III
	5.68	0.1	17.11		16.28	9.72	Phase IV (case II)
0.4	5.68	0.1	5.30	0.00	0.00	0.00	Phase I
	5.68	0.1	7.49	4.50	0.00	0.00	Phase II
	5.68	0.1	7.94	3.86	0.00	2.74	Phase III
	5.68	0.1	16.08		15.03	8.59	Phase IV (case II)
0.8	5.68	0.1	5.30	0.00	0.00	0.00	Phase I
	5.68	0.1	7.49	4.50	0.00	0.00	Phase II
	5.68	0.1	7.65	3.50	0.00	2.61	Phase III
	5.68	0.1	14.81		13.33	7.15	Phase IV (case II)

Table 3.1 Values for the scaled radii at critical stages of the tumor growth for various values of the parameter γ.

Conclusion: As γ increases, the overall tumor growth decreases. This means that an increase in the proportionality constant, λ, for the volume loss, or a decrease in the normal proliferation rate, s, results in an increase of the parameter γ and therefore in a decrease of the tumor growth (see figures 3.2 through 3.6).

2. The parameter $Q^2 = \frac{\beta_i(A/k)}{\hat{\sigma}(P/K)}$:

Description of variables:

β_i is the critical inhibitor concentration above which cell proliferation ceases (though the cells may still be viable, and consume small amount of nutrient).

K is the diffusion coefficient for the growth inhibitor in the tumor.

A is the normal nutrient consumption rate.

P is the inhibitor production rate.

k is the diffusion coefficient for the nutrient in the tumor.

$\hat{\sigma}$ is the critical nutrient concentration below which nutrient consumption by the cell falls.

Table 3.2 lists values for the scaled radii at critical stages of the tumor growth for various values of the parameter.

TABLE 3.2

$\gamma = 0.4 \quad b = 0.4 \quad \delta = 0.5$

Q	$\frac{\sigma_m}{\tilde{\sigma}}$	$\frac{\sigma_i}{\tilde{\sigma}}$	ξ	ρ	ς	η	End of
0.2	1.41	0.1	1.56	0.00	0.00	0.00	Phase I
	1.41	0.1	4.94	4.50	0.00	0.00	Phase II
	1.41	0.1	5.32	4.88	0.00	.99	Phase III
	1.41	0.1	8.67	8.58	8.40	3.60	Phase IV (case I)
	8	10^{-6}	6.48	0.00	0.00	0.00	Phase I
	8	10^{-6}	20.50	17.40	0.00	0.00	Phase II
	8	10^{-6}	21.98	18.84	0.00	2.71	Phase III
	8	10^{-6}	30.65	30.40	30.37	8.26	Phase IV (case I)
0.5	1.41	0.1	1.56	0.00	0.00	0.00	Phase I
	1.41	0.1	4.94	4.50	0.00	0.00	Phase II
	1.41	0.1	5.67	5.24	0.00	1.51	Phase III
	1.41	0.1	10.27	10.07	9.58	5.33	Phase IV (case I)
	5.68	0.1	5.30	0.00	0.00	0.00	Phase I
	5.68	0.1	7.49	4.50	0.00	0.00	Phase II
	5.68	0.1	7.94	3.91	0.00	2.02	Phase III
	5.68	0.1	14.41		13.75	6.87	Phase IV (case II)
0.8	1.41	0.1	1.56	0.00	0.00	0.00	Phase I
	1.41	0.1	4.94	4.50	0.00	0.00	Phase II
	1.41	0.1	6.35	5.93	0.00	2.37	Phase III
	1.41	0.1	11.26	10.96	10.09	6.43	Phase IV (case I)
	8	10^{-6}	6.48	0.00	0.00	0.00	Phase I
	8	10^{-6}	20.50	17.40	0.00	0.00	Phase II
	8	10^{-6}	21.98	18.84	0.00	2.71	Phase III
	8	10^{-6}	37.86	36.93	36.79	15.29	Phase IV (case I)
0.9	5.68	0.1	5.30	0.00	0.00	0.00	Phase I
	5.68	0.1	7.49	4.50	0.00	0.00	Phase II
	5.68	0.1	7.94	3.85	0.00	2.96	Phase III
	5.68	0.1	16.58		15.40	9.10	Phase IV (case II)
	8	10^{-6}	6.48	0.00	0.00	0.00	Phase I
	8	10^{-6}	20.50	17.40	0.00	0.00	Phase II
	8	10^{-6}	21.98	18.84	0.00	2.71	Phase III
	8	10^{-6}	38.79	37.75	37.59	16.16	Phase IV (case I)
1.15	5.68	0.1	5.30	0.00	0.00	0.00	Phase I
	5.68	0.1	7.49	4.50	0.00	0.00	Phase II
	5.68	0.1	7.94	3.85	0.00	3.47	Phase III
	5.68	0.1	17.75		16.24	10.28	Phase IV (case II)

Table 3.2 Values for the scaled radii at critical stages of the tumor growth for various values of the parameter Q.

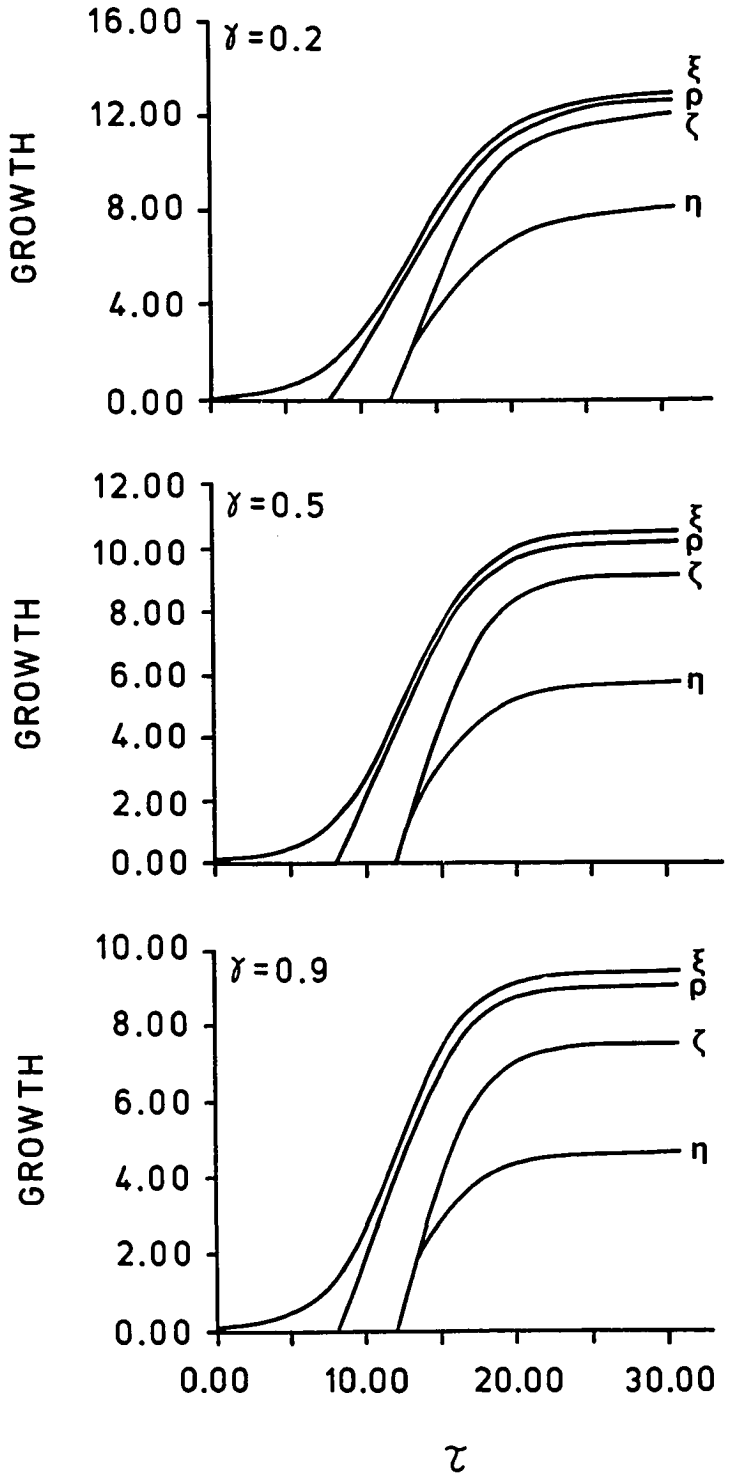

Figure 3.2. The full growth pattern of the tumor for different values of the parameter γ (i.e. $\gamma = 0.2$, $\gamma = 0.5$, $\gamma = 0.9$). The values used for the other parameters are: $Q = 0.8$, $b = 0.4$, $\delta = 0.5$.

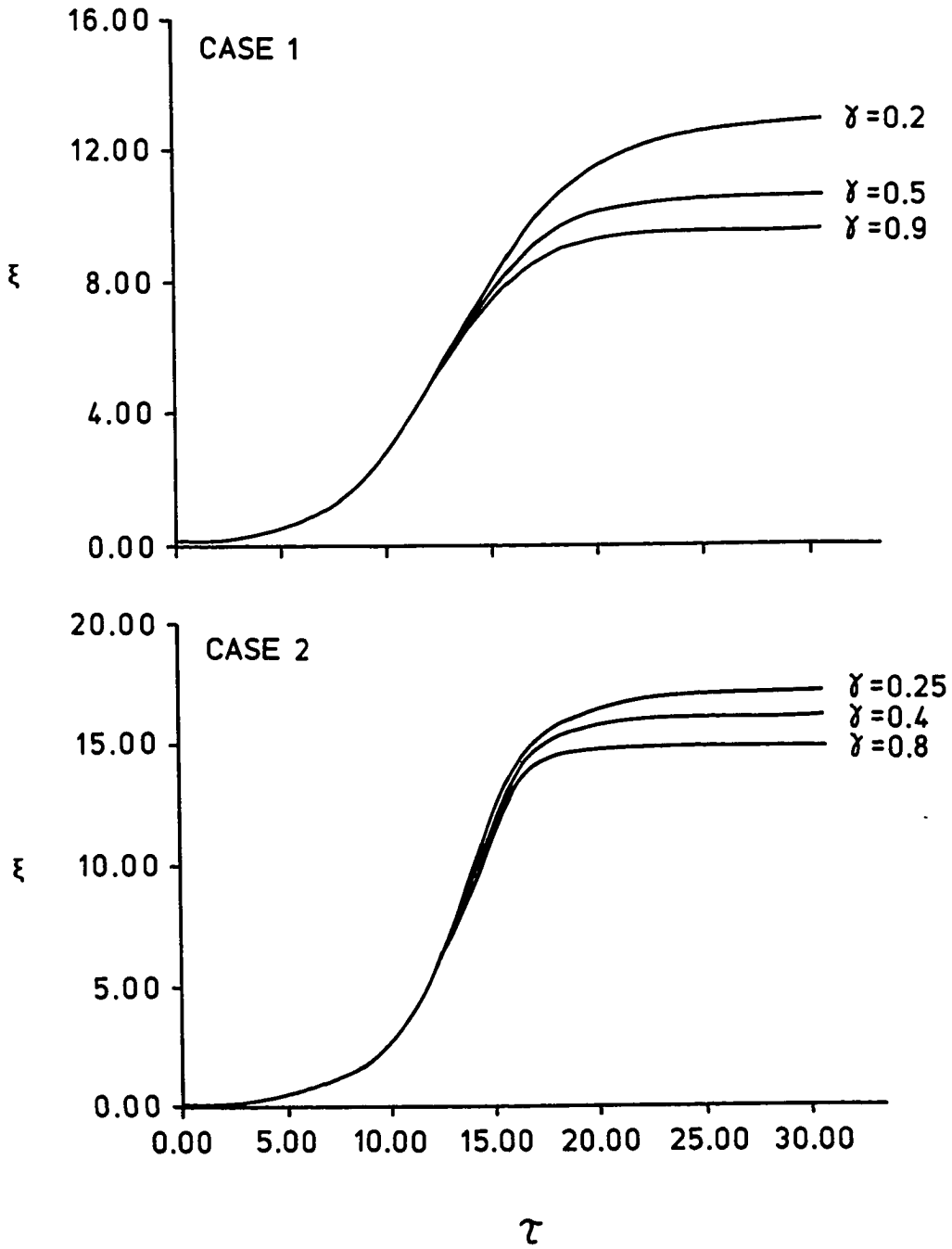

Figure 3.3. The change of the scaled outer tumor radius ξ as the parameter γ takes on various values (i.e. $\gamma = 0.2$, $\gamma = 0.5$, $\gamma = 0.9$ for case I, and $\gamma = 0.25$, $\gamma = 0.4$, $\gamma = 0.8$ for case II of phase IV of the growth development of the tumor). The values used for the other parameters are: $Q = 0.8$, $b = 0.4$, $\delta = 0.5$ for both cases.

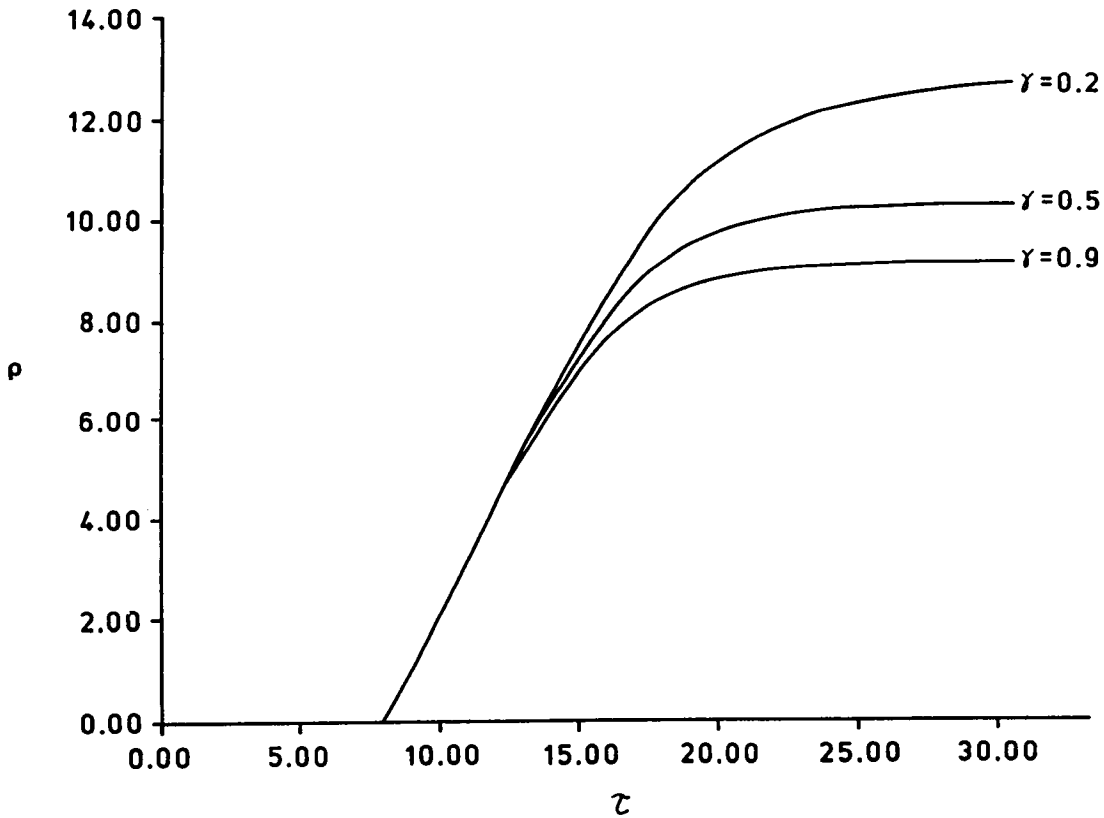

Figure 3.4. The change of the scaled inner radius ρ, the radius at which the concentration of nutrient $\sigma(r) < \hat{\sigma}$, as the parameter γ changes (i.e. $\gamma = 0.2$, $\gamma = 0.5$, $\gamma = 0.9$). The values used for the other parameters are: $Q = 0.8$, $b = 0.4$, $\delta = 0.5$.

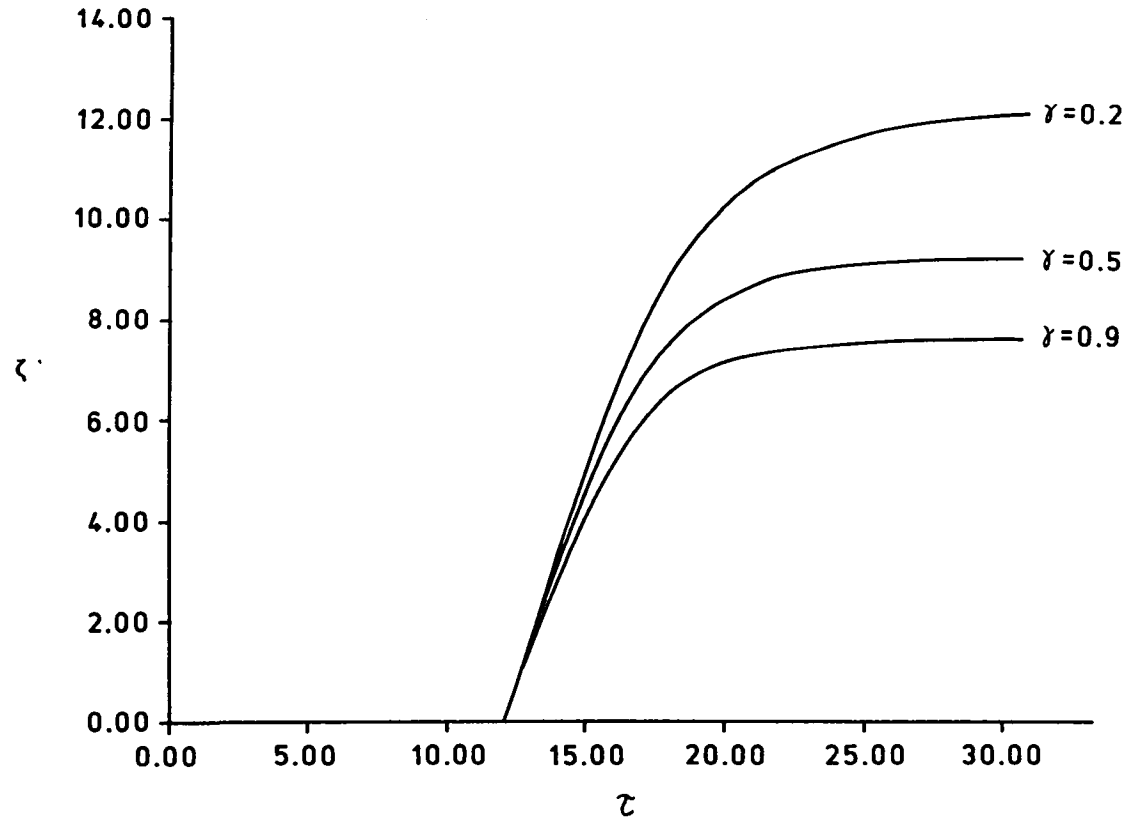

Figure 3.5. The change of the scaled inner radius ς, the radius at which the concentration of inhibitor $\beta(r) > \beta_i$, as the parameter γ changes (i.e. $\gamma = 0.2$, $\gamma = 0.5$, $\gamma = 0.9$). The values used for the other parameters are: $Q = 0.8$, $b = 0.4$, $\delta = 0.5$.

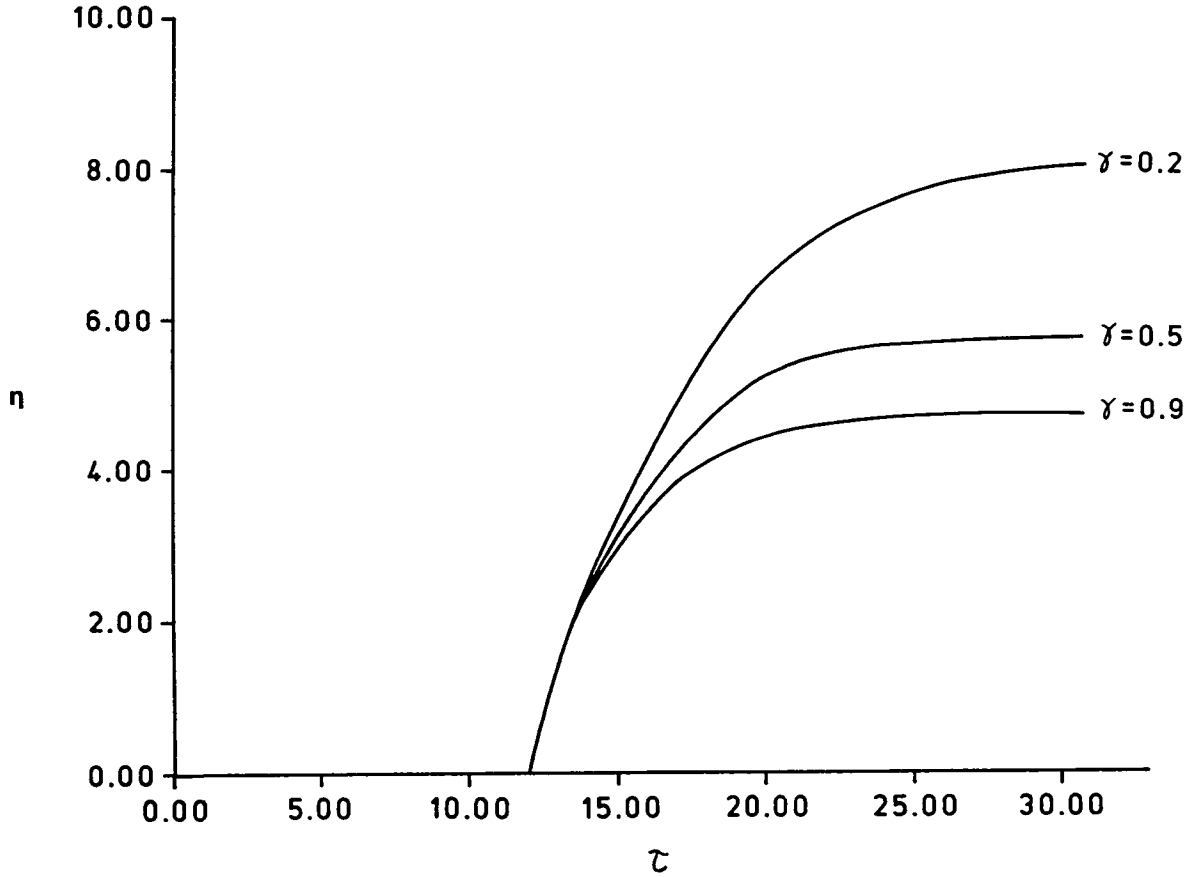

Figure 3.6. The change of the radius η of the necrotic core for various values of the parameter γ (i.e. $\gamma = 0.2$, $\gamma = 0.5$, $\gamma = 0.9$). The values used for the other parameters are: $Q = 0.8$, $b = 0.4$, $\delta = 0.5$.

Conclusion: As Q increases, the overall tumor growth increases. This means that an increase in the source term A/k for the nutrient consumption, or a decrease in the source term P/K for the inhibitor production results in an increase in the parameter Q and therefore in an increase in the tumor growth (see figures 3.7 through 3.11). From figure 3.10, initially, the rate of change of the scaled inner radius ς (the radius of the inhibited growth region) is greater for small values of the parameter Q than it is for large values. This occurs due to the fact that there is greater inhibitor production for smaller values of Q, and as a result the tumor cells undergo inhibition faster (i.e. ς reaches a given radius faster).

3. The parameter b:

Description of variables:

b is the measure of the degree of non-uniformity for the inhibitor production rate.

Constraints:

$$0 \leq b \leq 1$$

Table 3.3 lists values for the scaled radii at critical stages of the tumor growth for various values of the parameter.

TABLE 3.3

$\gamma = 0.4 \quad Q = 0.8 \quad \delta = 0.5$

b	$\frac{\sigma_\infty}{\hat{\sigma}}$	$\frac{\sigma_i}{\hat{\sigma}}$	ξ	ρ	ς	η	End of
0	1.41	0.1	1.56	0.00	0.00	0.00	Phase I
	1.41	0.1	4.94	4.50	0.00	0.00	Phase II
	1.41	0.1	6.02	5.59	0.00	1.96	Phase III
	1.41	0.1	10.90	10.64	9.94	6.02	Phase IV (case I)
	8	10^{-6}	6.48	0.00	0.00	0.00	Phase I
	8	10^{-6}	20.50	17.40	0.00	0.00	Phase II
	8	10^{-6}	21.98	18.84	0.00	2.71	Phase III
	8	10^{-6}	36.56	35.78	35.67	14.09	Phase IV (case I)
	5.68	0.1	5.30	0.00	0.00	0.00	Phase I
	5.68	0.1	7.49	4.50	0.00	0.00	Phase II
	5.68	0.1	7.94	3.88	0.00	2.44	Phase III
	5.68	0.1	15.38		14.51	7.88	Phase IV (case II)
0.5	5.68	0.1	5.30	0.00	0.00	0.00	Phase I
	5.68	0.1	7.49	4.50	0.00	0.00	Phase II
	5.68	0.1	7.94	3.88	0.00	2.85	Phase III
	5.68	0.1	16.31		15.21	8.83	Phase IV (case II)
0.7	1.41	0.1	1.56	0.00	0.00	0.00	Phase I
	1.41	0.1	4.94	4.50	0.00	0.00	Phase II
	1.41	0.1	6.67	6.62	0.00	2.75	Phase III
	1.41	0.1	11.57	11.23	10.09	6.83	Phase IV (case I)
	8	10^{-6}	6.48	0.00	0.00	0.00	Phase I
	8	10^{-6}	20.50	17.40	0.00	0.00	Phase II
	8	10^{-6}	21.98	18.84	0.00	2.71	Phase III
	8	10^{-6}	39.43	38.31	38.14	16.74	Phase IV (case I)
0.9	5.68	0.1	5.30	0.00	0.00	0.00	Phase I
	5.68	0.1	7.49	4.50	0.00	0.00	Phase II
	5.68	0.1	7.94	3.82	0.00	3.52	Phase III
	5.68	0.1	17.85		16.32	10.39	Phase IV (case II)
	8	10^{-6}	6.48	0.00	0.00	0.00	Phase I
	8	10^{-6}	20.50	17.40	0.00	0.00	Phase II
	8	10^{-6}	23.11	19.99	0.00	4.12	Phase III
	8	10^{-6}	42.34	40.83	40.58	19.37	Phase IV (case I)
0.99	1.41	0.1	1.56	0.00	0.00	0.00	Phase I
	1.41	0.1	4.94	4.50	0.00	0.00	Phase II
	1.41	0.1	7.79	7.39	0.00	4.01	Phase III
	1.41	0.1	11.64	11.26	9.43	7.19	Phase IV (case I)

Table 3.3 Values for the scaled radii at critical stages of the tumor growth for various values of the parameter b.

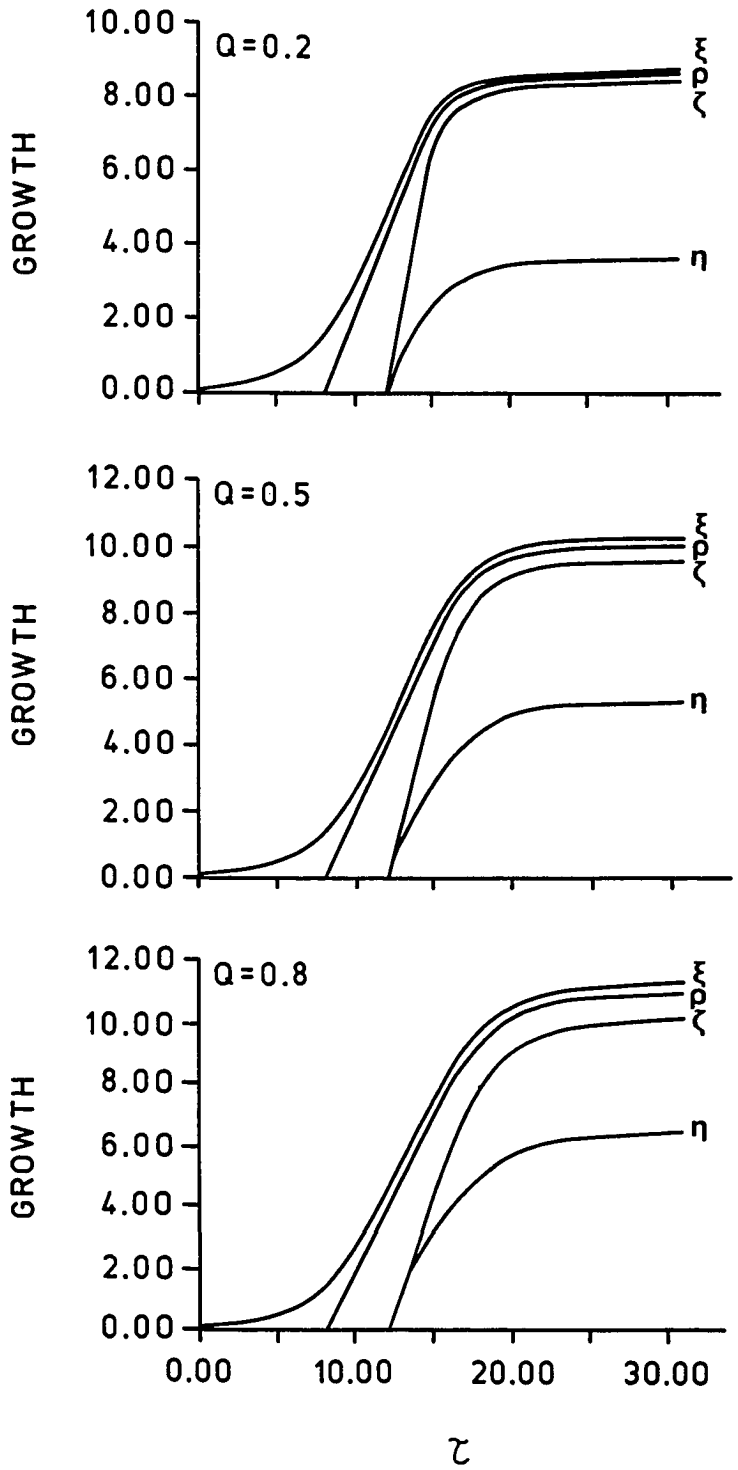

Figure 3.7. The full growth pattern of the tumor for different values of the parameter Q (i.e. $Q = 0.2$, $Q = 0.5$, $Q = 0.8$). The values used for the other parameters are: $\gamma = 0.4$, $b = 0.4$, $\delta = 0.5$.

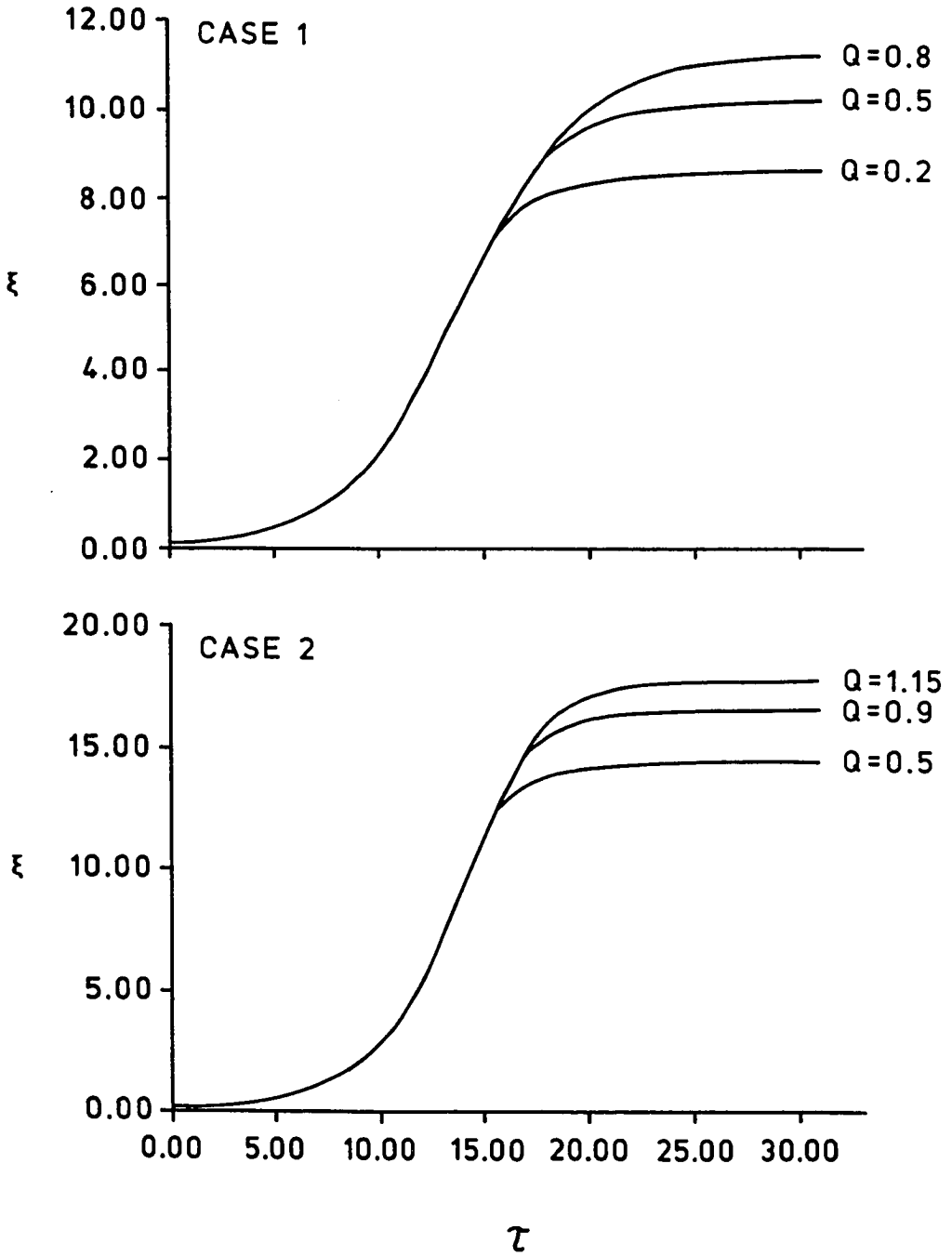

Figure 3.8. The change of the scaled outer tumor radius ξ as the parameter Q changes (i.e. $Q = 0.2$, $Q = 0.5$, $Q = 0.8$ for case I, and $Q = 0.5$, $Q = 0.9$, $Q = 1.15$ for case II of phase IV of the growth development of the tumor). The values used for the other parameters are: $\gamma = 0.4$, $b = 0.4$, $\delta = 0.5$ for both cases.

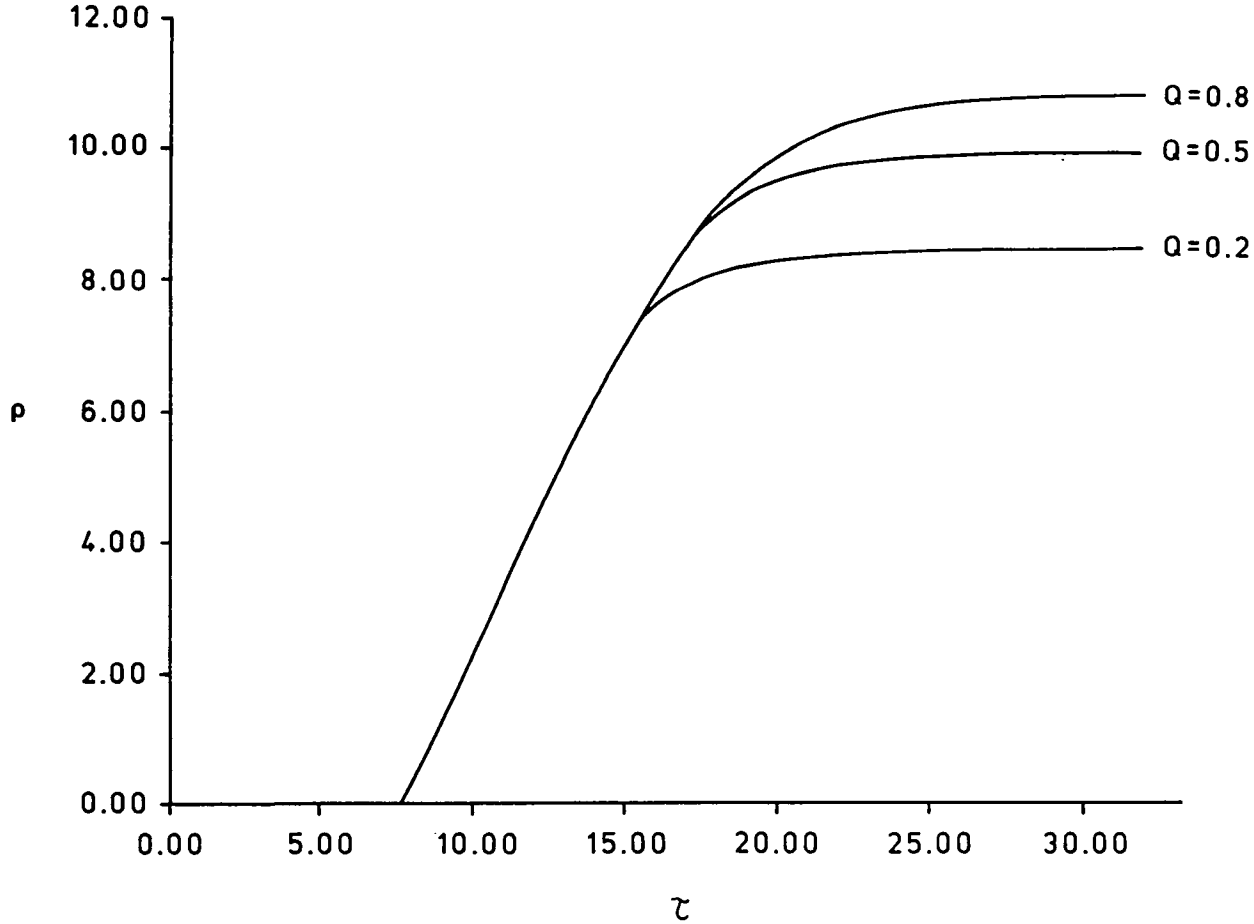

Figure 3.9. The change of the scaled inner radius ρ as the parameter Q changes (i.e. $Q = 0.2$, $Q = 0.5$, $Q = 0.8$). The values used for the other parameters are: $\gamma = 0.4$, $b = 0.4$, $\delta = 0.5$.

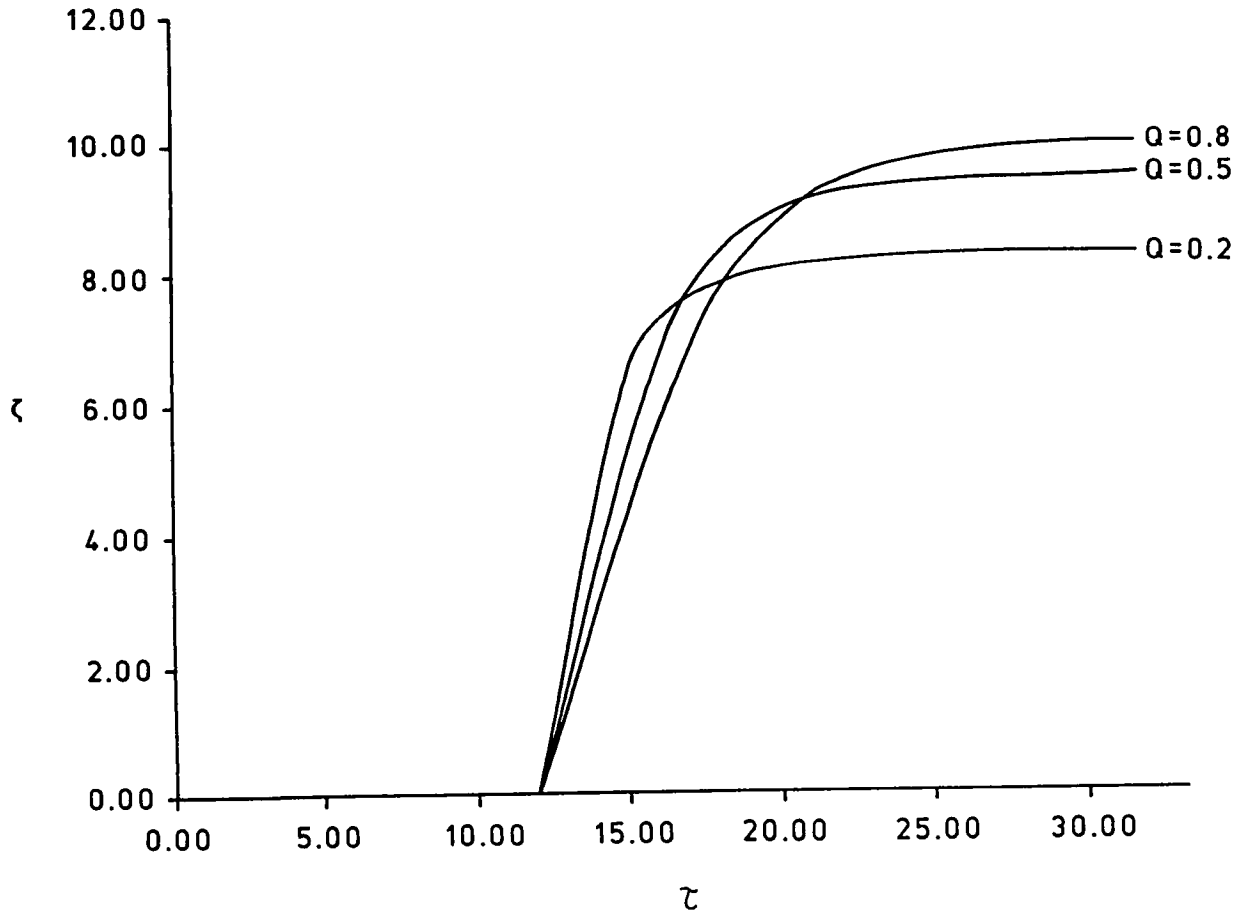

Figure 3.10. The change of the scaled inner radius ζ as the parameter Q changes (i.e. $Q = 0.2$, $Q = 0.5$, $Q = 0.8$). The values used for the other parameters are: $\gamma = 0.4$, $b = 0.4$, $\delta = 0.5$.

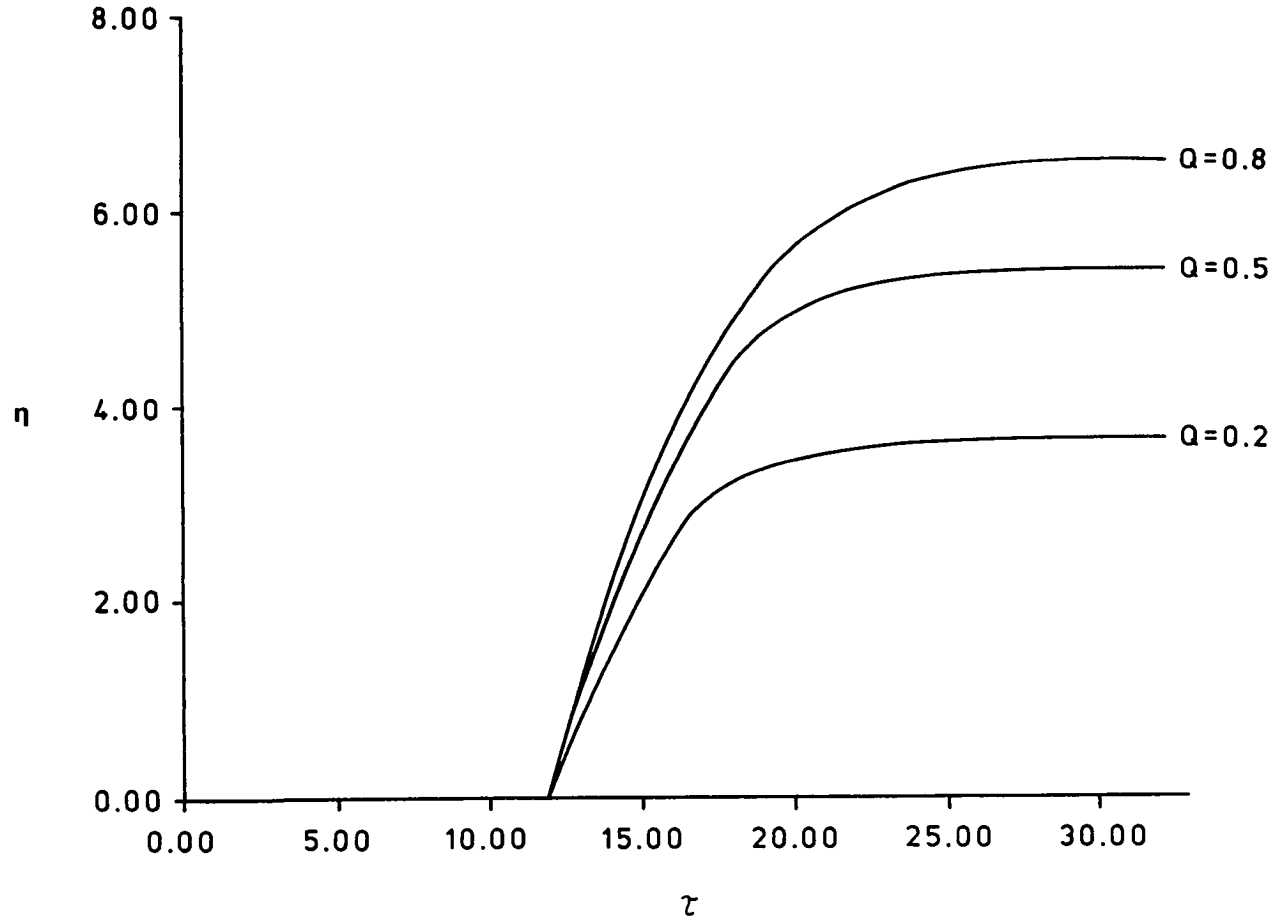

Figure 3.11. The change of the radius of the necrotic core for various values of the parameter Q (i.e. $Q = 0.2$, $Q = 0.5$, $Q = 0.8$). The values used for the other parameters are: $b = 0.4$, $\gamma = 0.4$, $\delta = 0.5$.

Conclusion: As the parameter b increases, the overall tumor growth increases. This means that an increase in b results in a decrease of the inhibitor concentration $\beta(r)$ (Figure 3.12) which in turn results in an increase of the growth of the mitotically active region due to the lack of enough inhibitor to reduce mitosis (see figures 3.12 through 3.17). From figure 3.16, the rate of change of the scaled inner radius ς is greater for small values of the parameter than for large values. This occurs due to the fact that there is greater concentration of inhibitor $\beta(r)$ for small values of b, and as a result, this concentration $\beta(r)$ reaches the critical level β_i nearer to the origin causing ς to reach a given radius faster.

4. The parameter δ:

Description of variables:

δ is the measure of the effect (if any) of non-zero inhibitor concentration on the nutrient consumption rate.

Constraints:

$$0 < \delta < 1$$

Table 3.4 lists values for the scaled radii at critical stages of the tumor growth for various values of the parameter δ.

TABLE 3.4

$\gamma = 0.4 \quad Q = 0.8 \quad b = 0.4$

δ	$\frac{\sigma_\infty}{\hat{\sigma}}$	$\frac{\sigma_i}{\hat{\sigma}}$	ξ	ρ	ς	η	End of
0.1	1.41	0.1	1.56	0.00	0.00	0.00	Phase I
	1.41	0.1	4.94	4.50	0.00	0.00	Phase II
	1.41	0.1	6.35	5.93	0.00	3.37	Phase III
	1.41	0.1	18.59	18.28	17.21	8.59	Phase IV (case I)
	8	10^{-6}	6.48	0.00	0.00	0.00	Phase I
	8	10^{-6}	20.50	17.40	0.00	0.00	Phase II
	8	10^{-6}	21.98	18.84	0.00	2.71	Phase III
	8	10^{-6}	67.22	64.72	64.03	15.47	Phase IV (case I)
	5.68	0.1	5.30	0.00	0.00	0.00	Phase I
	5.68	0.1	7.49	4.50	0.00	0.00	Phase II
	5.68	0.1	7.94	3.83	0.00	2.73	Phase III
	5.68	0.1	22.60		21.55	10.83	Phase IV (case II)
0.5	1.41	0.1	1.56	0.00	0.00	0.00	Phase I
	1.41	0.1	4.94	4.50	0.00	0.00	Phase II
	1.41	0.1	6.35	5.93	0.00	2.37	Phase III
	1.41	0.1	11.26	10.96	10.09	6.43	Phase IV (case I)
	8	10^{-6}	6.48	0.00	0.00	0.00	Phase I
	8	10^{-6}	20.50	17.40	0.00	0.00	Phase II
	8	10^{-6}	21.98	18.84	0.00	2.71	Phase III
	8	10^{-6}	37.86	36.93	36.79	15.29	Phase IV (case I)
	5.68	0.1	5.30	0.00	0.00	0.00	Phase I
	5.68	0.1	7.49	4.50	0.00	0.00	Phase II
	5.68	0.1	7.94	3.86	0.00	2.74	Phase III
	5.68	0.1	16.08		15.03	8.59	Phase IV (case II)
0.9	1.41	0.1	1.56	0.00	0.00	0.00	Phase I
	1.41	0.1	4.94	4.50	0.00	0.00	Phase II
	1.41	0.1	6.35	5.93	0.00	2.37	Phase III
	1.41	0.1	9.42	9.12	8.25	5.66	Phase IV (case I)
	8	10^{-6}	6.48	0.00	0.00	0.00	Phase I
	8	10^{-6}	20.50	17.40	0.00	0.00	Phase II
	8	10^{-6}	21.98	18.84	0.00	2.71	Phase III
	8	10^{-6}	30.13	29.21	29.07	13.15	Phase IV (case I)
	5.68	0.1	5.30	0.00	0.00	0.00	Phase I
	5.68	0.1	7.49	4.50	0.00	0.00	Phase II
	5.68	0.1	7.94	3.92	0.00	2.77	Phase III
	5.68	0.1	13.13		12.08	7.46	Phase IV (case II)

Table 3.4 Values for the scaled radii at critical stages of the tumor growth for various values of the parameter δ.

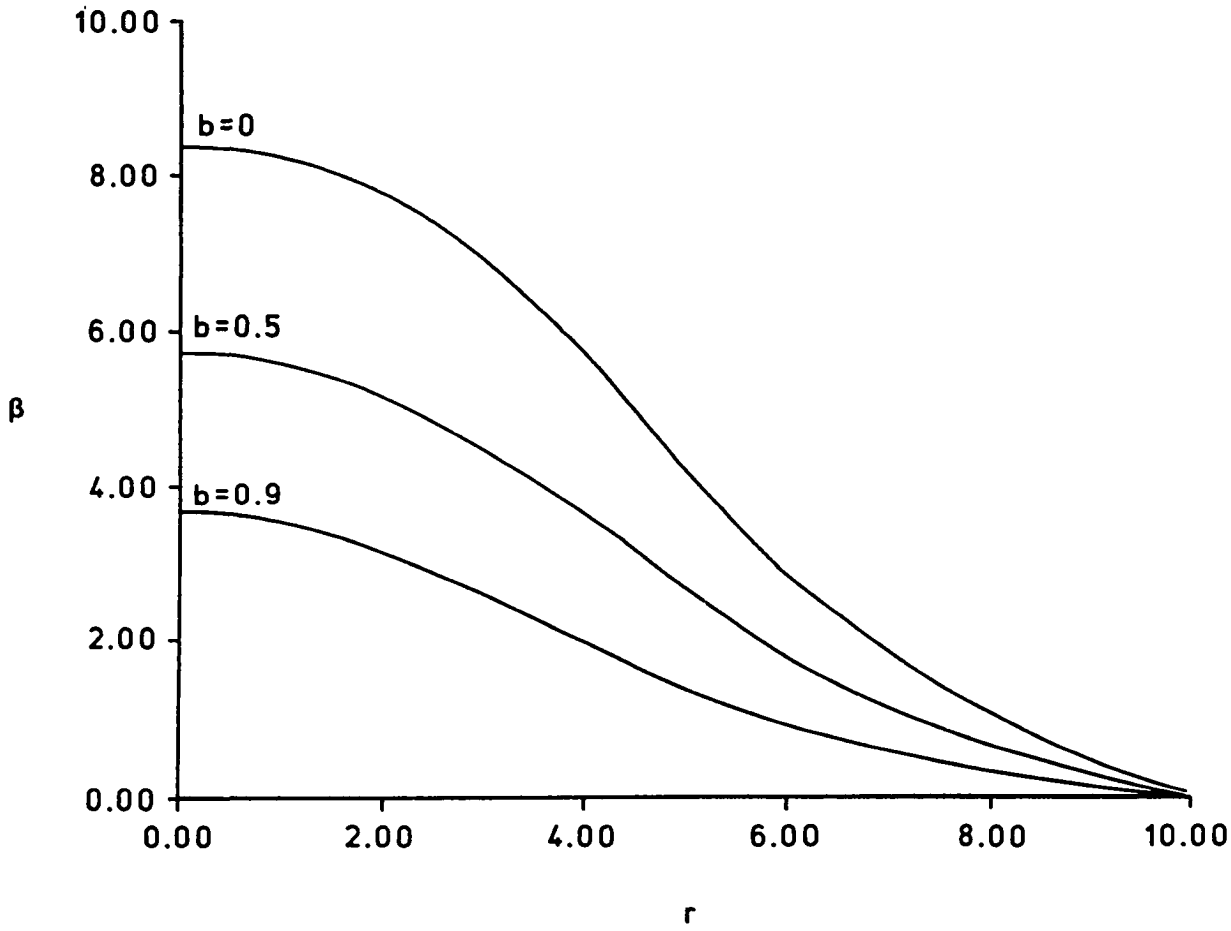

Figure 3.12. The change of the inhibitor concentration $\beta(r)$ as the parameter b takes on different values (i.e. $b = 0$, $b = 0.5$, $b = 0.9$).

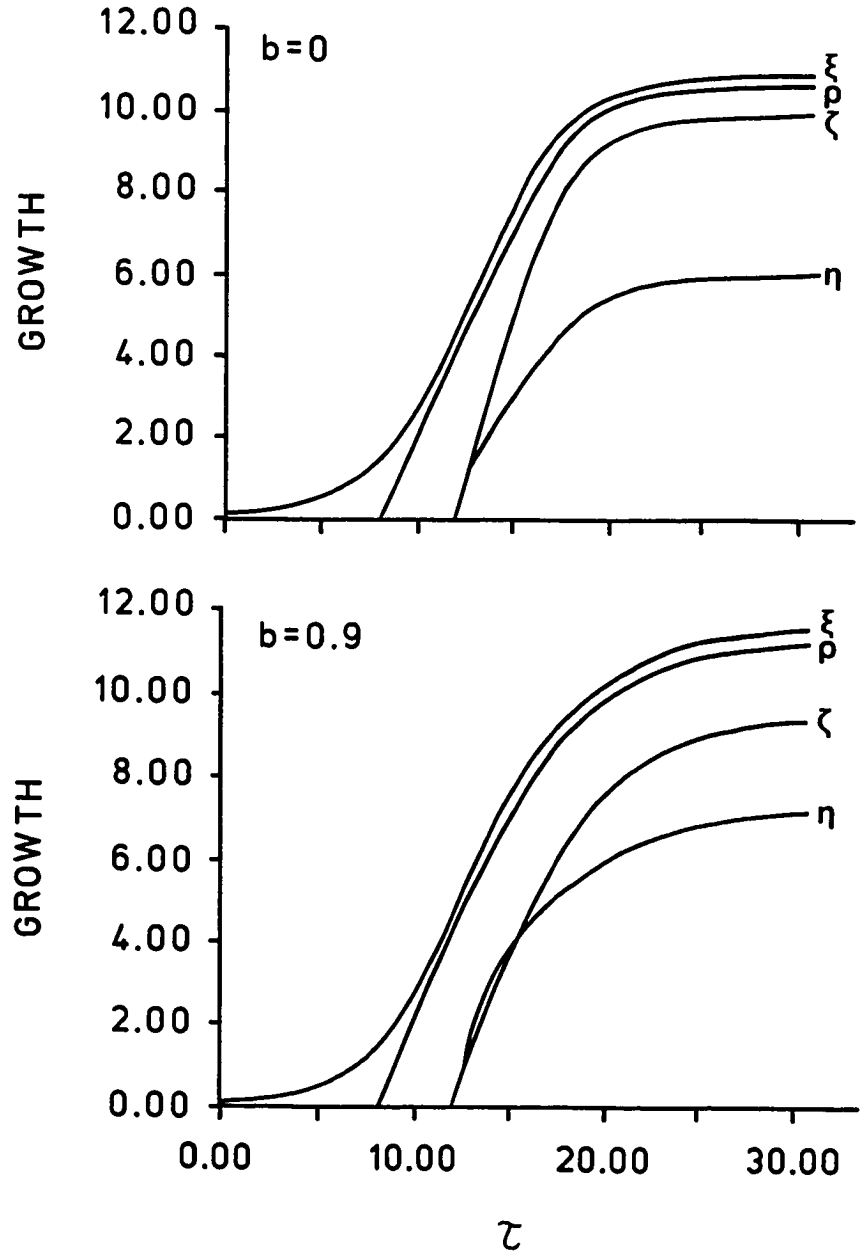

Figure 3.13. The full tumor growth pattern for different values of the parameter b (i.e. $b = 0$, $b = 0.9$). The values used for the other parameters are: $Q = 0.8$, $\gamma = 0.4$, $\delta = 0.5$.

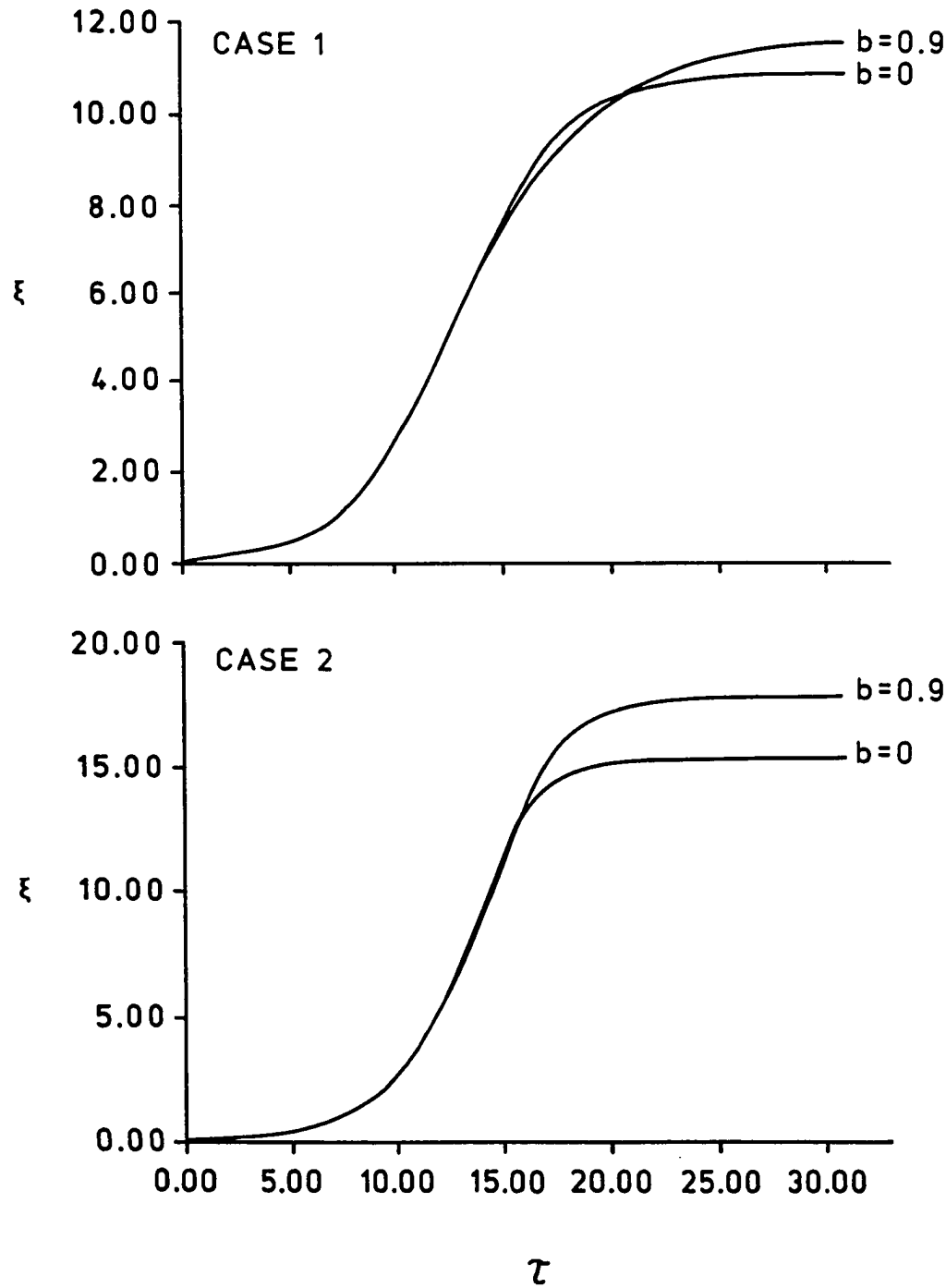

Figure 3.14. The change of the scaled outer tumor radius ξ as the parameter b changes (i.e. $b = 0$, $b = 0.9$ for both cases of phase IV of the growth development of the tumor). The values used for the other parameters are: $Q = 0.8$, $\gamma = 0.4$, $\delta = 0.5$ for both cases.

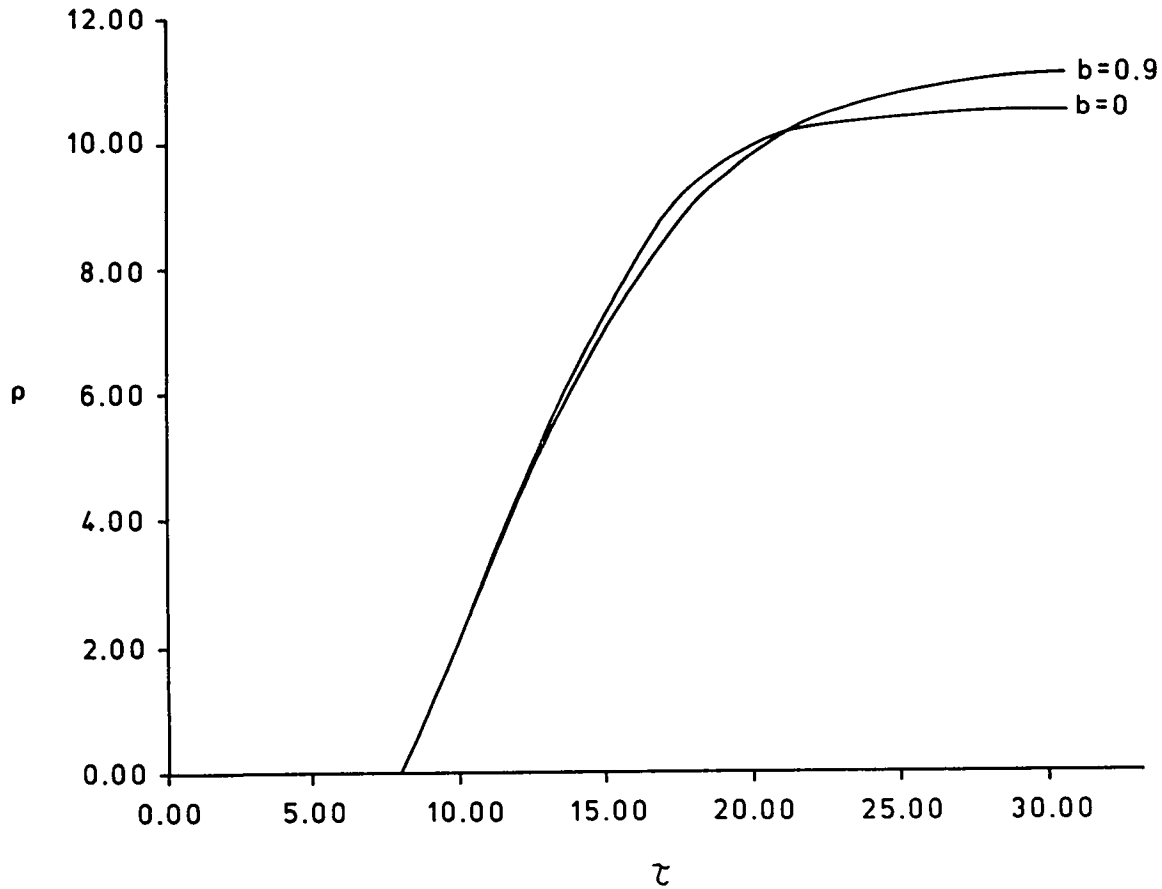

Figure 3.15. The change of the scaled inner radius ρ as the parameter b changes (i.e. $b = 0$, $b = 0.9$). The values used for the other parameters are: $Q = 0.8$, $\gamma = 0.4$, $\delta = 0.5$.

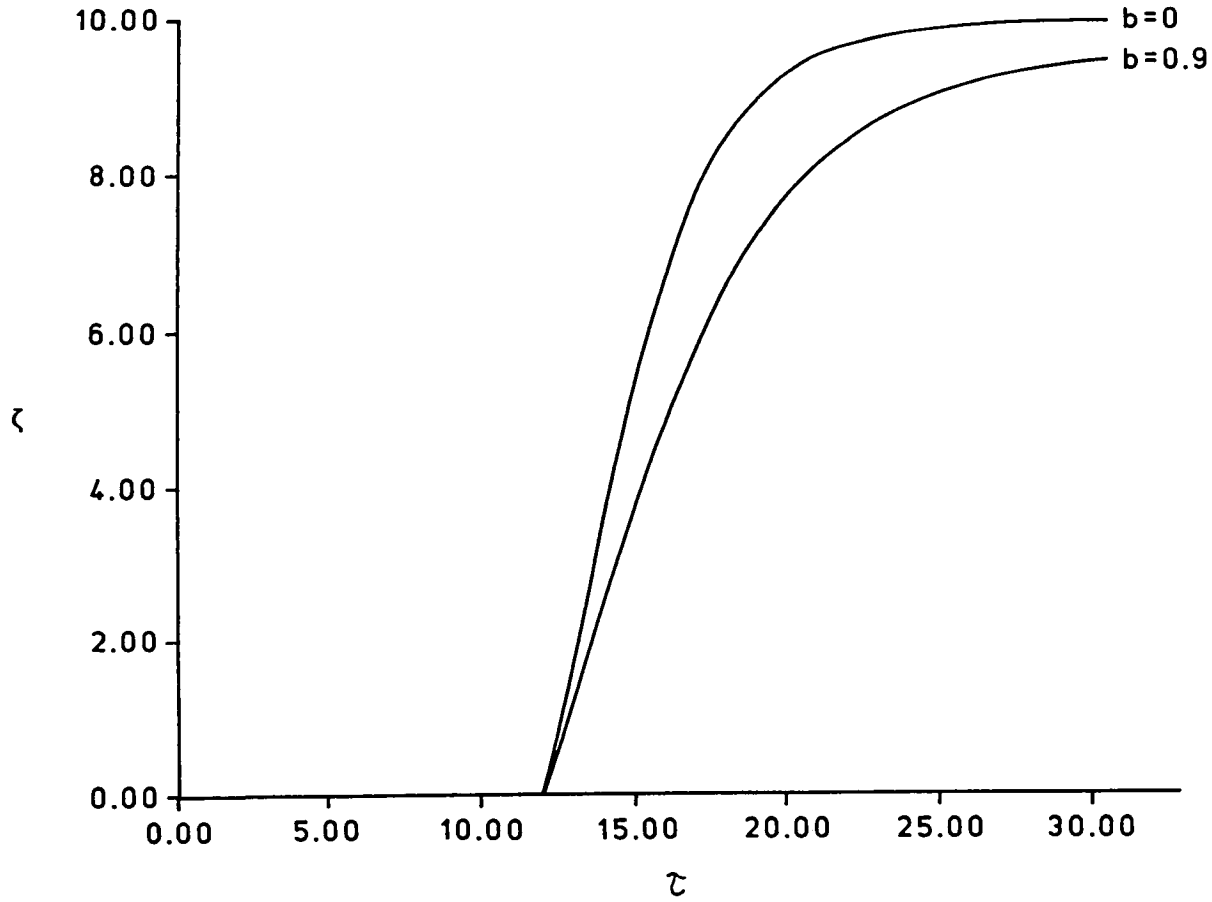

Figure 3.16. The change of the scaled inner radius ζ as the parameter b changes (i.e. $b = 0$, $b = 0.9$). The values used for the other parameters are: $Q = 0.8$, $\gamma = 0.4$, $\delta = 0.5$.

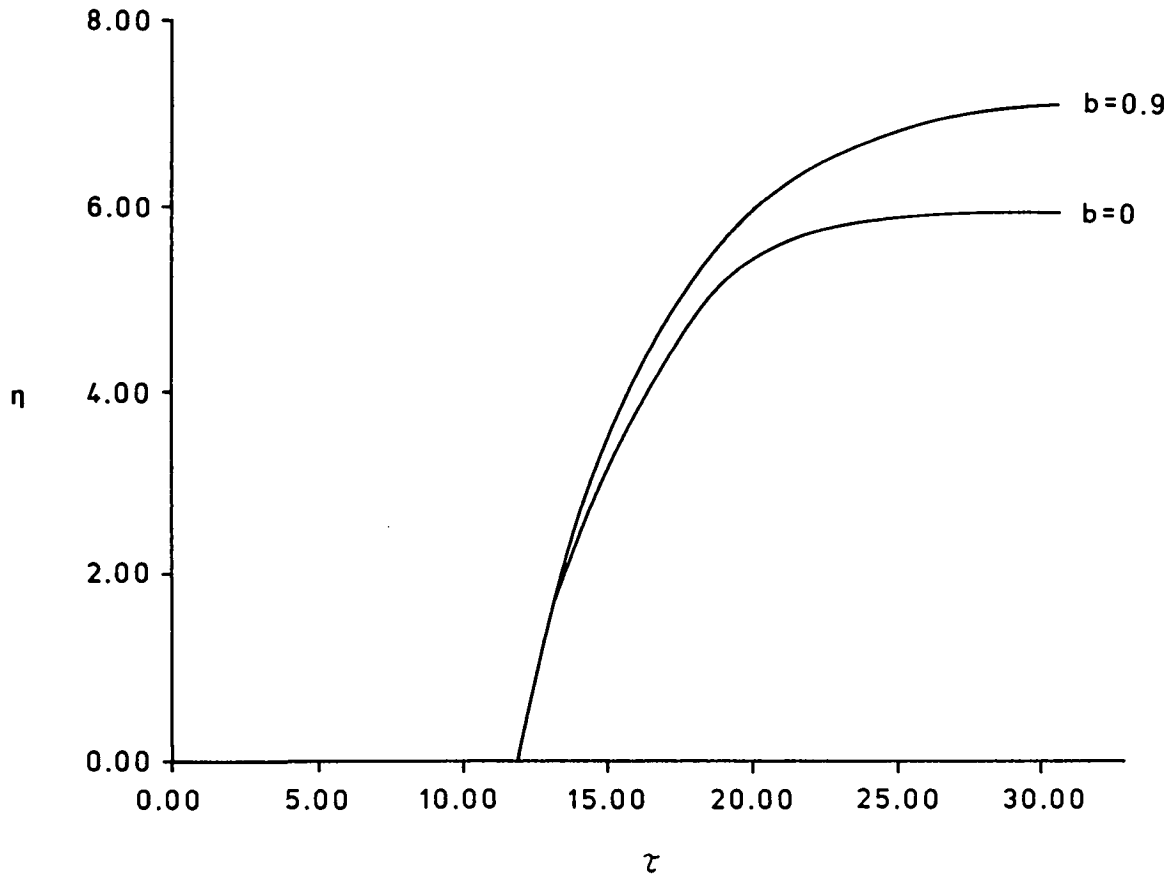

Figure 3.17. The change of the radius of the necrotic core η for various values of the parameter b (i.e. $b = 0$, $b = 0.9$). The values used for the other parameters are: $Q = 0.8$, $\gamma = 0.4$, $\delta = 0.5$.

Conclusion: As δ increases, the overall tumor growth decreases. This can be understood by noting that, as δ decreases, the concentration of nutrient $\sigma(r)$ decreases in the inhibited growth region ($R_i \leq r \leq R_g$) and in the mitotically active region ($R_g \leq r \leq \hat{R}$) (figure 3.18), but the flux of nutrient decreases in the inhibited growth region and increases in the mitotically active region (figure 3.19) causing the growth of the tissue to increase (see figures 3.18 through 3.24). From figures 3.23 and 3.24, initially, the rate of change of the scaled inner radii ς and η is greater for large values of δ than it is for small values. This occurs due to the fact that nutrient flux from the ambient medium is greater for small δ because more nutrient is "washed through" the system into the interior than for large δ.

The full growth pattern of the tumor for various values of the parameters γ, Q, b, and δ is shown in figures 3.2, 3.7, 3.13 and 3.20 respectively, while the change of the scaled outer tumor radius ξ and the change of the scaled radius of the necrotic core η as the above parameters take on different values is shown in figures 3.3, 3.8, 3.14, and 3.21 (for ξ), 3.6, 3.11, 3.17, and 3.24 (for η) respectively. Figures 3.4, 3.9, 3.15, and 3.22 show the change in the inner scaled radius ρ (the radius at which the concentration of nutrient $\sigma(r) = \hat{\sigma}$, the critical concentration) as the parameters γ, Q, b, and δ change respectively, and figures 3.5, 3.10, 3.16, and 3.23 show the change of the scaled inner radius ς (the radius at which the concentration of inhibitor ($\beta(r) = \beta_i$) as the above parameters are varied respectively.

These various parameters that determine the growth pattern of the present model could be prescribed by clinical or experimental data (Appendix II, King et

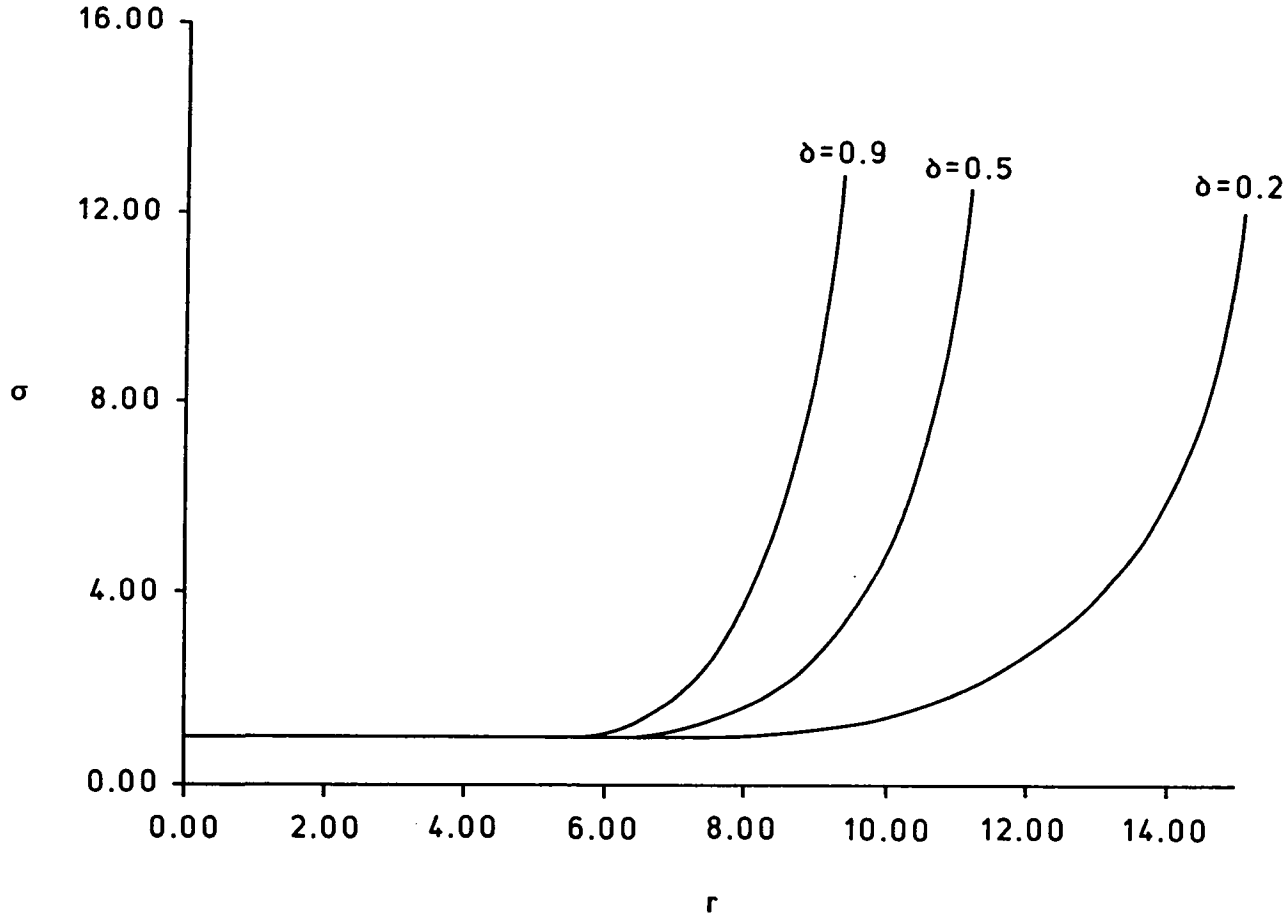

Figure 3.18. The change of the nutrient concentration $\sigma(r)$ as the values of the parameter δ are varied (i.e. $\delta = 0.2$, $\delta = 0.5$, $\delta = 0.9$).

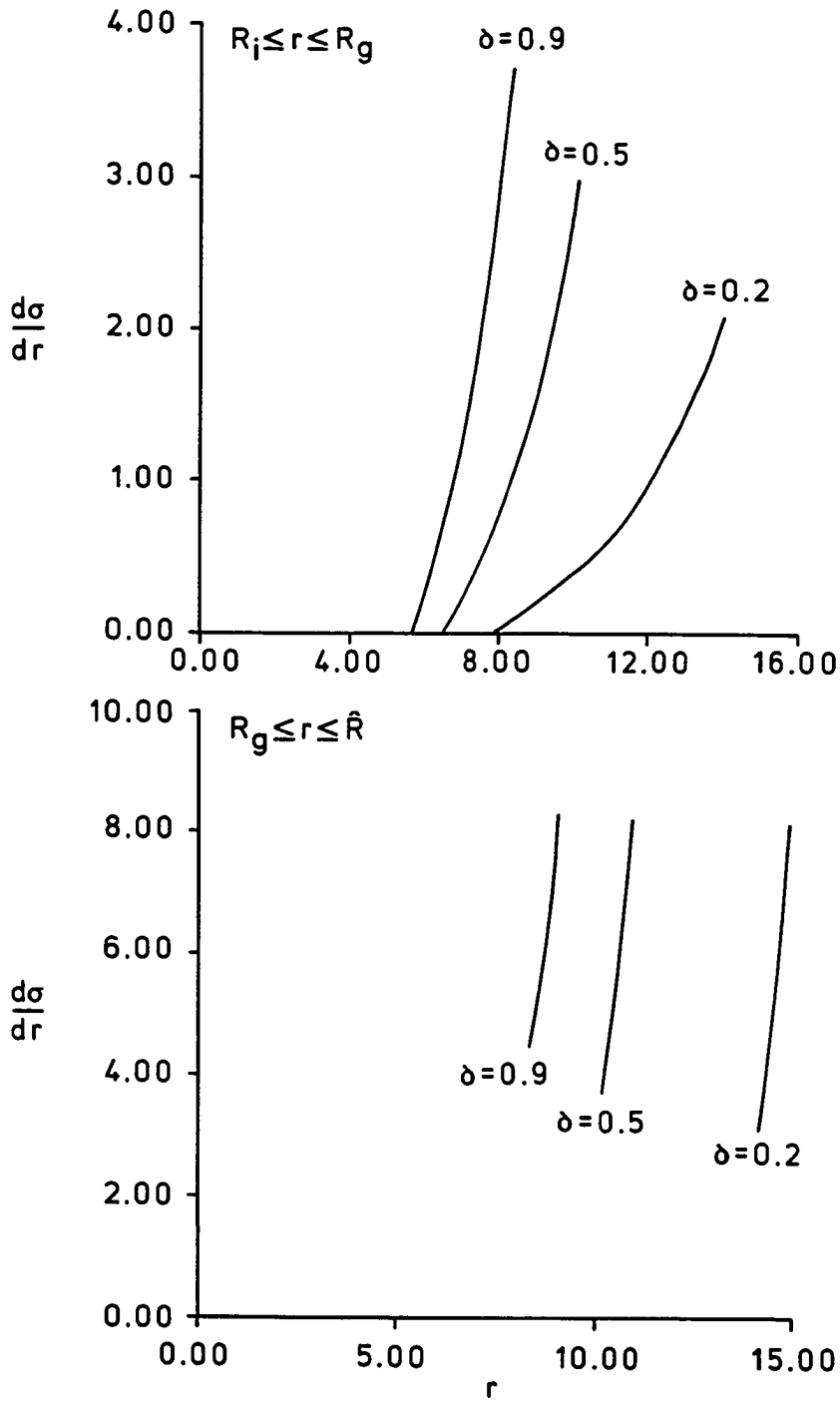

Figure 3.19. The change of the nutrient flux $\frac{d\sigma}{dr}$ in the inhibited growth region $(R_i \leq r \leq R_g)$ and in the mitotically active region $(R_g \leq r \leq \hat{R})$ as the values of the parameter δ are varied (i.e. $\delta = 0.2$, $\delta = 0.5$, $\delta = 0.9$).

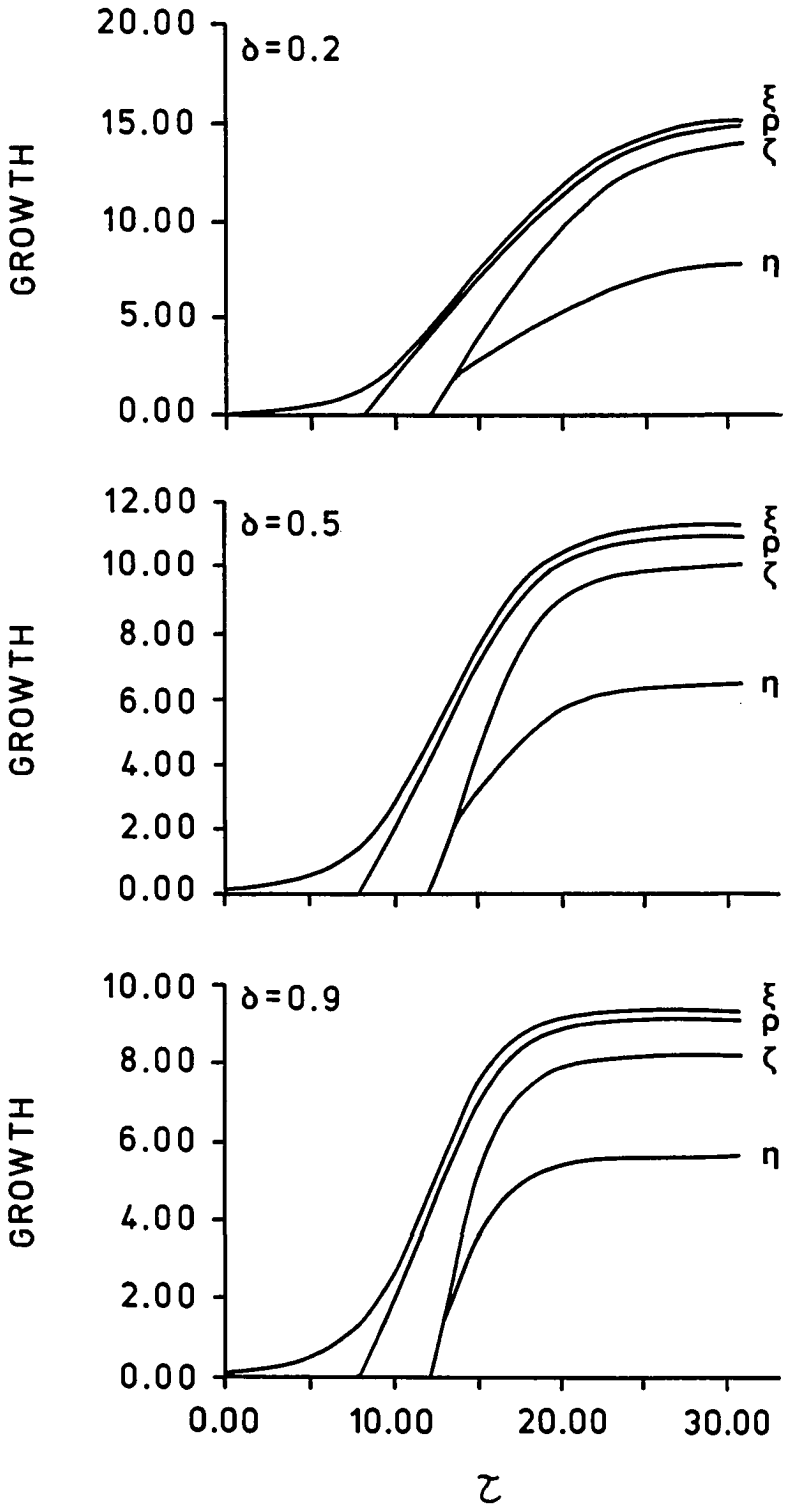

Figure 3.20. The full tumor growth pattern for different values of the parameter δ (i.e. $\delta = 0.2$, $\delta = 0.5$, $\delta = 0.9$). The values used for the other parameters are: $Q = 0.8$, $\gamma = 0.4$, $b = 0.4$.

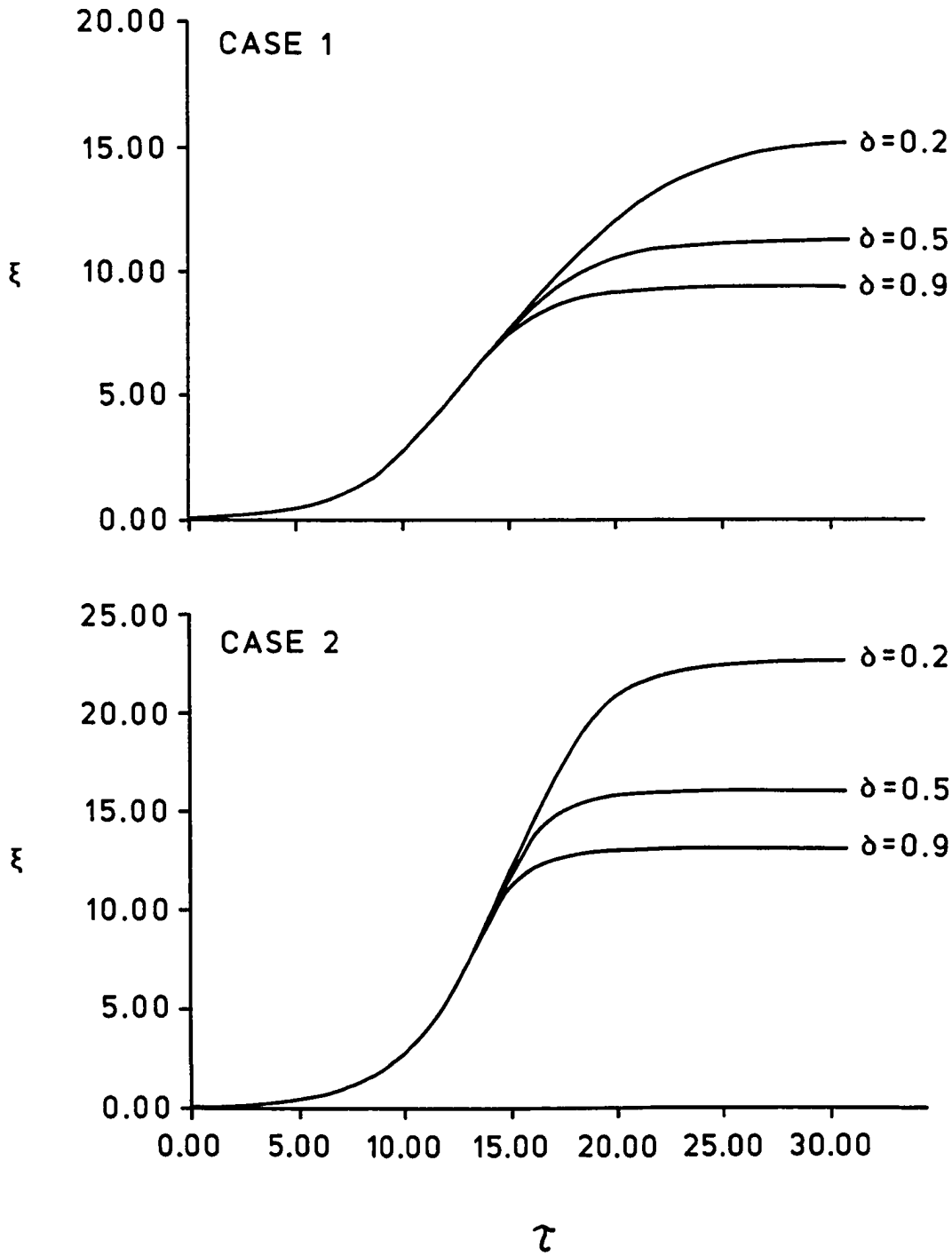

Figure 3.21. The change of the scaled outer tumor radius ξ as the parameter changes (i.e. $\delta = 0.2$, $\delta = 0.5$, $\delta = 0.9$ for both cases of phase IV of the growth development of the tumor). The values used for the other parameters are: $Q = 0.8$, $b = 0.4$, $\gamma = 0.4$ for both cases.

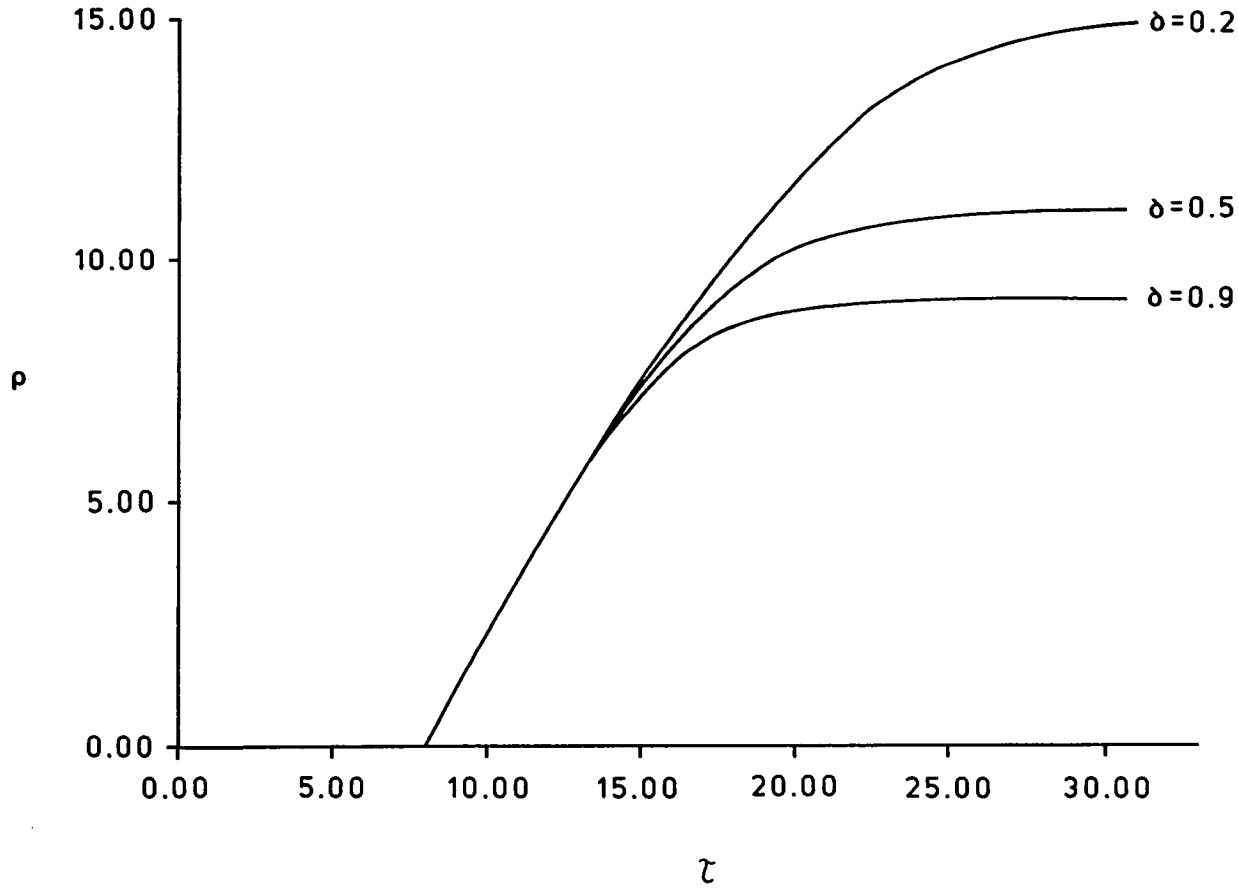

Figure 3.22. The change of the scaled inner radius ρ as the parameter δ changes (i.e. $\delta = 0.2$, $\delta = 0.5$, $\delta = 0.9$). The values used for the other parameters are: $Q = 0.8$, $\gamma = 0.4$, $b = 0.4$.

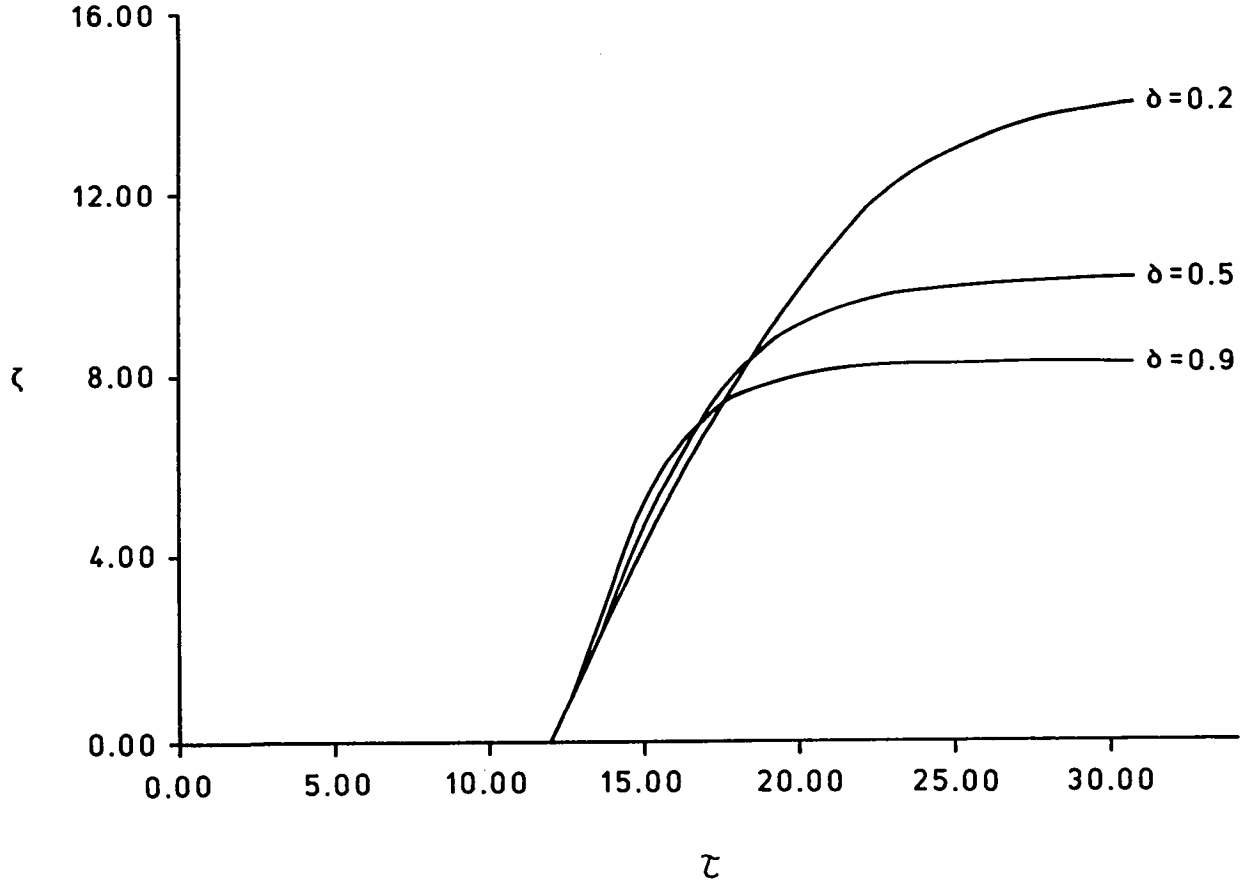

Figure 3.23. The change of the scaled inner radius ζ for different values of the parameter δ (i.e. $\delta = 0.2$, $\delta = 0.5$, $\delta = 0.9$). The values used for the other parameters are: $Q = 0.8$, $\gamma = 0.4$, $b = 0.4$.

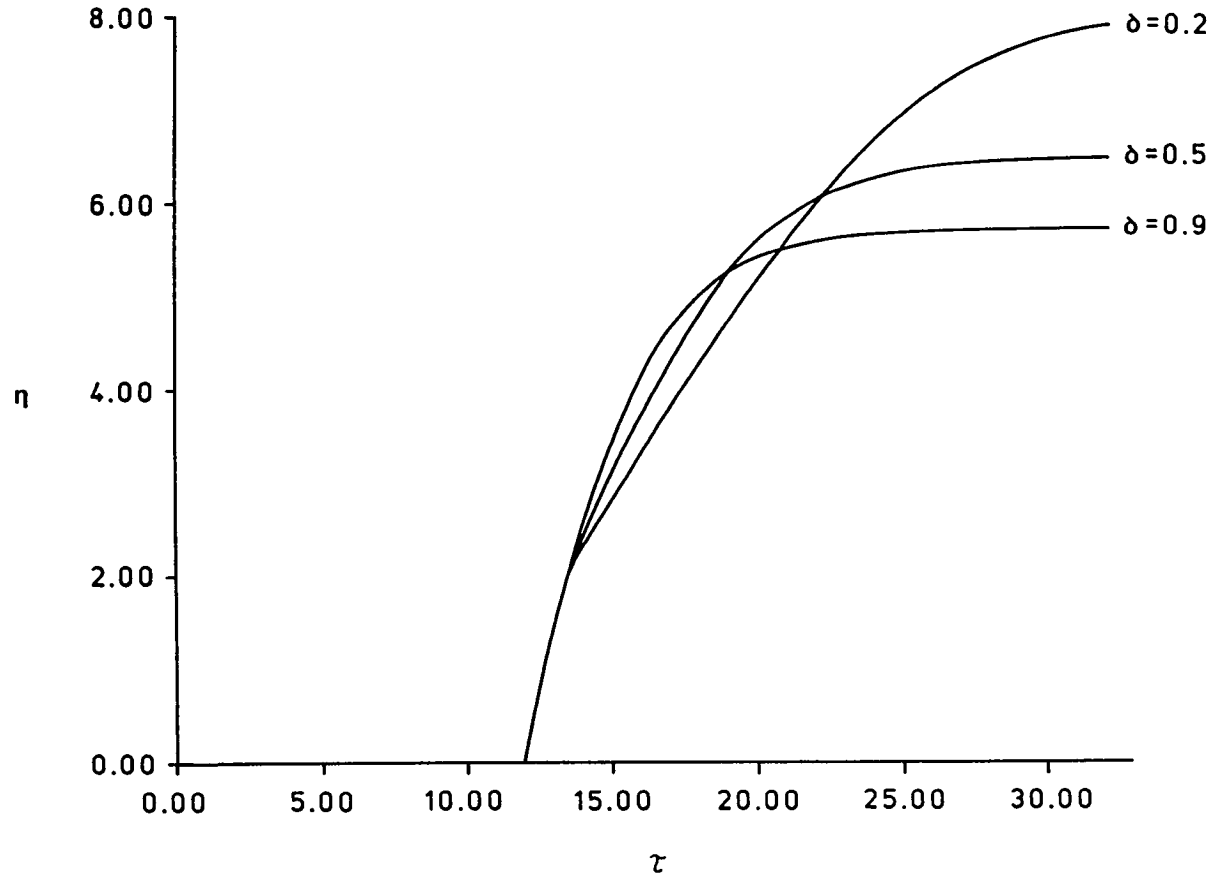

Figure 3.24. The change of the radius of the necrotic core η for various values of the parameter δ (i.e. $\delta = 0.2$, $\delta = 0.5$, $\delta = 0.9$). The values used for the other parameters are: $Q = 0.8$, $\gamma = 0.4$, $b = 0.4$.

al., 1986, 1988; Schultz & King, 1986) to provide important knowledge in understanding the basic biological mechanisms of tumor growth and consequently offer useful material to other areas within medical sciences.

Chapter 4

The Effects of Growth Inhibitor on the Stability of Tissue Growth

In this chapter, two spherically symmetric time-independent diffusion models are constructed which examine different source distributions of growth inhibitor production. The first model posits that inhibition is due to necrotic waste diffusing into the surrounding region of living cells; in the second model the source of inhibition is taken to be a by-product of processes occuring within the region of living cells.

The additional assumption is made that the growth inhibitor is produced at uniform rates within the necrotic core for the former model and by the living cells for the latter. In practice, a combination of these and possibly other mechanisms, such as nutrient depletion, may be responsible for growth retardation in the prevascular stage of growth.

4.1 The Growth Inhibitor as a Product of Necrosis (Model I)

4.1.1 Formulation of the Model

The necrotic debris is assumed to be the source of the growth inhibitor in this model. As in Burton (1966) and Greenspan (1972), it is assumed that the solid tumor is a sphere of radius R and that the concentration of growth inhibitor, $\beta(r)$, depends only on the radial distance, r, from the center of the sphere. The diffusion equation that determines this local concentration of inhibitor produced by the dead cells is given by

$$\frac{\partial \beta}{\partial t} = K\nabla^2\beta - C\beta + PS(r). \qquad (4.1.1.1)$$

K is the diffusion coefficient, C is the decay or depletion constant, and P is the inhibitor production rate (molecules per unit volume per second). The source term $S(r)$ is defined by (see Figure 4.1)

$$S(r) = \begin{cases} 1, & 0 \leq r \leq R_i \\ 0, & R_i \leq r \leq R \end{cases}$$

and is indicative of uniform production of inhibitor within the necrotic core of radius R_i $(r \leq R_i)$. Note that $r = R$ defines the entire surface of the tissue. This system corresponds to inhibitor with local concentration $\beta(r)$ produced within the

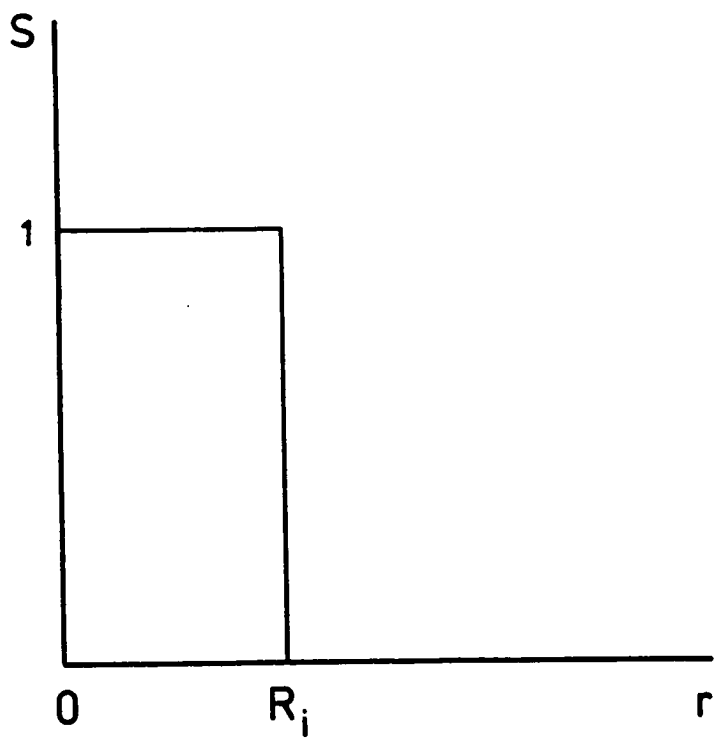

Figure 4.1. The radial dependence of the source term used in the diffusion equation for Model I.

necrotic core $r \leq R_i$ at a constant rate P, diffusing with a diffusion coefficient K, and being depleted throughout the tissue at a rate $-C\beta$. Since the diffusion time for multicellular spheroids is small (of the order of minutes) compared to their growth time (of the order of days), we may consider the tissue size to be stationary and compute the steady state distribution of growth inhibitor by setting the time derivative equal to zero. The system to be solved is therefore

$$-\frac{K}{r^2}\frac{d}{dr}\left[r^2\frac{d\beta}{dr}\right] + C\beta(r) = \begin{cases} P, & 0 \leq r \leq R_i \\ 0, & R_i \leq r \leq R \end{cases} \qquad (4.1.1.2)$$

subject to the conditions that

(i) $\beta(r)$ be bounded at the origin;

(ii) $\beta(r)$ and $\dfrac{d\beta}{dr}$ are continuous at $r = R_i$;

(iii) at steady state, the flux inside the tissue at the boundary $r = R$ is equal to the leakage flux, i.e. $K\dfrac{d\beta}{dr} + D\beta(r) = 0$.

(D is the permeability of the tissue surface).

Let $u = r\beta(r)$. Then the above system (4.1.1.2) is reduced to:

$$\frac{d^2u}{dr^2} - \frac{C}{K}u(r) = \begin{cases} \dfrac{P}{K}r & , \quad 0 \leq r \leq R_i \\ 0 & , \quad R_i \leq r \leq R, \end{cases} \qquad (4.1.1.3)$$

whence

$$u(r) = A_1 \cosh Mr + A_2 \sinh Mr + \frac{P}{C}r, \quad 0 \leq r \leq R_i$$

and

$$u(r) = B_1 \cosh Mr + B_2 \sinh Mr, \quad R_i \leq r \leq R.$$

Thus,

$$\begin{aligned}
\beta(r) &= \frac{A_1}{r} \cosh Mr + \frac{A_2}{r} \sinh Mr + \frac{P}{C}, \quad 0 \leq r \leq R_i \\
\beta(r) &= \frac{B_1}{r} \cosh Mr + \frac{B_2}{r} \sinh Mr, \quad R_i \leq r \leq R.
\end{aligned}$$

The arbitrary constants A_1, A_2, B_1, B_2 are evaluated by applying the boundary conditions to get

$$A_1 = 0$$

$$\begin{aligned}
A_2 &= -\frac{P}{RR_iX}\left\{\left[M - \frac{1}{MRR_i} + \frac{1}{\psi R_i}\right] \sinh M(R - R_i)\right. \\
&+ \left.\left[\frac{M}{\psi} - \frac{1}{R} + \frac{1}{R_i}\right] \cosh M(R - R_i)\right\}
\end{aligned}$$

$$\begin{aligned}
B_1 &= \frac{P}{RR_i^2X}\left\{[\sinh MR_i - MR_i \cosh MR_i] \times\right. \\
&\left.\times \left[\left(\frac{1}{MR} - \frac{1}{\psi}\right) \sinh MR - \cosh MR\right]\right\}
\end{aligned}$$

$$\begin{aligned}
B_2 &= -\frac{P}{RR_i^2X}\left\{[\sinh MR_i - MR_i \cosh MR_i] \times\right. \\
&\left.\left[\left(\frac{1}{MR} - \frac{1}{\psi}\right) \cosh MR - \sinh MR\right]\right\}
\end{aligned}$$

where

$$X = \frac{C}{R^2 R_i^2 \psi}[\psi MR\cosh MR + MR\sinh MR - \psi\sinh MR]$$

Thus, the corresponding solution to the system (4.1.1.2) is:

$$\beta(r) = \frac{P}{C}\left\{1 - \frac{\mu\sinh Mr}{M^2 Rrn\sinh MR}\right\}, \quad 0 \le r \le R_i \tag{4.1.1.4}$$

and

$$\beta(r) = \frac{P\psi\nu\kappa}{CrMn\sinh MR}, \quad R_i \le r \le R, \tag{4.1.1.5}$$

where

$$\mu = (M^2 RR_i\psi - \psi + MR)\sinh M(R - R_i)$$
$$+(M^2 RR_i - MR_i\psi + MR\psi)\cosh M(R - R_i) \tag{4.1.1.6}$$

$$\nu = \left(\frac{1}{MR} - \frac{1}{\psi}\right)\sinh M(R - r) - \cosh M(R - r) \tag{4.1.1.7}$$

$$n = \psi\left(\coth MR - \frac{1}{MR}\right) + 1 \tag{4.1.1.8}$$

$$\kappa = \sinh MR_i - MR_i\cosh MR_i \tag{4.1.1.9}$$

$$M = (C/K)^{1/2} \tag{4.1.1.10}$$

$$\psi = \frac{(CK)^{1/2}}{D}. \tag{4.1.1.11}$$

4.1.2 Regions of Stability

As in Shymko and Glass (1976) , it is assumed that mitosis is controlled by a discontinuous switch-like mechanism. This means that if in any region within the tumor the concentration of growth inhibitor $\beta(r)$ is less than a critical value θ, mitosis occurs within that region. On the other hand, if the concentration is greater than or equal to θ mitosis is inhibited. Stable tissue growth is reached when mitosis is completely inhibited throughout the tissue. The tissue growth will, therefore, be stable in the domain for which

$$\beta(R) \geq \theta\,, \tag{4.1.2.1}$$

where

$$\beta(R) = \frac{P\psi[MR_i \cosh MR_i - \sinh MR_i]}{CMR \sinh MR[\psi(\coth MR - \frac{1}{MR}) + 1]}\,.$$

However, in many mammalian tissues, in some tissue cultures and in cancerous tissue, growth is never completely inhibited. For these cases, a peripheral mitotic zone will exist even at the stable tissue size. Let W be the width of this mitotic zone overlaying the necrotic core of radius R_i, then $R_i = R - W$ and (4.1.2.1) becomes

$$\frac{P\psi[M(R-W)\cosh M(R-W) - \sinh M(R-W)]}{CMR \sinh MR[\psi(\coth MR - \frac{1}{MR}) + 1]} \geq \theta \tag{4.1.2.2}$$

If

$$\omega = \frac{PK}{D^2\theta}$$

then

$$\frac{P}{C\theta} = \frac{\omega}{\psi^2}$$

and (4.1.2.2) can be written as

$$\begin{aligned} &\omega\left\{\left(1-\tfrac{W}{R}\right)\left[\coth MR\cosh MW-\sinh MW\right]\right. \\ &\left.-\tfrac{1}{MR}\left[\cosh MW-\coth MR\sinh MW\right]\right\} \\ &\geq \psi+\psi^2\left(\coth MR-\tfrac{1}{MR}\right). \end{aligned} \tag{4.1.2.3}$$

If we further assume that W is proportional to R, i.e. $W = \alpha R$, $0 < \alpha < 1$ then (4.1.2.3) yields

$$\begin{aligned} &\omega\{(1-\alpha)[\coth MR\cosh \alpha MR-\sinh \alpha MR] \\ &-\tfrac{1}{MR}[\cosh \alpha MR-\coth MR\sinh \alpha MR]\} \\ &\geq \psi+\psi^2\left(\coth MR-\tfrac{1}{MR}\right). \end{aligned} \tag{4.1.2.4}$$

Figure (4.2) shows the graph of the equality in (4.1.2.4) ($\beta(R) = \theta$) for different values of α. The regions of stability are the intervals on the R axis for which

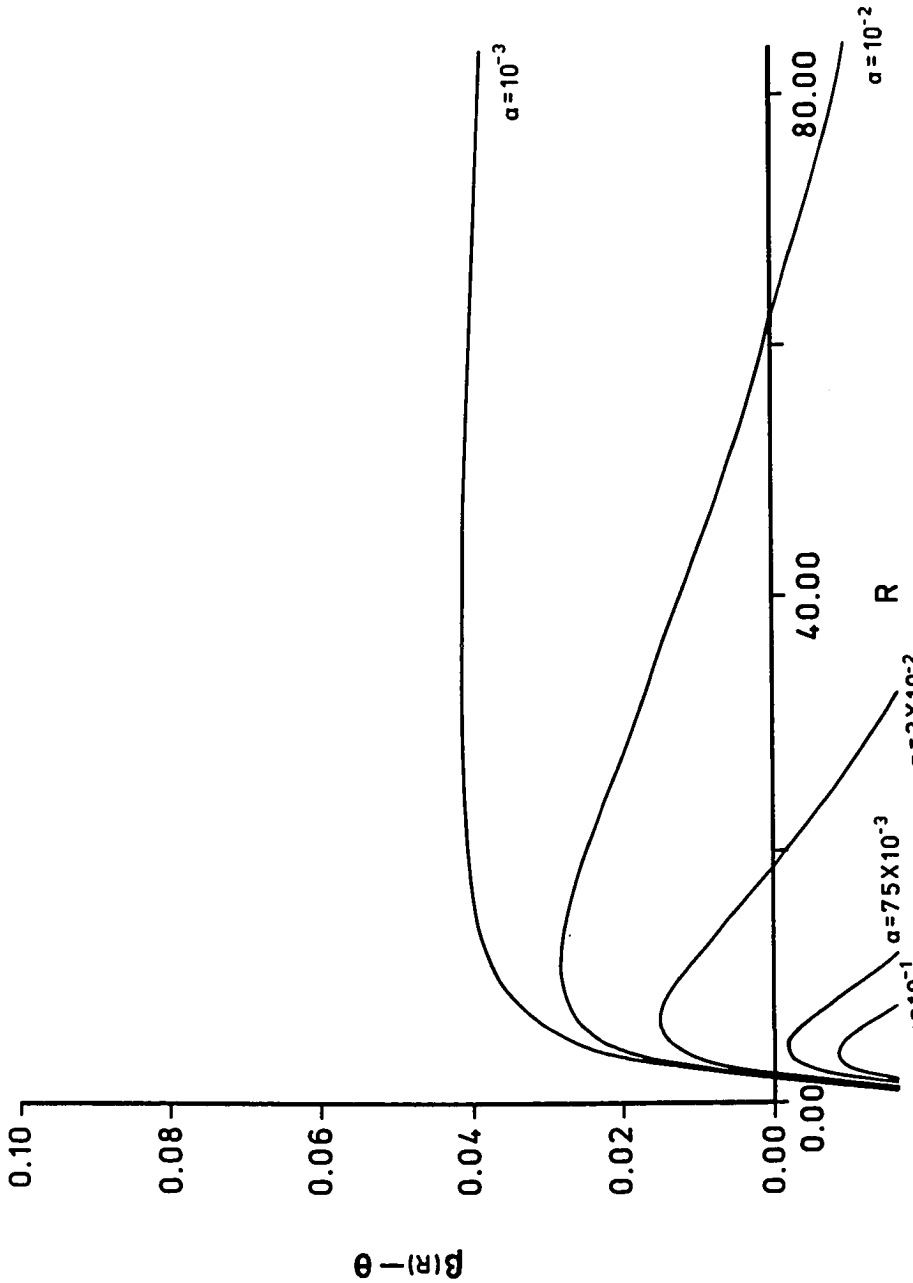

Figure 4.2. Stability diagram based on the inequality (4.1.2.4) for $\psi = 0.05$, $\omega = 0.1$, $M = 10cm^{-1}$ and different values of α (Model I).

$\beta(R) - \theta \geq 0$. The values used for M, ψ, and ω are: $M = 10cm^{-1}, \psi = 0.05$ and $\omega = 0.1$ which are the same as those used in Shymko and Glass (1976). The results from this figure show that as α increases, $W = \alpha R$ increases for given R, and hence the mitotically active region grows causing the system to become less stable.

Note that if R is small enough for given α the growth of the spheroid is unstable until the limiting size $R = R_1$ is reached. If $R > R_2$ initially, growth is limitless (see Figure 4.3). The dependence of the domain of stability ΔR on α is schematically indicated in Figure 4.4.

4.1.3 The Limiting Peripheral Width W_{L_1}

Some further analysis is of interest in this model. To find the *limiting* peripheral width W_{L_1}, which is the size of the peripheral mitotic zone at the time that stability is reached (if it is), the equation $\beta(R - W_{L_1}) = \theta$ must be solved for W_{L_1} as $R \to \infty$.

$$\beta(R - W_{L_1}) = \frac{P\psi[\sinh M(R - W_{L_1}) - M(R - W_{L_1})\cosh M(R - W_{L_1})]}{CM(R - W_{L_1})\sinh MR[\psi(\coth MR - \frac{1}{MR}) + 1]} \times \times \left[(\frac{1}{MR} - \frac{1}{\psi})\sinh MW_{L_1} - \cosh MW_{L_1}\right]$$

as $R \to \infty$,

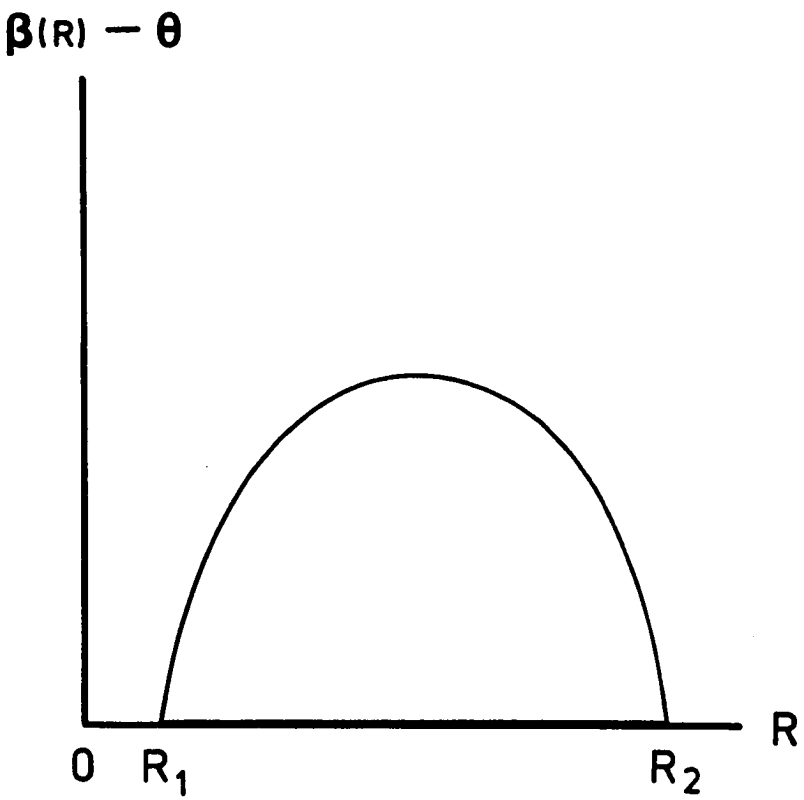

Figure 4.3. The domain of stability (Model I).

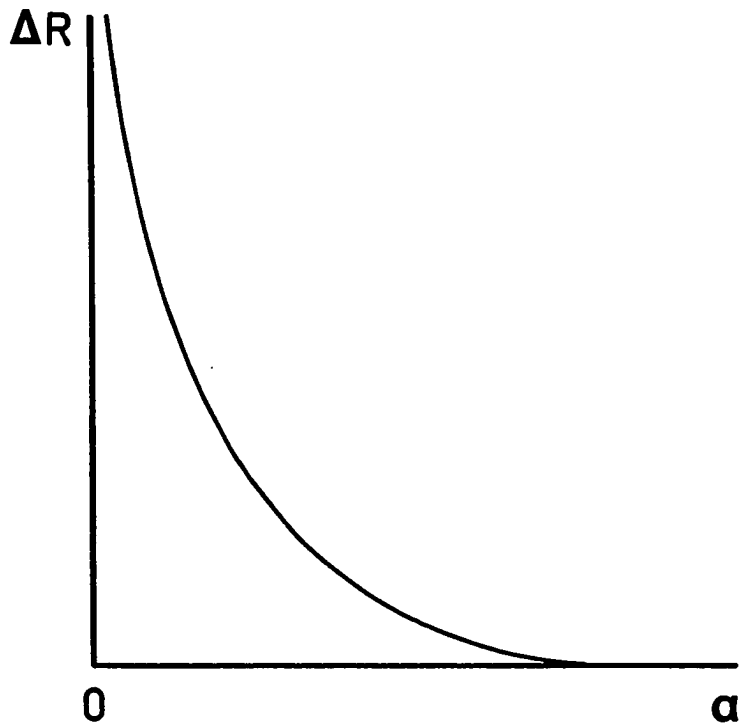

Figure 4.4. The dependence of the domain of stability on α (Model I).

$$\beta(R-W_{L_1}) = \frac{P\psi}{CM}\left\{-\frac{M(\cosh MW_{L_1}-\sinh MW_{L_1}}{\psi+1}\times \right.$$
$$\left.\times\left(-\frac{1}{\psi}\sinh MW_{L_1}-\cosh MW_{L_1}\right)\right\}$$

or

$$\frac{P(\psi-1)e^{-2MW_{L_1}}}{2C(\psi+1)}+\frac{P}{2C}=\theta\,. \qquad (4.1.3.1)$$

Recall that $\frac{P}{C\theta}=\frac{\omega}{\psi^2}$, and (4.1.3.1) now becomes

$$e^{-2MW_{L_1}}+\frac{\psi+1}{\psi-1}=\frac{2\psi^2(\psi+1)}{\omega(\psi-1)}\,.$$

Thus,

$$W_{L_1}=-\frac{1}{2M}\ln\left[\frac{(\psi+1)(2\psi^2-\omega)}{\omega(\psi-1)}\right]\,. \qquad (4.1.3.2)$$

The graph of W_{L_1} as a function of ω for given ψ is shown in Figure 4.5. An increase in the inhibitor production rate P results in an increase in ω. This generates more mitotically inactive tissue which results in a decrease of W_{L_1}. Note that an increase in the diffusion coefficient K or a decrease in either the permeability D of the tissue surface or in the critical value θ of the inhibitor concentration

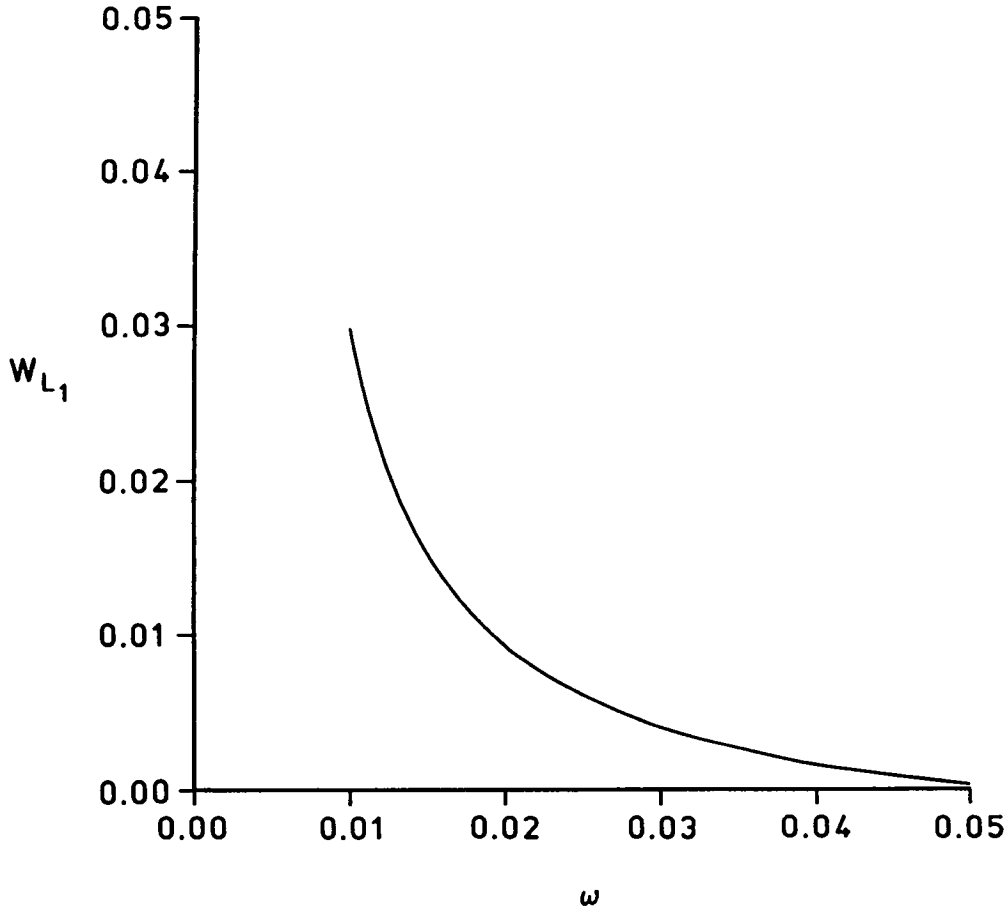

Figure 4.5. The behavior of the limiting peripheral width (Model I).

(or both) may also result in an increase in ω. The data used to graph W_{L_1} is again taken from Shymko and Glass (1976) (i.e $\psi = 0.05$, $M = 10cm^{-1}$, $0.01 \leq \omega \leq 0.1$). In what follows, we investigate the domains of ψ and ω. Appropriate values must be given to these parameters so that W_{L_1} is defined (i.e. > 0), and at the same time no "catastrophic" behavior of W_{L_1} occurs. Catastrophic behavior of W_{L_1} occurs when

$$\frac{(\psi+1)(2\psi^2-\omega)}{\omega(\psi-1)} \to 0$$

i.e. as

$$\omega \to (2\psi^2)^-.$$

W_{L_1} is defined i.e. (> 0), when

$$0 < \frac{(\psi+1)(2\psi^2-\omega)}{\omega(\psi-1)} < 1, \tag{4.1.3.3}$$

which implies that

$$2\psi^2 < \omega < \psi^2 + \psi, \quad \psi < 1 \tag{4.1.3.4}$$

or

$$\psi^2 + \psi < \omega < 2\psi^2, \quad \psi > 1. \tag{4.1.3.5}$$

Clearly, for $\psi > 0$,

$$\psi^2 + \psi > 2\psi^2 \quad \text{if and only if} \quad \psi < 1$$

and

$$\psi^2 + \psi < 2\psi^2 \quad \text{if and only if} \quad \psi > 1.$$

4.2 The Growth Inhibitor as a Product of Waste From Living Cells (Model II)

4.2.1 Formulation of the Model

In this second model, no inhibition is associated with necrosis. The metabolic processes of living cells are assumed to be the source of the chemical inhibitor. This, by implication, defines the existence of an "inert" necrotic core.

The local concentration $\beta(r)$ of growth inhibitor produced by the living cells is described by the same diffusion equation (4.1.1.1) and boundary conditions and is subject to the same assumptions as the local concentration of growth inhibitor in Model I. The source term $S(r)$ now is defined by (See Figure 4.6)

$$S(r) = \begin{cases} 0, & 0 \le r \le R_i \\ 1, & R_i \le r \le R. \end{cases}$$

The system to be solved is therefore

$$-\frac{K}{r^2}\frac{d}{dr}\left[r^2\frac{d\beta}{dr}\right] + C\beta(r) = \begin{cases} 0, & 0 \le r \le R_i \\ P, & R_i \le r \le R \end{cases} \qquad (4.2.1.1)$$

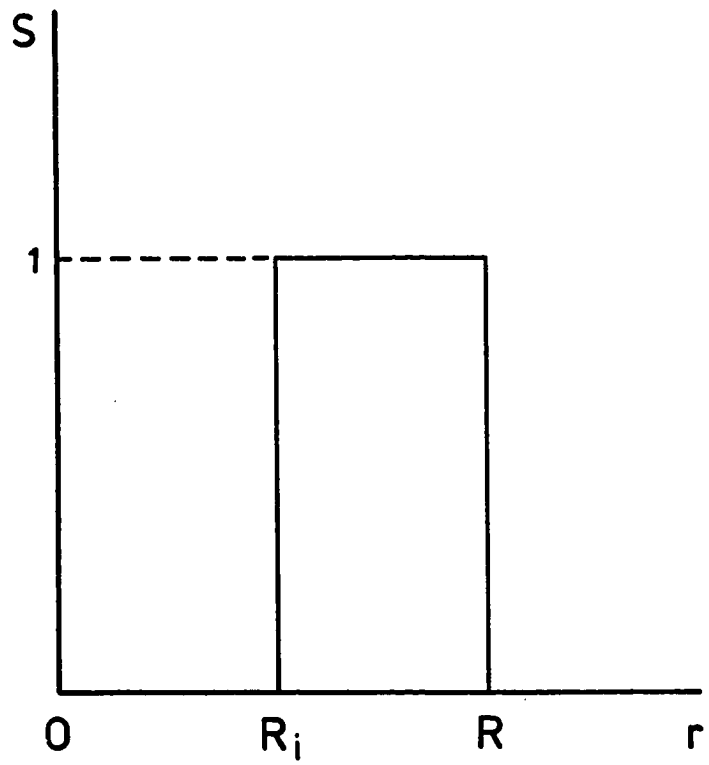

Figure 4.6. The radial dependence of the source term used in the diffusion equation for Model II.

or

$$\frac{d^2u}{dr^2} - \frac{C}{K}u(r) = \begin{cases} 0, & 0 \le r \le R_i \\ \dfrac{P}{K}r, & R_i \le r \le R, \end{cases} \qquad (4.2.1.2)$$

where

$$u = r\beta(r)$$

and

$$u(r) = C_1 \cosh Mr + C_2 \sinh Mr, \qquad 0 \le r \le R_i$$
$$u(r) = D_1 \cosh Mr + D_2 \sinh Mr + \frac{P}{C}r, \quad R_i \le r \le R.$$

Thus,

$$\beta(r) = \frac{C_1 \cosh Mr}{r} + \frac{C_2 \sinh Mr}{r}, \qquad 0 \le r \le R_i$$
$$\beta(r) = \frac{D_1 \cosh Mr}{r} + \frac{D_2 \sinh Mr}{r} + \frac{P}{C}, \quad R_i \le r \le R.$$

The arbitrary constants C_1, C_2, D_1, and D_2 are eliminated by applying the boundary conditions to get

$$C_1 = 0$$

$$C_2 = -\frac{P}{R_i X}\left\{\frac{M}{\psi R_i} + \frac{1}{R}\left[\left(\frac{1}{R} - \frac{1}{R_i} - \frac{M}{\psi}\right)\cosh M(R - R_i) +\right.\right.$$

$$+ \quad \left(\frac{1}{MRR_i} - M - \frac{1}{\psi R_i}\right) \sinh M(R - R_i)\Big]\Big\}$$

$$D_1 = \frac{P}{RR_i^2 X}\left[\sinh MR_i - MR_i \cosh MR_i\right] \times$$
$$\times \left[\cosh MR - \sinh MR\left(\frac{1}{MR} - \frac{1}{\psi}\right)\right]$$

$$D_2 = -\frac{PM}{\psi R_i^2 X} - \frac{P}{RR_i^2 X}\left[\sinh MR_i - MR_i \cosh MR_i\right] \times$$
$$\times \left[\sinh MR - \left(\frac{1}{MR} - \frac{1}{\psi}\right)\cosh MR\right]$$

where X is the same as in Model I. Thus, the corresponding solution to the system (4.2.1.1) is

$$\beta(r) = \frac{P(\mu - M^2R^2)\sinh Mr}{CM^2 rRn \sinh MR}, \qquad 0 \le r \le R_i \qquad (4.2.1.3)$$

and

$$\beta(r) = \frac{P}{C}\left\{1 - \frac{\psi\nu\kappa + MR\sinh Mr}{Mrn \sinh MR}\right\}, \qquad R_i \le r \le R \qquad (4.2.1.4)$$

where μ, ν, n, κ, M, and ψ are given by (4.1.1.6), (4.1.1.7), (4.1.1.8), (4.1.1.9), (4.1.1.10), and (4.1.1.11) respectively.

4.2.2 Regions of Stability

As in Model I, the tissue will be stable in the region for which $\beta(R) \geq \theta$. Thus,

$$\frac{P}{C}\left\{1 - \frac{MR\sinh MR - \psi(\sinh MR_i - MR_i\cosh MR_i)}{MR\sinh MR[\psi(\coth MR - \frac{1}{MR}) + 1]}\right\} \geq \theta\,. \qquad (4.2.2.1)$$

The assumptions that $W = \alpha R$ and that $\frac{P}{C\theta} = \frac{\omega}{\psi^2}$ are used again in (4.2.2.1) to obtain

$$\begin{aligned}
&\omega\left\{\coth MR + \frac{\cosh \alpha MR - \coth MR\sinh \alpha MR - 1}{MR}\right. \\
&\left. - \frac{MR(1-\alpha)[\coth MR\cosh \alpha MR - \sinh \alpha MR}{MR}\right\} \\
&\geq \psi + \psi^2\left(\coth MR - \frac{1}{MR}\right) \qquad (4.2.2.2)
\end{aligned}$$

Figure 4.7 shows the graph of $\beta(R) = \theta$ for different values of α. The intervals for which $\beta(R) - \theta \geq 0$ are the regions of stability. The same values as in Model I are used for ψ, ω, and M. The results of this figure show that as α increases, the width of the mitotic zone increases. Since the inhibitor is produced within the living tissue, increase in W results in an increase of the inhibitor production and therefore in an increase of the region of stability. The dependence of the domain of stability, ΔR, on α is schematically indicated in Figure 4.8.

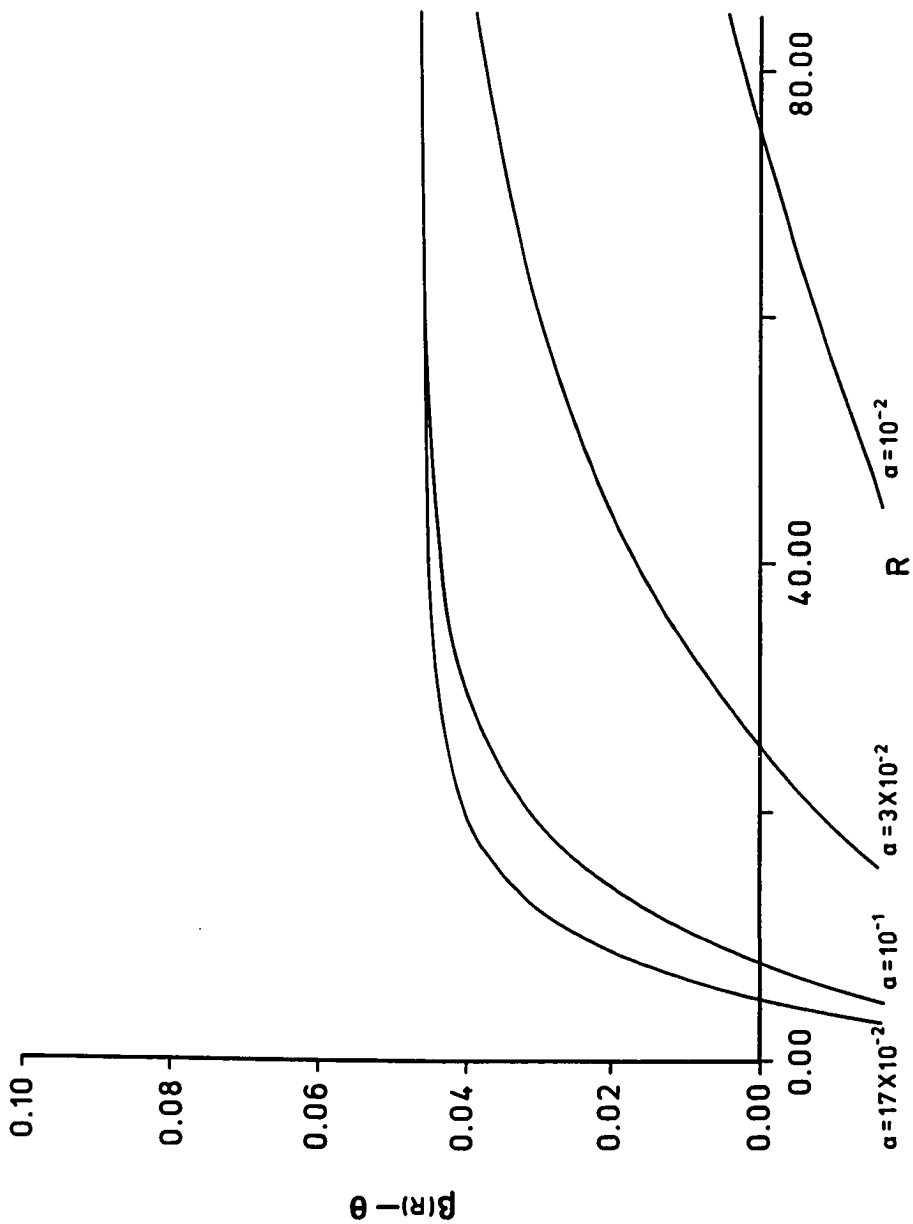

Figure 4.7. Stability diagram based on the inequality (4.2.2.2) for $\psi = 0.05$, $\omega = 0.1$, $M = 10cm^{-1}$ and different values of α (Model II).

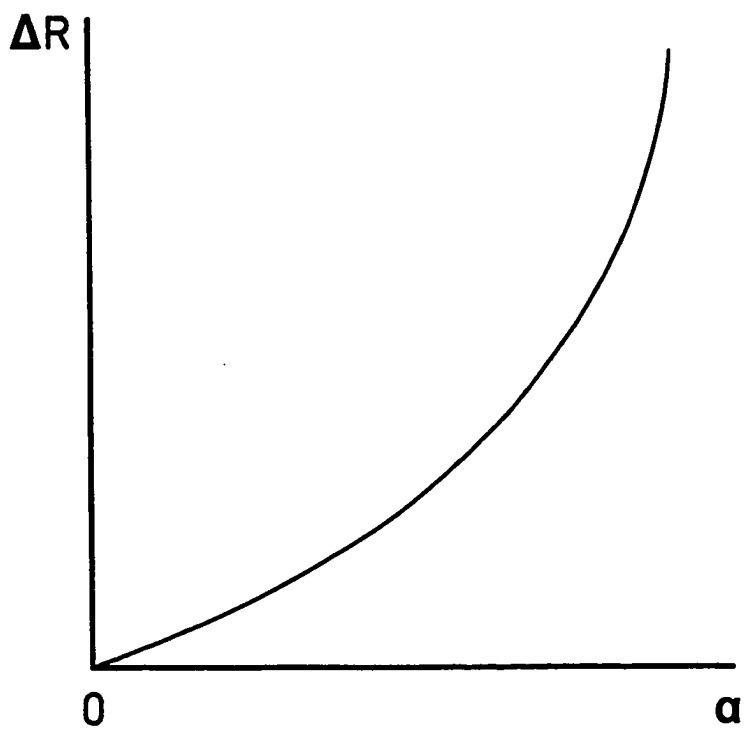

Figure 4.8. The dependence of the domain of stability on α (MODEL II).

4.2.3 The Limiting Peripheral Width W_{L_2}

The limiting peripheral width W_{L_2} can be found by solving the equation

$\beta(R - W_{L_2}) = \theta$ for W_{L_2} as $R \to \infty$.

$$\beta(R - W_{L_2}) = \frac{P}{C}\left\{1 - \frac{MR\sinh M(R - W_{L_2}) - \psi(\sinh M(R - W_{L_2})}{M(R - W_{L_2})\sinh MR[\psi(\coth MR - \frac{1}{MR}) + 1]}\right.$$

$$\left. - \frac{M(R - W_{L_2})\cosh M(R - W_{L_2})[\cosh MW_{L_2} - \left(\frac{1}{MR} - \frac{1}{\psi}\right)\sinh MW_{L_2}]}{M(R - W_{L_2})\sinh MR[\psi(\coth MR - \frac{1}{MR}) + 1]}\right\}$$

as $R \to \infty$,

$$\begin{aligned}\beta(R - W_{L_2}) &= \frac{P}{C}\left\{1 - \frac{\cosh MW_{L_2} - \sinh MW_{L_2}}{\psi + 1}\right. \\ &+ \left.\frac{(M\sinh MW_{L_2} - M\cosh MW_{L_2})(\psi\cosh MW_{L_2} + \sinh MW_{L_2})}{M(\psi + 1)}\right\}\end{aligned}$$

or

$$\frac{3MP(\psi + 1) + MP(\psi - 1)e^{-2MW_{L_2}} - 2PMe^{-MW_{L_2}}}{2MC(\psi + 1)} = \theta\,, \qquad (4.2.3.1)$$

which by using the fact that $\frac{P}{C\theta} = \frac{\omega}{\psi^2}$ becomes

$$e^{-MW_{L_2}} - \frac{2}{(\psi - 1)}e^{-MW_{L_2}} = \frac{(\psi + 1)(2\psi^2 - 3\omega)}{\omega(\psi - 1)}\,.$$

Thus,

$$W_{L_2} = -\frac{1}{M} \ln \left\{ \frac{1 \pm \sqrt{(\psi^2 - 1)(\frac{2\psi^2}{\omega} - 3) - 1}}{\psi - 1} \right\}. \qquad (4.2.3.2)$$

As in Model I, the domains of ω and ψ are determined below. Catastrophic behavior of W_{L_2} occurs if

$$\frac{1 \pm \sqrt{(\psi^2 - 1)(\frac{2\psi^2}{\omega} - 3) - 1}}{\psi - 1} \to 0.$$

For the (-) root, the catastrophic behavior of W_{L_2} occurs when

$$\sqrt{(\psi^2 - 1)(\frac{2\psi^2}{\omega} - 3) - 1} = 1$$

i.e. when

$$\omega = \frac{2\psi^2(1 - \psi^2)}{1 - 3\psi^2}.$$

The (+) root has no catastrophic behavior. W_{L_2} is defined i.e. (> 0) when

$$0 < \frac{1 \pm \sqrt{(\psi^2 - 1)(\frac{2\psi^2}{\omega} - 3) - 1}}{\psi - 1} < 1 \qquad (4.2.3.3)$$

which after some algebra implies the following:

(i) For the (+) root:

$$\omega > \max\left(\frac{\psi^2(1-\psi^2)}{2\psi-1-2\psi^2}, 0\right), \quad \psi > 1$$

and

$$\omega < \frac{2\psi^2(1-\psi^2)}{2-3\psi^2}, \quad \psi > 1.$$

(ii) For the (−) root:

$$\omega > \max\left(\frac{2\psi^2(1-\psi^2)}{1-3\psi^2}, 0\right), \quad \psi > 1$$

and

$$\omega < \frac{\psi^2(1-\psi^2)}{2\psi-1-2\psi^2}, \quad \psi > 1$$

or

$$\omega > \max\left(\frac{\psi^2(1-\psi^2)}{2\psi-1-2\psi^2}, 0\right), \quad \psi < 1$$

and

$$\omega < \frac{2\psi^2(1-\psi^2)}{1-3\psi^2}, \quad \psi < 1$$

with obvious restrictions on ψ such that $\omega > 0$.

The results from these two models indicate that there is a considerable degree of sensitivity of growth patterns to the location and nature of inhibitor sources and enables comparisons to be made with relevant in-vitro data, as it becomes available, which in turn will provide indications as to which model is most appropriate.

Chapter 5

Existence and Uniqueness of Solutions to Two Classes of Nonlinear Time-independent Diffusion Equations

A study of the existence and uniqueness of solutions to two classes of nonlinear time-independent diffusion equations is presented in this chapter.

5.1 Oxygen Diffusion in a Multicellular Spheroid

The first non-linear spherically symmetric time-independent diffusion equation is:

$$\frac{1}{r^2}\frac{d}{dr}\left[r^2\frac{d\sigma}{dr}\right] = h(\sigma, r) \quad , \quad R_i \leq r \leq R_0 \tag{5.1.1}$$

subject to boundary conditions:

$$\begin{aligned} \sigma(R_i) &= \sigma_i \\ \sigma(R_0) &= \sigma_\infty > \sigma_i \,, \end{aligned} \tag{5.1.2}$$

where $\sigma(r)$ is the oxygen concentration, h an arbitrary oxygen consumption rate, R_i the radius of the necrotic core, and R_0 the radius of the spherical tumor. Our goal is to determine conditions on $h(\sigma, r)$ under which a unique solution to problem (5.1.1) exists.

The following sequence of transformations are used to take advantage of a standard formulation using Green's functions:

1. Let $\sigma(r) = \sigma_\infty y(r)$. Then (5.1.1) becomes

$$\begin{aligned} r\sigma_\infty \frac{d^2y}{dr^2} + 2\sigma_\infty \frac{dy}{dr} &= rh(\sigma_\infty y, r), \qquad R_i \le r \le R_0 \\ y(R_i) &= \frac{\sigma_i}{\sigma_\infty} \\ y(R_0) &= 1. \end{aligned} \tag{5.1.3}$$

2. Let $r = R_0 x$, $\dfrac{\sigma_i}{\sigma_\infty} = \eta$, and $\dfrac{R_i}{R_0} = \delta_1$ to get

$$\begin{aligned} \sigma_\infty x \frac{d^2y}{dx^2} + 2\sigma_\infty \frac{dy}{dx} &= R_0^2 x h(\sigma_\infty y, R_0 x), \qquad \delta_1 \le x \le 1 \\ y(\delta) &= \eta \\ y(1) &= 1. \end{aligned} \tag{5.1.4}$$

3. Let $\ell = \dfrac{x - \delta_1}{1 - \delta_1}$ which yields the system

$$\frac{\sigma_\infty}{(1-\delta_1)^2}[\ell(1-\delta_1) + \delta_1]\frac{d^2y}{d\ell^2} + \frac{2\sigma_\infty}{1-\delta_1}\frac{dy}{d\ell} =$$

$$= R_0^2[\ell(1-\delta_1)+\delta_1]h(\sigma_\infty y, R_0[\ell(1-\delta_1)+\delta_1]), \quad 0<\ell\le 1$$

$$y(0)=\eta$$

$$y(1)=1. \tag{5.1.5}$$

4. Let $y(\ell)=v(\ell)+u(\ell)$, where $u(\ell)=\eta+(1-\eta)\ell$ and (5.1.5) now becomes

$$\frac{\sigma_\infty}{(1-\delta_1)^2}[\ell(1-\delta_1)+\delta_1]\frac{d^2v}{d\ell^2}+\frac{2\sigma_\infty}{1-\delta_1}\frac{dv}{d\ell}=$$
$$= R_0^2[\ell(1-\delta_1)+\delta_1]h\left(\sigma_\infty(u+v), R_0\left[\ell(1-\delta_1)+\delta_1\right]\right)$$
$$-\frac{2\sigma_\infty(1-\eta)}{1-\delta_1}, \quad 0\le\ell\le 1$$

$$v(0)=0$$

$$v(1)=0$$

which in simplified form is

$$\frac{d^2}{d\ell^2}[(\ell+\alpha)v(\ell)+2(1-\eta)]=$$
$$=\frac{R_0^2}{\sigma_\infty}(1-\delta_1)^2[\ell+\alpha]h(\sigma_\infty(u+v), R_0[\ell(1-\delta_1)+\delta_1]), \quad 0\le\ell\le 1$$

$$v(0)=0$$

$$v(1)=0\ . \tag{5.1.6}$$

5. Finally, let $P(\ell)=(\ell+\alpha)v(\ell)+2(1-\eta)$ to get

$$\frac{d^2P}{d\ell^2} = \frac{R_0^2}{\sigma_\infty}(1-\delta_1)^2[\ell+\alpha]h(\sigma_\infty(u+v), R_0[\ell(1-\delta_1)+\delta_1]\,,\ 0 \le \ell \le 1$$

$$P(0) = 0$$

$$P(1) = 0$$

or

$$\begin{aligned} \frac{d^2P}{d\ell^2} \ &+\ \lambda f(y,\ell) = 0\,, \quad 0 \le \ell \le 1 \\ P(0) \ &=\ 0 \\ P(1) \ &=\ 0 \end{aligned} \tag{5.1.7}$$

where

$$\lambda = (1-\delta)^2$$

and

$$f(y,\ell) = -\frac{R_0^2}{\sigma_\infty}(\ell+\alpha)h(y,x)\,.$$

The Green's function method is used to solve this system. Thus, if $G(\ell,\xi)$ is the Green's function then the system to be solved is reduced to

$$\frac{d^2G}{d\ell^2} = \delta(\ell-\xi)\ \ ,\ \ 0 \le \ell \le 1$$

with

$$G(\ell,\xi)\,|_{\ell=0} \;=\; 0$$

$$G(\ell,\xi)\,|_{\ell=1} \;=\; 0\,.$$

For $\ell \neq \xi$, $\delta(\ell-\xi)=0$. (Note that $\delta(\ell-\xi)$ is the Dirac's delta function). Thus,

$$\frac{d^2G}{d\ell^2}=0 \;\;,\;\; 0\leq \ell<\xi$$

$$G(\ell,\xi)\,|_{\ell=0}=0$$

and

$$\frac{d^2G}{d\ell^2}=0 \;\;,\;\; \xi<\ell\leq 1$$

$$G(\ell,\xi)\,|_{\ell=1}=0\,.$$

The solution to this Green's function problem is

$$G(\ell,\xi)=\begin{cases}(1-\xi)\ell & 0\leq \ell<\xi\\ (1-\ell)\xi\,, & \xi<\ell\leq 1\,.\end{cases} \tag{5.1.8}$$

Therefore, the solution to (5.1.7) is given by the integral equation

$$P(\ell) = \lambda \int_0^1 K(\ell, \xi, P(\xi)) d\xi \,, \tag{5.1.9}$$

where

$$K(\ell, \xi, P(\xi)) = G(\ell, \xi) f(\xi, P(\xi)) \tag{5.1.10}$$

and $G(\ell, \xi)$ is given by (5.1.8). The integral equation (5.1.9) has a unique solution $P \in L_2[0,1]$ provided that (see Appendix I and Griffel (1981)):

(i) K satisfies a Lipschitz condition

$$|K(\ell, \xi, z_1) - K(\ell, \xi, z_2)| \leq N(\ell, \xi)|z_1 - z_2| \quad \forall z_1, z_2 \,,$$

where N is square integrable with

$$\int_0^1 \int_0^1 |N(\ell, \xi)|^2 d\ell d\xi = Q^2 < \infty \,,$$

(ii) $K(\ell, \xi, 0)$ is continuous for $\ell, \xi \in [0,1]$,

(iii) $|\lambda| < Q^{-1}$.

It is assumed that $\left|\frac{\partial f}{\partial P}\right| \leq M$ for $0 \leq \ell \leq 1$ and all P. By the Mean Value Theorem,

$$\begin{aligned} |K(\ell, \xi, z_1) - K(\ell, \xi, z_2)| &= |G(\ell, \xi)| \left|\frac{\partial f(P, \varsigma)}{\partial P}\right| |z_1 - z_2| \\ &\leq M|G(\ell, \xi)|\,|z_1 - z_2| \text{ for some } \varsigma \in (z_1, z_2). \end{aligned}$$

Hence,

$$N(\ell,\xi) = M|G(\ell,\xi)|.$$

It follows that

$$\begin{aligned} Q^2 &= \int_0^1\int_0^1 M^2|G(\ell,\xi)|^2 d\ell d\xi \\ &= M^2\left\{\int_0^1\left[\int_0^\xi \left|G(\ell,\xi)\right|^2 d\ell + \int_\xi^1 \left|G(\ell,\xi)\right|^2 d\ell\right] d\xi\right\} \\ &= M^2\left\{\int_0^1\left[\int_0^\xi \ell^2(1-\xi)^2 d\ell + \int_\xi^1 \xi^2(1-\ell)^2 d\ell\right] d\xi\right\} = M^2\frac{1}{90} \end{aligned}$$

i.e.

$$Q = \frac{M}{3\sqrt{10}}.$$

Therefore, there exists a unique solution to (5.1.9) provided

$$M = \sup_P\left|\frac{\partial f}{\partial P}\right| < \frac{3\sqrt{10}}{\lambda}, \tag{5.1.11}$$

which is a known result for systems of the type (5.1.7).

5.2 A Re-examination of Oxygen Diffusion in a Multicellular Spheroid

A more complete model from the biological standpoint can be constructed from system (5.1.1) by taking into consideration the flux of oxygen at the interfaces R_i

and R_0. Thus, system (5.1.1) can be re-examined with the appropriate boundary conditions to get

$$\frac{1}{r^2}\frac{d}{dr}\left[r^2\frac{d\sigma}{dr}\right] = h(\sigma, r) \quad , \quad R_i \leq r \leq R_0 \tag{5.2.1}$$

subject to:

$$\begin{aligned} \sigma'(R_i) &= 0 \\ \sigma'(R_0) &= m(1-\sigma(R_0)) \end{aligned} \tag{5.2.2}$$

(note that σ' denotes that the derivative is taken), where m is a constant representing the permeability of the tissue surface. Again the following sequence of transformations are made:

1. Let $r = R_0 x$ to get

$$\begin{aligned} x\frac{d^2\sigma}{dx^2} + 2\frac{d\sigma}{dx} &= R_0^2 x h(\sigma, R_0 x) \quad , \quad \delta_1 \leq x \leq 1 \\ \sigma'(\delta_1) &= 0 \\ \sigma'(1) &= m(1-\sigma(1)) \end{aligned} \tag{5.2.3}$$

where

$$\delta_1 = \frac{R_i}{R_0}$$

2. Let $\ell = \dfrac{x-\delta_1}{1-\delta_1}$. Then (5.2.3) in simplified form becomes

$$
\begin{aligned}
(\ell+\alpha)\frac{d^2\sigma}{d\ell^2}+2\frac{d\sigma}{d\ell} &= \lambda R_0^2(\ell+\alpha)h(\sigma, R_0[\ell(1-\delta_1)+\delta_1] \ , \ 0\le \ell \le 1 \\
\sigma'(0) &= 0 \\
\sigma'(1) &= m(1-\sigma(1))
\end{aligned}
\tag{5.2.4}
$$

where $\alpha = \dfrac{\delta_1}{1-\delta_1}$ and $\lambda = (1-\delta_1)^2$.

3. Finally by letting $\sigma(\ell) = v(\ell) + 1$, system (5.2.4) is reduced to

$$
\begin{aligned}
(\ell+\alpha)\frac{d^2v}{d\ell^2}+2\frac{dv}{d\ell} &= \phi(\sigma,\ell) \ , \ 0\le \ell \le 1 \\
v'(0) &= 0 \\
v'(1) &+ mv(1) = 0,
\end{aligned}
\tag{5.2.5}
$$

where

$$\phi(\sigma,\ell) = \lambda f(\sigma,\ell)$$

and

$$f(\sigma,\ell) = R_0^2(\ell+\alpha)h(\sigma,\ell)\,.$$

The Green's function method is used again in order to solve this system. The solution of

$$(\ell+\alpha)\frac{d^2v}{d\ell^2}+2\frac{dv}{d\ell} = 0$$

satisfying $v'(0) = 0$ is:

$$v_1(\ell) = 1 \ , \ 0 \leq \ell < \xi \, ,$$

where the solution of

$$(\ell + \alpha)\frac{d^2v}{d\ell^2} + 2\frac{dv}{d\ell} = 0$$

satisfying $v'(1) + mv(1) = 0$ is:

$$v_2(\ell) = \frac{1}{\ell + \alpha} - \frac{1}{1 + \alpha} + \frac{1}{m(1 + \alpha)^2} \ , \ \xi < \ell \leq 1 \, .$$

The Wronskian of v_1 and v_2 is then given by

$$W(\xi) = v_1(\xi)v_2'(\xi) - v_2(\xi)v_1'(\xi) = -\frac{1}{(\xi + \alpha)^2} \, .$$

Then

$$G(\ell, \xi) = \begin{cases} G_1(\ell, \xi) \ , \ 0 \leq \ell < \xi \\ G_2(\ell, \xi) \ , \ \xi < \ell \leq 1 \end{cases}$$

or

$$G(\ell,\xi)=\begin{cases} C_1(\xi)v_1(\ell) \text{ for } \ell<\xi \\ C_2(\xi)v_2(\ell) \text{ for } \ell>\xi, \end{cases}$$

where

$$C_1(\xi)=\frac{-v_2(\xi)}{-\frac{1}{\xi+\alpha}}$$

and

$$C_2(\xi)=\frac{-v_1(\xi)}{-\frac{1}{\xi+\alpha}}.$$

Thus,

$$G(\ell,\xi)=\begin{cases} \dfrac{m(1+\alpha)(1-\xi)+(\xi+\alpha)}{m(1+\alpha)^2}, & \ell<\xi \\ (\xi+\alpha)\dfrac{m(1+\alpha)(1-\ell)+(\ell+\alpha)}{m(1+\alpha)^2(\ell+\alpha)}, & \ell>\xi. \end{cases} \tag{5.2.6}$$

(note that since the differential operator is not self-adjoint, $G(\ell,\xi)$ is not symmetric). Consequently, the corresponding solution to (5.2.5) is given by

$$v(\ell)=\int_0^1 G(\ell,\xi)\phi(\xi)d\xi=\lambda\int_0^1 K(\ell,\xi,v(\xi))d\xi, \tag{5.2.7}$$

where

$$K(\ell, \xi, v(\xi)) = G(\ell, \xi) f(\xi, v(\xi)) \tag{5.2.8}$$

and $G(\ell, \xi)$ is given by (5.2.6). The conditions under which (5.2.7) has a unique solution were stated in Section 5.1. Once more we assume that $\left|\frac{\partial f}{\partial v}\right| \leq M$ for $0 \leq \ell \leq 1$ and all v, and by the Mean Value Theorem

$$\begin{aligned} |K(\ell, \xi, z_1) - K(\ell, \xi, z_2)| &= |G(\ell, \xi)| \left|\frac{\partial f(v, \varsigma)}{\partial v}\right| |z_1 - z_2| \\ &\leq M|G(\ell, \xi)||z_1 - z_2| \text{ for some } \varsigma \in (z_1, z_2) \end{aligned}$$

i.e.

$$N(\ell, \xi) = M|G(\ell, \xi)|\,.$$

It follows that

$$\begin{aligned} Q^2 &= \int_0^1 \int_0^1 M^2 |G(\ell, \xi)|^2 d\ell d\xi \\ &= M^2 \left\{ \int_0^1 \left[\int_0^\xi \left(\frac{m(1+\alpha)(1-\xi) + (\xi+\alpha)}{m(1+\alpha)^2} \right)^2 d\ell \right. \right. \\ &+ \left. \left. \int_\xi^1 \left((\xi+\alpha) \frac{m(1+\alpha)(1-\ell) + (\ell+\alpha)}{m(1+\alpha)^2(\ell+\alpha)} \right)^2 d\ell \right] d\xi \right\} \\ &= M^2 \Lambda, \end{aligned}$$

where

$$
\begin{aligned}
\Lambda \;=\; & \frac{6\alpha^2+2\alpha+9}{12}+\frac{2\beta^2(1+3\ln\beta)}{9}+\frac{2(1-3\ln\beta)(\beta^2+\alpha^3 m)}{9m\beta} \\
& -\frac{3\alpha^2+\alpha+1}{3\beta}+\frac{\alpha^2(8m^2+3)}{6m^2\beta^3}-\frac{\alpha(1+3\alpha)}{3m\beta^3}+\frac{(4\alpha+1)(2m^2+1)}{12m^2\beta^4} \\
& +\frac{6(3\alpha^2+\alpha+1)\ln\beta-2\alpha^3(1-3\ln\alpha)}{9m\beta^2}
\end{aligned}
$$

with $\beta = (1+\alpha)$. For given m, Λ is a monotone increasing function of α (see Fig. 5.1). Thus, $Q = M\sqrt{\Lambda}$, and a unique solution to (5.2.7) exists provided

$$
M = \sup_{v}\left|\frac{\partial f}{\partial v}\right| < \frac{\sqrt{\Lambda}}{\lambda\Lambda}.
$$

It is worth noting that since the metabolic reactions in a cell are catalyzed by enzymes (Lin, 1976; McElwain, 1978), it is possible to express the oxygen consumption rate $h(\sigma, r)$ in (5.1.1) and (5.2.1) by means of Michaelis-Menten kinetics:

$$
h(\sigma, r) = \frac{V\sigma}{\sigma + k_m}
$$

where V is the maximum reaction rate, and k_m the Michaelis-Menten constant.

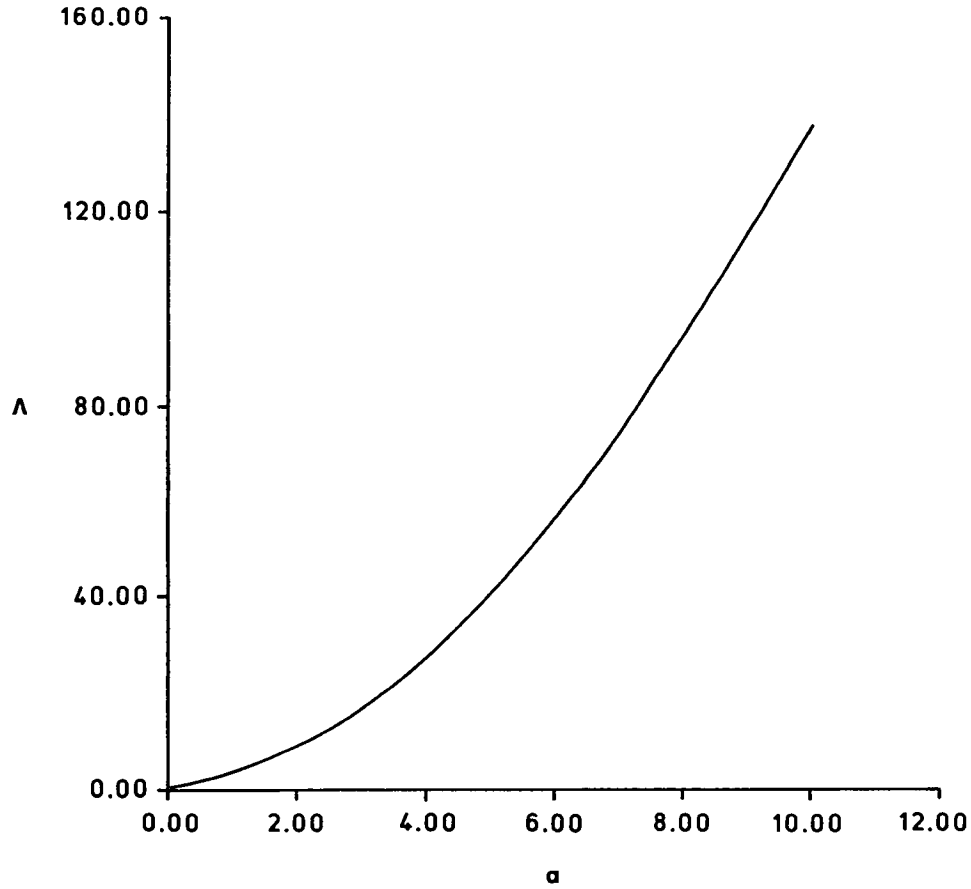

Figure 5.1. The upper bound Λ as a function of α (where $\alpha = \dfrac{\delta_1}{1-\delta_1}$ and $\delta_1 = \dfrac{R_i}{R_0}$)

Chapter 6

Concluding Remarks

Various mathematical models of prevascular tumor growth by diffusion have been developed and analyzed. The objective of all these models has been to provide qualitative descriptions of tumor growth characteristics.

The results obtained from the one-dimensional problem (modeled in a long tube with a small cross sectional area α), in which the effects of non-uniform inhibitor production and uniform nutrient consumption on the growth of tumor tissue were examined, indicate that there is a significant difference between the growth pattern predicted by the Greenspan (1974) model, in which the effects of uniform inhibitor production and uniform nutrient consumption were investigated, and that predicted by this model for the same values of the parameters Q and γ. For example, as the nonuniformity parameter b is varied from zero (uniform production of inhibitor) to unity (maximum nonuniformity of inhibitor production), there is a considerable relative increase in the asymptotic steady state outer "radius", and also in the corresponding inner necrotic core size. There is little

change in the radius separating the region of the inhibited grown cells from the region of the proliferating cells. This indicates that the limiting size of the culture is determined primarily in this model by the nature of the inhibitor production.

The interesting and suggestive results obtained from the one-dimensional model motivated the study of a more sophisticated spherically symmetric growth model, in which the source of the growth inhibitor is assumed to be the necrotic debris. The combined effects of non-uniform nutrient consumption and non-uniform inhibitor production on the growth rate of a spherically symmetric multicellular spheroid were examined in this model, and the time evolution of the various outer and inner radii of interest were analyzed as a function of these various influences. A four-layer structure in the dormant steady state was predicted, and successive stages of growth were examined. This is a deterministic model in that the evolution of a multicellular spheroid from an initial form is determined by an integro-differential equation, the kernel of which depends on the solutions of the spatially dependent spherically symmetric diffusion equations for the concentration of nutrient and growth inhibitor. The behavior of the model is determined by the four parameters Q, γ, b and δ. These parameters depend on information about the various diffusion processes that take place such as: measure of the degree of non-uniformity, volume loss, inhibitor production rates, nutrient consumption rates, and cell proliferation rates. Specific bounds from experimental data, as it becomes available, can be placed on the values of the parameters mentioned so that growth characteristics of multicellular spheroids in vitro can be predicted. At

this time there is relatively little data available, and the emphasis here has been to indicate the general characteristics and qualitative features of tumor growth by using data from existing models in the literature. The model was most closely compared to the models by Greenspan (1972) and McElwain & Ponzo (1977). The results showed a significant difference between the growth patterns of these models and the ones predicted here. This is largely due to the combined effects of non-uniform inhibitor production and non-uniform nutrient consumption.

Comparisons of the results obtained from the two mathematical models developed for the control of the growth of a tumor by diffusion of mitotic inhibitor indicate a considerable degree of sensitivity of growth patterns to the location and nature of inhibitor sources. The predictions from these models enable comparisons to be made with relevant in vitro data, as it becomes available, which in turn will provide indications as to which model is most appropriate.

The analysis of the mathematical behavior with attention to the existence and uniqueness of solutions to non-linear diffusion equations is of value. Loss of uniqueness of solutions of the governing diffusion equations that occur in tumor growth models may correspond to the onset of instabilities in the system, and bifurcation of solutions.

It is hoped that the qualitative information gathered from the present study will serve as a theoretical framework within which to analyze growth characteristics of multicellular spheroids and ultimately solid tumors in the light of experimental and clinical data.

References

Adam, J.A. 1986, "A Simplified Mathematical Model of Tumor growth," *Math. Biosci.* **81**, 224-229.

Adam, J.A. 1987, "A Mathematical Model of Tumor Growth. II. Effects of Geometry and Spatial Nonuniformity on Stability," *Math. Biosci.* **86**, 183-211

Adam, J.A. 1987, "A Mathematical Model of Tumor Growth. III. Comparison with Experiment," *Math. Biosci.* **86**, 213-227.

Anderson, N. and A.M. Arthurs, 1980, "Complemantary Variational Principles for Diffusion Problems with Michaelis-Menten Kinetics," *Bull. Math. Biol.* **42**, 131-135.

Arve, B.H. and A.I. Liapis, 1988, "Oxygen Tension in Tumors Predicted by a Diffusion with Absorption Model Involving a Moving Free Boundary," *Mathl. Comput. Modeling,* **10**, 159-174.

Bullough, W.S. 1965, "Mitotic and Functional Homeostatis: A Speculative Review," *Cancer Res.* **25**, 1683-1727.

Bullough, W.S. and J.U.R. Deol, 1971, "The Pattern of Tumor Growth," *Symp. Soc. Exp. Biol.* **XXV**, 255-275.

Burton, A.C. 1966, "Rate of Growth of Solid Tumors as a Problem of Diffusion," *Growth,* **30**, 157-176.

Deakin, A.S. 1975, "Model for the Growth of a Solid in Vitro Tumor," *Growth,* **39**, 159.

Do, D.D. and P.F. Greenfield, 1981, " A Finite Integral Transform Technique for Solving the Diffusion-reaction Equations with Michaelis-Menten Kinetics," *Math. Biosci.* **54**, 31-47.

Folkman, J. 1974, "Tumor Angiogenesis," *Adv. Cancer Res.* **19**, 331-338.

Folkman, J. and H.P. Greenspan, 1975, "Influence of Geometry on Control of Cell Growth," *Biochem. Biophys. Acta.* **417**, 211-236.

Folkman, J. and M. Hochberg, 1973, "Self-regulation of Growth in Three Dimensions," *J. Exp. Med.* **138**, 745-753.

Folkman, J. and M. Klagsbrun, 1987, "Angiogenic Factors," *Science,* **235**, 442-447.

Franko, A.J. and H.I. Freedman, 1984, "Model of Diffusion on Oxygen to Spheroids Grown in Stationary Medium - I. Complete Spherical Symmetry," *Bull. Math. Biol.* **46**, 205-217.

Franko, A.J. and R.M. Sutherland, 1979, "Oxygen Diffusion Distance and the Development of Necrosis in Multicell Spheroids," *Radiat. Res.* **79**, 439-453.

Franko, A.J. and R.M. Sutherland, 1979, "Radiation Survival of Cells from Spheroids Grown in Different Oxygen Concentrations," *Radiat. Res.* **79**, 454-467.

Freyer, J.P. and R.M. Sutherland, 1983, "Determination of Diffusion Constants for Metabolites in Multicell Tumor Spheroids," *Oxygen Transport to Tissue-IV,* Plenum Publishing Corporation, 463-475.

Freyer, J. P., E. Tustanoff, A.J. Franko, and R.M. Sutherland, 1984, "In Situ Oxygen Consumption Rates of Cells in V-79 Multicellular Spheroids During Growth," *J. Cell Physiol,* **118**, 53-61.

Gatenby, R.A., L.R. Coia, and M.P. Richter, 1985, "Oxygen Tension in Human Tumors: In-vivo Mapping Using CT-guided Probes," *Radiology,* **156**, 211-214.

Glass, L. 1973. "Instability and Mitotic Patterns in Tissue Growth," *J. Dyn. Syst. Meas. Control,* **95**, 324-327.

Goldacre, R.J. and G. Sylven, 1962, "On the Access of Blood-borne Dyes to Various Tumor Regions," *Br. J. Cancer.* **16**, 306.

Greenspan, H.P. 1972, "Models for the Growth of a Solid Tumor by Diffusion," *Stud. Appl. Math.* **52**, 317-340.

Greenspan, H.P. 1974, "On the Self-inhibited Growth of Cell Cultures," *Growth,* **38**, 81-95.

Griffel, D.H. 1981, *Applied Functional Analysis,* Ellis Horwood Limited, Chichester, England.

Grossman, U. 1984, "Profiles of Oxygen Partial Pressure and Oxygen Consumption Inside Multicellular Spheroids," *Recent Results in Cancer Research,* **95**, 150-161.

Hiltman, P. and P. Lory, 1983, "On Oxygen Diffusion in a Spherical Cell with Michaelis-Menten Oxygen Uptake Kinetics," *Bull. Math. Biol.* **45**, 661-664.

Jain, R.K. and J. Wei, 1977, "Dynamics of Drug Transport in Solid Tumors: Distributed Parameter Model," *J. Bioengineering,* **1**, 313-330.

King, W.E., D.S. Schultz, and R.A. Gatenby, 1986, "Multi-region Models for Discribing Oxygen Tension Profiles in Human Tumors," *Chem. Eng. Commun.* **47**, 73-91.

King, W.E., D.S. Schultz, and R.A. Gatenby, 1988, "An Analysis of Systematic Tumor Oxygenation Using Multi-region Models," *Chem. Eng. Commun.* **64**, 137-153.

Laird, A.K. 1965, "Dynamics of Tumor Growth. Comparison of Growth Rates and Extrapolation of Growth Curve to One Cell," *Br. J. Cancer,* **19**, 278.

Landry, J., J.P. Freyer, and R.M. Sutherland, 1982, "A Model for the Growth of Multicellular Spheroids," *Cell Tissue Kinet.* **15**, 585-594.

Liapis, A.I., G.G. Lipscomb, and O.K. Crosser, 1982, "A Model of Oxygen Diffusion in Absorbing Tissue," *Mathematical Modeling,* **3**, 83-92.

Lin, S.H. 1976, "Oxygen Diffusion in a Spherical Cell with Nonlinear Oxygen Uptake Kinetics," *J. Theor. Biol.* **60**, 449-457.

Lin, S.H. 1979, "Nonlinear Diffusion in Biological Systems," *Bull. Math. Biol.* **41**, 151-162.

McElwain, D.L.S. 1978, "A Re-examination of Oxygen Diffusion in a Spherical Cell with Michaelis-Menten Oxygen Uptake Kinetics," *J. Theor. Biol.* **71**, 255-263.

McElwain, D.L.S. 1981, "A Comment on Lin's Paper on Nonlinear Diffusion in Biological Systems," *Bull. Math. Biol.* **43**, 117-120.

McElwain, D.L.S. and P.J. Ponzo, 1977, "A Model for the Growth of Solid Tumor with Non-uniform Oxygen Consumption," *Math. Biosci.* **35**, 267-279.

McElwain, D.L.S., R. Callcott, and L.E. Morris, 1979, "A Model of Vascular Compression in Solid Tumors," *J. Theor. Biol.* **78**, 405-415.

Mueller-Klieser, W.F. 1984, "Method for the Determination of Oxygen Consumption Rates and Diffusion Coefficients in Multicellular Spheroids," *Biophys. J.* **46**, 343-348.

Mueller-Klieser, W.F. and R.M. Sutherland, 1982, "Oxygen Tensions in Multicell Spheroids of Two Cell Lines," *Br. J. Cancer,* **45**, 256-263.

Mueller-Klieser, W.F. and R. M. Sutherland, 1984, "Oxygen Consumption and Oxygen Diffusion Properties of Multicellular Spheroids from Two Different Cell Lines," *Adv. Exp. Med. Biol.* (Preprint).

Mueller-Klieser, W.F., J.P. Freyer, and R.M. Sutherland, 1983. "Evidence for a Major Role of Glucose in Controlling Development of Necrosis in EMT6/RO Multicell Tumor Spheroids," *Oxygen Transport to Tissue-IV*, Plenum Publishing Corporation, 487-495.

Old, L.J. 1988, "Tumor Necrosis Factor," *Scientific American*, May, 59.

Poste, G. and R. Greig, 1983, "The Experimental and Clinical Implications of Cellular Heterogeneity in Malignant Tumors," *J. Cancer Res. Clin. Oncol.* **106**, 159-170.

Schultz, D.S. and W.E. King, 1987, "On the Analysis of Oxygen Diffusion in Biological Systems," *Math. Biosci.* **83**, 179-190.

Shymko, R.M. and L. Glass, 1976, "Cellular and Geometric Control of Tissue Growth and Mitotic Instability," *J. Theor. Biol.* **63**, 355-374.

Sutherland, R.M. 1988, "Cell and Environment Interactions in Tumor Microregions: The Multicell Spheroid Model," *Science*, **240**, 177-184.

Sutherland, R.M. and R.E. Durand, 1976, "Radiation Response of Multicellular Spheroids - AnIn vitro Tumor Model," *Curr. Top. Radiat. Res.* **11**, 87-139.

Swan, G.W. 1981, "Optimization of Human Cancer Radiotherapy," *Lecture Notes in Biomathematics*, **42**, Springler - Verlag.

Tannock, I. 1976, "Oxygen Distribution in Tumours: Influence on Cell Proliferation and Implications for Tumour Therapy," *Adv. Exp. Med. Biol.* **75**, 597-603.

Tannock, I. F. 1968, "The Relation Between Cell Proliferation and the Vascular System in a Transplanted Mouse Mammary Tumor," *Br. J. Cancer*, **22**, 258-273.

Thews, G. and P. Vaupel, 1976, "Oxygen Supply Conditions in Tumor Tissue in Vivo," *Adv. Exp. Med. Biol.* **75**, 537-546.

Tosaka, N. and S. Miyaka, 1982, "Analysis of a Nonlinear Diffusion Problem with Michaelis-Menten Kinetics by an Integral Equation Method," *Bull. Math. Biol.* **44**, 841-849.

Vaupel, P., S. Frinak, and H.I. Bicher, 1981, "Heterogeneous Oxygen Partial Pressure and pH Distribution in C3H Mouse Mammary Adenocaricinoma," *Cancer Res.* **41**, 2008-2013.

Wette, R., I.N. Katz, and E.Y. Rodin, 1974, "Stochastic Processes for Solid Tumor Kinetics I. Surface Regulated Growth," *Math. Biosci.* **19**, 231-255.

Wette, R., I.N. Katz, and E.Y. Rodin, 1974, "Stochastic Processes for Solid Tumor Kinetics II. Diffusion Regulated Growth," *Math. Biosci.* **21**, 311-388.

Appendix I

Existence and Uniqueness for Integral Equations

Theorem The integral equation

$$u(x) - \lambda \int_a^b K(x, y, u(y))dy = f(x) \qquad \text{(AI.1)}$$

has a unique solution $u \in L_2[a, b]$, provided that

(i) $f \in L_2[a, b]$;

(ii) K satisfies a Lipschitz condition with respect to its third arguement,

$$| K(x, y, z_1) - K(x, y, z_2) | \leq N(x, y) | z_1 - z_2 | \qquad \forall z_1, z_2 \qquad \text{(AI.2)}$$

where N is square-integrable, with

$$\int_a^b \int_a^b | N(x, y) |^2 dxdy = P^2, \text{ say}; \qquad \text{(AI.3)}$$

(iii) $K(x, y, 0)$ is continuous for $x, y \in [a, b]$;

(iv) $| \lambda | < 1/P$

Proof Define an operator T by

$$(Tu)(x) = f(x) + \lambda \int_a^b K(x, y, u(y))dy$$

We must first show that T maps $L_2[a, b]$ into itself. Since $L_2[a, b]$ is a vector space, and $f \in L_2[a, b]$, Tu will belong to $L_2[a, b]$ if $\int_a^b K(x, y, u(y))dy$ does. Now, using

the Lipschitz condition,

$$
\begin{aligned}
&| K(x,y,u) - K(x,y,0) | \leq N(x,y) | u |, \\
&| K(x,y,u | \leq | K(x,y,0) | + N(x,y) | u |, \\
&| \int_a^b K(x,y,u(y))dy | \leq \int_a^b | K(x,y,0) | dy \\
&\qquad + \int_a^b N(x,y) | u(y) | dy
\end{aligned}
$$

Each term on the right is square-integrable, the first because it is continuous, the second because it is the result of applying the integral operator with kernel N to the function $| u | \in L_2[a,b]$. Hence,

$$\int_a^b K(x,y,u(y))dy$$

is square-integrable, and we have shown that T maps $L_2[a,b]$ into itself.

We must show that T is a contraction. We have, for any u_1 and u_2 in $L_2[a,b]$ and any $x \in [a,b]$,

$$
\begin{aligned}
| Tu_1(x) - Tu_2(x) | &= | \lambda \int_a^b [K(x,y,u_1(y)) - K(x,y,u_2(y))]dy | \\
&\leq | \lambda | \int_a^b N(x,y) | u_1(y) - u_2(y) | dy \\
&\leq | \lambda | \left\{ \int_a^b | N(x,y) |^2 dy \int_a^b | u_1(y) - u_2(y) |^2 dy \right\}^{\frac{1}{2}}
\end{aligned}
$$

by the Cauchy-Schwarz inequality. Hence,

$$\| Tu_1 - Tu_2 \| \leq | \lambda | \| \left\{ \int_a^b | N(x,y) |^2 \, dy \, \| u_1 - u_2 \|^2 \right\}^{\frac{1}{2}} \|$$
$$= | \lambda | P \| u_1 - u_2 \| .$$

So condition (iv) ensures that T is a contraction on $L_2[a,b]$, and the equation $Tu = u$, which is just equation (AI.1), has exactly one solution (Griffel, 1981).

Appendix II

Related Observations for Multicellular Spheroids [1]

There are several recent experimental studies of oxygen consumption rates and tensions in multicellular spheroids during growth. We briefly summarize the findings of two of the most relevant to this study: that of Freyer et al. (1984) and that of Mueller-Klieser and Sutherland (1982), referring to them respectively as (F) and (MKS).

In the former study, 0_2 consumption rates in V-79 Chinese hamster cells in multicellular spheriods were measured as a function of the spheroid diameter. The in situ consumption was equal to that of exponentially growing cells for spheroids less than 200 μm in diameter, after which the consumption rate decreased to one fourth of the initial rate for spheroids between 200 and 400 μm in diameter. Thereafter it remained constant for further spheroid growth. Comparison of consumption rates for cells before and after dissociation from the spheroid structure indicated that the spheroid microenvironment accounted for only 20% of the change in 0_2 consumption rates. Furthermore, the study indicated that cell-cell contact, cell packing and cell volume were not critical parameters. "Plateau-phase" cells had a fivefold lower rate of 0_2 consumption than exponential cells, indicating that the spheroid quiescent cell population may account for a significant

[1] Taken from a paper by Adam and Maggelakis submitted to the Bulletin of Mathematical Biology

part of the intrinsic alteration in 0_2 consumption of cells in spheroids.

In (MKS), 0_2 tensions ($P0_2$) were measured with microelectrodes in multicellular spheroids from both V-79 and EMT_6/R_0 cells. The $P0_2$ profiles were characterized by a diffusion-depleted zone surrounding the spheroids, and by a steep drop in $P0_2$ within the spheroids over mean distances of 220 μm (EMT6/R0) and 188 μm (V-79) from the spheroid surfaces respectively. Smaller spheroids were found to exhibit parabolic $P0_2$ profiles while larger ones showed a low central plateau. The region of steep decrease in each case identifies the thickness of the viable rim; the plateau region is created by the absence of 0_2 consumption in the central necrotic core– a fact built into the model presented in Chapter 3. (MKS) give estimates of average $P0_2$ values at which central necrosis may arise in each type of spheroid under the growth conditions described.

There are four basic parameters in the model presented in Chapter 3: Q, γ, b, and δ. The first two are the most biologically meaningful, given their definitions; b, while it may be of considerable relevance to biological systems in which growth inhibitory factors are produced, is also (for the purposes of this model) a measure of the sensitivity of this type of model to non-uniform source terms. Variations in b indicate the degree to which the model responds in terms of the dormant steady state. δ is somewhat of an ad-hoc parameter introduced to account for the effects of inhibitor concentration on the nutrient consumption rate. However, it is certainly necessary to have some measure of this interaction, and there is some indication that this is well justified (see point (vii) below). The question naturally

arises as to what insight is provided by experimental work into the appropriate parameter domains for this model. Only partial answers can be given to this question at the present time, but some helpful information is available, and it is to this that we will now devote some attention. Specifically, we will address certain data and points that are raised in (F) and (MKS) and examine briefly some of the implications for the model of tumor growth presented here. From (F) we note the following points:

(i) Low central 0_2 tensions occur in V-79 spheroids. This is of course a feature of this and other diffusion models.

(ii) For $0 < t < 6$ days, the mean 0_2 consumption rate was the same as that of exponentially growing cells in suspension, for $R_0 < 100\mu m$. For $6 < t < 12$ days, this rate decreased rapidly for cells in spheroids for which $100\ \mu m < R_0 < 200\mu m$, to a value one fourth of the initial value. For $R_0 > 200\mu m$, no further change in consumption occurred, through the spheroids continued to grow.

This means that we can fix the end of the first phase of growth (Phase I: exponential growth) in the model as $t_1 = 6$ days (or other appropriate units of time) and, given the normal proliferation rate s, we can estimate $\tau_1 = st_1$ to a reasonable degree of accuracy. Further, if we identify the lowest non-zero relative consumption rate in our model with the above-mentioned factor of $1/4$, it follows from the postulated form for consumption rates that $\sigma_i/\hat{\sigma} = 1/4$.

As an alternative to estimating the time τ_1 to the end of phase I, we can use information on τ_1 from tables 3.1-3.4 to give predictions of the normal proliferation rate s. The beginning of the second phase occurs when $\sigma(0) = \hat{\sigma}$, and the outer tumor radius at this point is given by, dimensionally,

$$R_0 = \{(\frac{6k\hat{\sigma}}{A})(\frac{\sigma_\infty}{\hat{\sigma}} - 1)\}^{1/2} \qquad \text{(AII.1)}$$

approximately $100\mu m$ from the data discussed above. Again, information can be taken from the tables or graphs of $\xi(\tau)$ to find those parameters that best fit the above data. The second phase ends when $\sigma(0) = \sigma_i$; a necrotic core is initiated. This occurs when the radius $\hat{R} = (k\hat{\sigma}/A)^{1/2}\rho_c$, where

$$\frac{\sigma_i}{\hat{\sigma}} = \frac{\rho_c}{\sinh \rho_c} \qquad \text{(AII.2)}$$

This in turn gives a value of R_0 at this point via a transcendental equation (see Chapter III), or the corresponding parameter values can be read from the model predictions, given $R_0 \approx 200\mu m$. Related to this is the estimate given in (F) of the diameter of the spheroid when necrosis first occurs, namely $\approx 370\mu m$.

(iii) At no time during the experiments did the volume of the necrotic core exceed 10% of the total spheroid volume. For perfect spherical symmetry, assumed here, this places an upper bound on the ratio R_i/R_0 of $(10)^{-1/3} \approx 0.46$. However, it is not clear whether or not the spheroids had reached a dormant steady state during these observations.

(iv) The initial 0_2 consumption rate for spheroids with $R_0 < 200\mu m$ was found to be $\approx 2.5 \times 10^{-8}$ moles/cm^3/sec. This fixes the value of A in the diffusion

equation for nutrient consumption.

(v) As R_0 increased from $\approx 200\mu m$ to $\approx 310\mu m$ the thickness of the viable cell rim was observed to decrease slightly from a mean of $180\mu m$ to the mean of $170\mu m$; however the value of one standard deviation was about $20\mu m$ so this may not be a significant trend. Extrapolation of this data yielded the estimate of R_0 when necrosis first appears, discussed in point (ii) above. It may be appropriate to identify this rim thickness with an 0_2-penetration depth.

(vi) The experimental work appears to demonstrate that the reduced rate of 0_2 consumption per unit volume for spheroid cells is due to a reduced cellular rate of consumption, not reduced cell packing in the spheroid. Furthermore, it appears that this reduction is due largely to some effect independent of the spheroid microenvironment which appears to be an intrinsic property of spheroid-derived cells. This in turn, the authors remark, indicates that the effect of decreasing spheroid surface area to volume ratio is small. The present model incorporated the assumptions of (non-uniform) inhibitor production and (non-uniform) 0_2 consumption as related factors determining the overall growth characteristics of spherical tumors, consistent with the observations.

(vii) The effects of toxic products from the necrotic core on mean cellular 0_2 utilization appears to be minimal. This indicates that small values of the

parameter δ used in Phase IV are more appropriate than values close to unity.

(viii) Plateau-phase cells had a five-fold lower consumption rate than exponentially growing cells, although there was a 40% volume reduction associated with cells in this phase.

(ix) The proliferative status of the cells does have a significant effect on cellular 0_2 utilization. A large fraction of V-79 spheroids ($R_0 > 250\mu m$) consists of non-cycling cells: from this it may be assumed that proliferating cells exist primarily in an outer zone $\approx 50 - 70\mu m$ in thickness. This corresponds in Case 1 of Phase IV in this model to $R_0 - \hat{R}$; or to $R_0 - R_g$ in Case 2. Furthermore, the experimental results predict that quiescent cells first appear when $R_0 \approx 50 - 75\mu m$, increasing in number until a maximal percentage is reached at $R_0 \approx 250 - 300\mu m$. This initial radius is slightly smaller than that discussed in point (ii) above; it may be that an appreciable drop in 0_2 consumption rate occurs well after quiescent cells first appear– a reasonably large number of them are necessary to effect any change in the measurements.

There are a number of features of both multicellular spheroid and tumor growth that are not incorporated in the present model, and therefore represent a challenge to future theoretical work: In (MKS) such features are noted:

(i) Restrictions in blood supply, as they may occur in solid tumors with increasing weight, can lead to a decrease in nutrient concentration, such as

0_2 in the tumor capillaries. This situation can be simulated in spheroids by lowering the 0_2 content in the growth medium.

(ii) Metabolism of 0_2 is influenced by glucose levels (see Mueller- Klieser et al. (1983)) and vice versa: this could certainly impede a good theoretical estimate of 0_2 concentration in spheroids.

(iii) Additional complications arise from the effects of factors in the interstitial milieu of spheroids (eg. pH) which might also influence tumor cell metabolism.

(iv) There is in fact a decrease of 0_2 in the medium directly surrounding the spheroid, lowering the $P0_2$ at the surface considerably below that in the bulk of the medium. This point has been addressed in detail recently by Franko and Freedman (1984), but these authors were not concerned there with the subsequent growth equations discussed in this model.

A further aspect of the diffusion problems discussed here concerns values for the diffusion constants k and K used in the model. Mueller-Klieser (1984) has described a method for determining 0_2 consumption rates and diffusion constants in multicellular spheroids. The method utilizes measured $P0_2$ gradients withing the spheroids; the diffusion constant of interest was in fact Krogh's constant, equal to the product of 0_2 solubility with the 0_2 diffusivity. Further work along these lines, for both EMT6 and V-79 spheroids, can be found in the article by Mueller-Klieser and Sutherland (1984). Freyer and Sutherland (1983) determined diffusion con-

stants for Glucose and Thymidine; Mueller-Klieser et al. (1983) found evidence for a major role of Glucose in controlling the development of necrosis in EMT6 spheroids. Landry et al (1982) developed a model for growth of multicellular spheroids using some observations by Folkman and Hochberg (1973) and theoretical work of Shymko and Glass (1976). The latter work has been extended (Adam, 1986,1987a,b) to allow for non-uniform inhibitor production, and also to allow for the presence of a necrotic core (see Chapter 4).

Franko and Sutherland (1979) discussed the relationship between oxygen diffusion distances and development of necrosis in spheroids. The thickness of the viable cell rim in V-79 spheroids was measured for different 0_2 (and glucose) concentrations, and they found that in general the square of the thickness increased linearly with the theoretically derived 0_2 diffusion distance. This indicated that 0_2 diffusion distance is a major influence in the development of necrosis. They found a correspondingly smaller effect from variations in the glucose concentrations.

Tannock (1976) has studied the of 0_2 distribution in tumors on cell proliferation and its implications for tumor therapy. In particular, in some human and animal tumors, cylindrical cords of tumor cells with a central capillary and peripheral necrosis have been observed. This relatively simple morphology may be used to identify any relationships that may exist between cellular kinetics and the concentration of metabolites or drugs that diffuse from blood vessels (see also the articles by Thews and Vaupel (1976), and Grossman (1984)).

The next task in the process of formulating realistic mathematical models

of tumor spheroid growth by diffusion is to synthesise all pertinent information provided by the above experimental and theoretical papers, and other related studies, to obtain numerical values (or at least tight bounds) on the parameters $Q(A, k, P, K, \beta_i, \hat{\sigma}), \gamma, b$ and δ, and to compare model predictions with experimental results. If, as seems likely at this time, complete information is unavailable, then whatever is available can be used to define a subspace of that parameter space, and the model curves used to make predictions about the otherwise in accessible features, e.g. possible values of b (as was done in Adam (1987,1989), or the ratio β_i/P, etc.

As a complementary level of description, the mathematical model discussed here and in Chapter 3 is of interest as an (in general) nogeneral) nonlinear diffusion problem. As such, the analysis of existence, uniqueness and stability of solutions to the diffusion equations and the governing growth equation is of value (see Chapter 5). This, coupled with a detailed understanding of the mathematical model itself, and the associated computer simulation of solutions to the model can form the basis for a further level of description in deterministic models of tumor growth.

Appendix III

Computer Program: Growth

```
C ************************************************************
C *                                                          *
C *                     PROGRAM GROWTH                       *
C *                                                          *
C ************************************************************
C *                                                          *
C * PROGRAM "GROWTH" SOLVES THE INTEGRO-DIFFERENTIAL         *
C * EQUATIONS, THAT DESCRIBE THE GROWTH PATTERN OF THE       *
C * TUMOR, FOR EACH STAGE OF THE GROWTH DEVELOPMENT USING    *
C * A FOURTH ORDER RUNGE-KUTTA METHOD. THESE GROWTH          *
C * EQUATIONS DEPEND ON THE RELATIONSHIPS BETWEEN THE        *
C * VARIOUS DIMENSIONLESS INNER TUMOR RADII "RO", "ZHTA",    *
C * "HTA" AND THE CONCENTRATIONS OF THE NUTRIENT AND         *
C * GROWTH INHIBITOR. THE EQUATIONS THAT GIVE THESE          *
C * RELATIONSHIPS ARE SOLVED SEVERAL TIMES DURING EACH       *
C * STEP OF THE METHOD. THE TUMOR GROWTH IS CHARACTERIZED    *
C * BY FOUR PHASES.                                          *
C *                                                          *
C ************************************************************
C *                                                          *
C *    PARAMETERS                                            *
C *    ----------                                            *
C *                                                          *
C *        GAMA: IS THE RATIO OF THE PROPORTIONALITY         *
C *              CONSTANT FOR THE VOLUME LOSS TERM           *
C *              (LAMBDA) AND THE NORMAL PROLIFERATION       *
C *              RATE OF CELLS (s).                          *
C *                                                          *
C *           Q: IS A MEASURE OF THE COMPETING EFFECTS       *
C *              OF NUTRIENT CONSUMPTION/DIFFUSION AND       *
C *              INHIBITOR PRODUCTION/DIFFUSION.             *
C *                                                          *
C *          B1: MEASURES THE DEGREE OF NON-UNIFORMITY       *
C *              OF THE NHIBITOR PRODUCTION.                 *
C *                                                          *
C *       DELTA: MEASURES THE EFFECT (IF ANY) OF NON-ZERO    *
C *              INHIBITOR ON NUTRIENT CONSUMPTION RATE.     *
C *                                                          *
C *   VARIABLES                                              *
C *  -----------                                             *
C *                                                          *
C *       SIGMA: THE RATIO OF SIGMAINF/SIGMAHAT.             *
C *                                                          *
C *    SIGMAINF: IS THE CONCENTRATION OF THE NUTRIENT        *
C *              IN THE AMBIENT MEDIUM OF THE TUMOR.         *
C *                                                          *
C *    SIGMAHAT: IS THE CRITICAL NUTRIENT CONCENTRATION      *
C *              BELOW WHICH NUTRIENT CONSUMPTION BY THE     *
C *              CELL FALLS.                                 *
C *                                                          *
C *          S1: THE RATIO OF SIGMAI/SIGMAHAT.               *
C *                                                          *
C *      SIGMAI: IS THE CRITICAL NUTRIENT CONCENTRATION      *
C *              BELOW WHICH TUMOR CELLS DIE.                *
C *                                                          *
C *         XSE: THE OUTER TUMOR RADIUS AT TIME (t).         *
C *                                                          *
```

```
C *          RO: INNER TUMOR RADIUS AT WHICH THE                *
C *              CONCENTRATION OF NUTRIENT EQUALS THE           *
C *              CRITICAL CONCENTRATION (SIGMAHAT).             *
C *                                                             *
C *        ZHTA: INNER TUMOR RADIUS AT WHICH THE                *
C *              CONCENTRATION OF INHIBITOR EQUALS THE          *
C *              CRITICAL CONCENTRATION, BETAI, ABOVE           *
C *              WHICH ALL CELL PROLIFERATION CEASES.           *
C *                                                             *
C *         HTA: RADIUS OF THE NECROTIC CORE.                   *
C *                                                             *
C *         ROC: IS THE VALUE THAT THE INNER TUMOR              *
C *              RADIUS "RO" TAKES AT THE ONSET OF              *
C *              NECROSIS.                                      *
C *                                                             *
C *           A: LOWER BOUND OF THE TIME INTERVAL WITHIN        *
C *              WHICH TUMOR GROWTH TAKES PLACE.                *
C *                                                             *
C *           B: UPPER BOUND OF THE TIME INTERVAL WITHIN        *
C *              WHICH TUMOR GROWTH TAKES PLACE.                *
C *                                                             *
C *                                                             *
C *  SUBROUTINES                                                *
C *  -----------                                                *
C *                                                             *
C *     RADIRO: SOLVES FOR THE SCALED INNER RADIUS "RO"         *
C *     WHICH IS REQUIRED IN ORDER TO OBTAIN THE SOLUTION       *
C *     OF THE GROWTH EQUATION THAT DESCRIBES PHASE-2.          *
C *                                                             *
C *     RADIXC: SOLVES FOR THE SCALED OUTER TUMOR RADIUS        *
C *             "XSEC" WHICH IS THE OUTER RADIUS AT THE         *
C *             END OF PHASE-1.                                 *
C *                                                             *
C *     RADIRC: SOLVES FOR THE SCALED INNER RADIUS "ROC"        *
C *             WHICH IS REQUIRED IN ORDER TO SOLVE FOR         *
C *             THE OUTER TUMOR "XSEC".                         *
C *                                                             *
C *        SYS: SOLVES A SYSTEM OF NONLINEAR EQUATIONS          *
C *             FOR THE INNER TUMOR RADII "RO" AND "HTA".       *
C *             THESE RADII ARE REQUIRED IN ORDER TO            *
C *             SOLVE THE GROWTH EQUATION THAT DESCRIBES        *
C *             PHASE-3 OF THE TUMOR DEVELOPMENT.               *
C *                                                             *
C *       SYST: SOLVES A SYSTEM OF NONLINEAR EQUATIONS          *
C *             FOR THE INNER TUMOR RADII "RO", "ZHTA",         *
C *             AND "HTA". THESE RADII ARE REQUIRED IN          *
C *             ORDER TO SOLVE THE GROWTH EQUATION THAT         *
C *             DESCRIBES PHASE-4 (CASE-1) OF THE               *
C *             TUMOR DEVELOPMENT.                              *
C *                                                             *
C *       SYS1: SOLVES A SYSTEM OF NONLINEAR EQUATIONS          *
C *             FOR THE INNER TUMOR RADII "ZHTA" AND            *
C *             "HTA". THESE RADII ARE REQUIRED IN ORDER        *
C *             TO SOLVE THE GROWTH EQUATION THATDESCRIBES      *
C *             PHASE-4 (CASE-2) OF THE TUMOR DEVELOPMENT.      *
C *                                                             *
C *     FCTEVL: EVALUATES THE RIGHT-HAND SIDE OF THE            *
```

```
C *              GROWTH EQUATION THAT DESCRIBES PHASE-2      *
C *              OF THE TUMOR DEVELOPMENT.                   *
C *                                                          *
C *      FUNCTN: EVALUATES THE RIGHT-HAND SIDE OF THE        *
C *              GROWTH EQUATION THAT DESCRIBES PHASE-3      *
C *              OF THE TUMOR DEVELOPMENT.                   *
C *                                                          *
C *       FNCT2: EVALUATES THE RIGHT-HAND SIDE OF THE        *
C *              GROWTH EQUATION THAT DESCRIBES PHASE-4      *
C *              (CASE-1) OF THE TUMOR DEVELOPMENT.          *
C *                                                          *
C *       FNCT1: EVALUATES THE RIGHT-HAND SIDE OF THE        *
C *              GROWTH EQUATION THAT DESCRIBES PHASE-4      *
C *              (CASE-2) OF THE TUMOR DEVELOPMENT.          *
C *                                                          *
C ************************************************************
C
C
C
      DIMENSION XSIN(100)
      REAL K1,K2,K3,K4
C
C
C  FILES ARE CREATED TO STORE THE DATA FOR THE VARIOUS
C  TUMOR RADII.
C
C        "XSE.DAT"  DATA FOR THE EVOLUTION OF THE
C         OUTER TUMOR RADIUS.
C
C         "RO.DAT"  DATA FOR THE EVOLUTION OF THE
C                   INNER TUMOR RADIUS "RO".
C
C       "ZHTA.DAT"  DATA FOR THE EVOLUTION OF THE
C                   INNER TUMOR RADIUS "ZHTA".
C
C         "HTA.DAT"  DATA FOR THE EVOLUTION OF THE
C                   RADIUS OF THE NECROTIC CORE "HTA".
C
C
          OPEN(UNIT=1,FILE='XSE.DAT')
          OPEN(UNIT=2,FILE='RO.DAT')
          OPEN(UNIT=3,FILE='HTA.DAT')
          OPEN(UNIT=4,FILE='ZHTA.DAT')
C
C
C    ENTER THE APPROPRIATE DATA
C
C
      WRITE(*,*)' ENTER A LOWER BOUND OF INTERVAL [A,B]: '
      READ(*,*)A
      WRITE(*,*)' ENTER AN UPPER BOUND OF NTERVAL [A,B]: '
      READ(*,*)B
      WRITE(*,*)' ENTER NUMBER OF SUBINTERVALS: '
      READ(*,*)N
      WRITE(*,*)' ENTER SIGMAINF/SIGMAHAT: '
      READ(*,*)SIGMA
      WRITE(*,*)' ENTER SIGMAI/SIGMAHAT: '
```

```
      READ(*,*)S1
      WRITE(*,*)' ENTER INITIAL GUESS FOR XSE: '
      READ(*,*)XSI
      WRITE(*,*)' ENTER INITIAL GUESS FOR ROC: '
      READ(*,*)ROC
      WRITE(*,*)' ENTER INITIAL GUESS FOR RO: '
      READ(*,*)RO0
      WRITE(*,*)' ENTER INITIAL GUESS FOR HTA: '
      READ(*,*)HTA0
      WRITE(*,*)' ENTER INITIAL GUESS FOR ZHTA: '
      READ(*,*)ZHTA
      WRITE(*,*)' ENTER A VALUE FOR GAMA: '
      READ(*,*)GAMA
      WRITE(*,*)' ENTER A VALUE FOR Q: '
      READ(*,*)Q
      WRITE(*,*)' ENTER A VALUE FOR THE PARAMETER B: '
      READ(*,*)B1
      WRITE(*,*)' ENTER A VALUE FOR DELTA: '
      READ(*,*)DELTA
      S=SIGMA-1.0
C
C
C                *****  PHASE-1  *****
C
C
      H=(B-A)/(FLOAT(N))
      SS=(6.0)*S
      XSEC1=SQRT(SS)
      DO 105 J=1,N

      TAU=(J-1)*H
      XSE0=XSI*EXP(TAU/3.0)
      RNEW=0.0
      ZNEW=0.0
      HNEW=0.0
C
C
C        CHECK FOR COMPLETION OF PHASE-1
C
C
       IF(XSE0.GT.XSEC1) GO TO 110
C
C
       WRITE(1,100)TAU,XSE0
       WRITE(2,100)TAU,RNEW
       WRITE(3,100)TAU,HNEW
       WRITE(4,100)TAU,ZNEW
C
105      CONTINUE

110          WRITE(*,*)' END OF PHASE-1',J,TAU,XSEC1
C
C
C
C
C
```

```
C
C
C                    *****  PHASE-2  *****
C
C
C
      T0=TAU
      WRITE(1,100)T0,XSE0
C
C
C       SOLVE FOR THE SCALED OUTER RADIUS "XSEC" AT
C       WHICH NECROSIS FIRST OCCURS.  PHASE-2
C       PROCEEDS UNTIL XSE=XSEC. THE VALUE OF THE
C       INNER RADIUS "RC" IS REQUIRED IN ORDER TO
C       SOLVE FOR "XSEC".
C
      CALL RADIRC(S1,ROC,RC)
      CALL RADIXC(S,RC,XSEC)
C
C
C       SOLVE FOR THE SCALED INNER TUMOR RADIUS "RO"
C       GIVEN "XSE" (FROM PHASE-1). THE KNOWLEDGE OF
C       "RO" IS REQUIRED IN ORDER TO SOLVE THE GROWTH
C       EQUATION THAT DESCRIBES PHASE-2.
C
C
C
       CALL RADIRO(S,XSE0,R0)
C
C
C     A FOURTH ORDER RUNGE-KUTTA PROCEDURE IS USED TO
C     SOLVE THE GROWTH EQUATION THAT DESCRIBES PHASE-2.
C
C
      DO 35 I=J,N
        CALL FCTEVL(S,XSE0,R0,F1)
        K1=H*F1
C
        XSE1=XSE0+(K1/2.0)
        CALL RADIRO(S,XSE1,R1)
        CALL FCTEVL(S,XSE1,R1,F2)
        K2=H*F2
C
        XSE2=XSE0+(K2/2.0)
        CALL RADIRO(S,XSE2,R2)
        CALL FCTEVL(S,XSE2,R2,F3)
        K3=H*F3
C
        XSE3=XSE0+K3
        CALL RADIRO(S,XSE3,R3)
        CALL FCTEVL(S,XSE3,R3,F4)
        K4=H*F4
C
        TNEW=(I*H)
        XSENEW=XSE0+((1.0/6.0)*(K1+(2.0*K2)+(2.0*K3)+K4))
        HNEW=0.0
```

```
        ZNEW=0.0
C
C
C     CHECK FOR COMPLETION OF PHASE-2
C
C
        IF(XSENEW.GT.XSEC) GO TO 250
C
        WRITE(1,100)TNEW,XSENEW
100     FORMAT(F15.10,1X,F15.10)
        CALL RADIRO(S,XSENEW,RNEW)
C
        WRITE(2,100)TNEW,RNEW
        WRITE(3,100)TNEW,HNEW
        WRITE(4,100)TNEW,ZNEW
C
        XSE0=XSENEW
        R0=RNEW

35    CONTINUE
C
250     WRITE(*,*)' END OF PHASE-2',I,TNEW,XSEC
        WRITE(*,*)' RO= ',RC
C
C
C                    *****  PHASE-3  *****
C
C
        TO=TNEW
        WRITE(1,100)TO,XSENEW
        XSE0=XSENEW
C
C
C      SOLVE THE NONLINEAR SYSTEM OF EQUATIONS
C      FOR "RO" AND "HTA".
C
C
        CALL SYS(S,S1,RO0,HTA0,XSE0,RO1,HTA1)
C
C
C      A FOURTH ORDER RUNGE-KUTTA PROCEDURE IS USED
C      TO SOLVE THE GROWTH EQUATION THAT DESCRIBES
C      PHASE-3.
C
      DO 50 I1=I,N
        CALL FUNCTN(S,XSE0,RO1,HTA1,GAMA,F)
        K1=H*F
C
        XSE1=XSE0+(K1/2.0)
        CALL SYS(S,S1,RO1,HTA1,XSE1,RO2,HTA2)
        CALL FUNCTN(S,XSE1,RO2,HTA2,GAMA,F)
        K2=H*F
C
        XSE2=XSE0+(K2/2.0)
        CALL SYS(S,S1,RO2,HTA2,XSE2,RO3,HTA3)
        CALL FUNCTN(S,XSE2,RO3,HTA3,GAMA,F)
```

```
        K3=H*F
C
        XSE3=XSE0+K3
        CALL SYS(S,S1,RO3,HTA3,XSE3,RO4,HTA4)
        CALL FUNCTN(S,XSE3,RO4,HTA4,GAMA,F)
        K4=H*F
C
        TNEW=(I1+1)*(H)
        XSENEW=XSE0+((1.0/6.0)*(K1+(2.0*K2)+(2.0*K3)+K4))
        ZNEW=0.0
C
C
C     CHECK FOR COMPLETION OF PHASE-3
C
C
        Q1=(HTA4**2)/3.0
        Q2=1.0-(HTA4/XSENEW)
        Q3=1.0-((3.0*B1)/4.0)
        EQ1=Q**2
        EQ2=Q1*Q2*Q3
        IF(EQ2.GE.EQ1) GO TO 60
C
        WRITE(1,100)TNEW,XSENEW
        CALL SYS(S,S1,RO4,HTA4,XSENEW,RONEW,HTANEW)
C
        WRITE(2,100)TNEW,RONEW
        WRITE(3,100)TNEW,HTANEW
C
        XSE0=XSENEW
        RO1=RONEW
        HTA1=HTANEW

50    CONTINUE
C
60      WRITE(*,*)' END OF PHASE-3',I1,TNEW,XSENEW
        WRITE(*,*)' RO,HTA= ',RO4,HTA4
C
C
C                  *****  PHASE-4  *****
C                   THE FOUR-LAYER CASE
C
C


        TO=TNEW
        WRITE(1,100)TO,XSENEW
        XSE0=XSENEW
        R0=RO4
        H0=HTA4
        Z0=ZHTA
C
C
C     SOLVE THE NONLINEAR SYSTEM OF EQUATIONS
C     FOR "RO", "ZHTA" AND "HTA".
C
C
      CALL SYST(S,S1,B1,Q,DELTA,XSE0,R0,H0,Z0,R1,H1,Z1)
```

```
C
      IF(Z1.GE.R1) GO TO 200

C
C
C     A FOURTH ORDER RUNGE-KUTTA PROCEDURE IS USED TO
C     SOLVE THE GROWTH EQUATION THAT DESCRIBES
C     PHASE-4 (CASE-1).
C
C
      DO 70 I2=I1,N
        XSIN(I2-1)=XSE0
        CALL FNCT2(S1,B1,DELTA,GAMA,XSE0,R1,Z1,H1,F)
        K1=H*F
C
        XSE1=XSE0+(K1/2.0)
        CALL SYST(S,S1,B1,Q,DELTA,XSE1,R1,H1,Z1,R2,H2,Z2)
        IF(Z2.GE.R2) GO TO 201
        CALL FNCT2(S1,B1,DELTA,GAMA,XSE1,R2,Z2,H2,F)
        K2=H*F
C
        XSE2=XSE0+(K2/2.0)
        CALL SYST(S,S1,B1,Q,DELTA,XSE2,R2,H2,Z2,R3,H3,Z3)
        IF(Z3.GE.R3) GO TO 202
        CALL FNCT2(S1,B1,DELTA,GAMA,XSE2,R3,Z3,H3,F)
        K3=H*F
C
        XSE3=XSE0+K3
        CALL SYST(S,S1,B1,Q,DELTA,XSE3,R3,H3,Z3,R4,H4,Z4)
        IF(Z4.GE.R4) GO TO 203
        CALL FNCT2(S1,B1,DELTA,GAMA,XSE3,R4,Z4,H4,F)
        K4=H*F
C
        TNEW=(I2+2)*H
        XSENEW=XSE0+((1.0/6.0)*(K1+(2.0*K2)+(2.0*K3)+K4))
        WRITE(*,*)' XSENEW= ',XSENEW
        XSIN(I2)=XSENEW
C
C
C     CHECK FOR COMPLETION OF PHASE-4 (CASE-1).
C
C
        IF((XSIN(I2)-XSIN(I2-1)).LT.(1.E-6)) GO TO 80
C
        WRITE(1,100)TNEW,XSENEW
        CALL SYST(S,S1,B1,Q,DELTA,XSENEW,R4,H4,Z4,RN,HN,ZN)
        IF(ZN.GE.RN) GO TO 204
C
        WRITE(2,100)TNEW,RN
        WRITE(3,100)TNEW,HN
        WRITE(4,100)TNEW,ZN
C
        XSE0=XSENEW
        R1=RN
        H1=HN
        Z1=ZN
        GO TO 70
```

```
201           Z0=Z2
              H0=H2
              XSE0=XSE1
              GO TO 200

202     Z0=Z3
        H0=H3
        XSE0=XSE2
        GO TO 200

203           Z0=Z4
              H0=H4
              XSE0=XSE3
              GO TO 200

204     Z0=ZN
        H0=HN
        XSE0=XSENEW
        GO TO 200

70    CONTINUE

80    WRITE(*,*)' END OF PHASE-4, CASE-1 ',I2,TNEW,XSENEW

      GO TO 96
C
C
C                    *****  PHASE-4  *****
C                     THE THREE-LAYER CASE
C
C
C
C     SOLVE THE NONLINEAR SYSTEM OF EQUATIONS
C     FOR "ZHTA" AND "HTA".
C
C
200   CALL SYS1(SIGMA,S1,B1,Q,DELTA,Z0,H0,XSE0,Z1,H1)
C
C
C     A FOURTH ORDER RUNGE-KUTTA PROCEDURE IS USED TO
C     SOLVE THE GROWTH EQUATION THAT DESCRIBES
C     PHASE-4 (CASE-2).
C
C
      DO 90 I2=I1,N
        XSIN(I2-1)=XSE0
        CALL FNCT1(DELTA,XSE0,Z1,H1,GAMA,F)
        K1=H*F
C
        XSE1=XSE0+(K1/2.0)
        CALL SYS1(SIGMA,S1,B1,Q,DELTA,Z1,H1,XSE1,Z2,H2)

        CALL FNCT1(DELTA,XSE1,Z2,H2,GAMA,F)
        K2=H*F
C
        XSE2=XSE0+(K2/2.0)
        CALL SYS1(SIGMA,S1,B1,Q,DELTA,Z2,H2,XSE2,Z3,H3)
```

```
C
C
C
      CALL FNCT1(DELTA,XSE2,Z3,H3,GAMA,F)
      K3=H*F
C
C
      XSE3=XSE0+K3
      CALL SYS1(SIGMA,S1,B1,Q,DELTA,Z3,H3,XSE3,Z4,H4)
      CALL FNCT1(DELTA,XSE3,Z4,H4,GAMA,F)
      K4=H*F
C
C
      TNEW=(I2+2)*H
      XSENEW=XSE0+((1.0/6.0)*(K1+(2.0*K2)+(2.0*K3)+K4))
      XSIN(I2)=XSENEW
C
C
C     CHECK FOR COMPLETION OF PHASE-4 (CASE-2).
C
C
      IF((XSIN(I2)-XSIN(I2-1)).LT.(1.E-6)) GO TO 95
C
      WRITE(1,100)TNEW,XSENEW
      CALL SYS1(SIGMA,S1,B1,Q,DELTA,Z4,H4,XSENEW,ZN,HN)
C
      WRITE(3,100)TNEW,HN
      WRITE(4,100)TNEW,ZN
C
      XSE0=XSENEW
      Z1=ZN
      H1=HN
90    CONTINUE
95    WRITE(*,*)' END OF PHASE-4, CASE-2 ',I2,TNEW,XSENEW
96      CLOSE(UNIT=1)
       STOP
      END
C
C
C
```

```
C ************************************************************
C *                                                          *
C *                    SUBROUTINE RADIRO                     *
C *                                                          *
C ************************************************************
C *                                                          *
C * THIS SUBROUTINE SOLVES FOR THE SCALED INNER RADIUS       *
C * "RO" WHICH IS REQUIRED IN ORDER TO SOLVE THE GROWTH      *
C * EQUATION THAT DESCRIBES PHASE-2. THE BISECTION           *
C * ALGORITHM IS USED AS A METHOD OF SOLUTION.               *
C *                                                          *
C ************************************************************
C
C
C
      SUBROUTINE RADIRO(S,XS0,R)

      DIMENSION SAVE(4),FCT(4),A(50),B(50),P(50),SOLT(4)
      RO=0.01

      CALL FNCT(S,XS0,RO,F1)

      J=1

      DO 40 I=1,100

         RO=I
         CALL FNCT(S,XS0,RO,F2)
         IF((F1*F2).LT.0.0) GO TO 45
         F1=F2
         GO TO 40

45           SAVE(J)=I-1
             FCT(J)=F1
             SAVE(J+1)=I
             FCT(J+1)=F2

             A(1)=SAVE(J)
             B(1)=SAVE(J+1)
             P(0)=0.0

         II=0
46       II=II+1

             IF(II.EQ.500) STOP 1111
             P(II)=(A(II)+B(II))/2.0
             CALL FNCT(S,XS0,P(II),F)
             IF(ABS(P(II)-P(II-1)).LT.(1.E-6)) GO TO 47
             IF((F*FCT(J)).GT.0.0) GO TO 48

                 A(II+1)=A(II)
                 B(II+1)=P(II)
                 GO TO 46

48               A(II+1)=P(II)
                 B(II+1)=B(II)
                 GO TO 46
```

```
47              SOLT(J)=P(II)
                J=J+2
                F1=F2

40    CONTINUE

            IF(SOLT(3).EQ.0.0) GO TO 49
            IF(SOLT(1).LE.SOLT(3)) GO TO 49
            R=SOLT(3)
            GO TO 51

49              R=SOLT(1)

51      RETURN

        END

C
C
C
C ************************************************************
C *                                                          *
C *                  SUBROUTINE RADIXC                       *
C *                                                          *
C ************************************************************
C *                                                          *
C *  THIS SUBROUTINE SOLVES FOR THE SCALED OUTER RADIUS      *
C *  "XSEC" WHICH IS THE OUTER TUMOR RADIUS AT THE END       *
C *  OF PHASE-2. THE BISECTION ALGORITHM IS USED AS A        *
C *  METHOD OF SOLUTION.                                     *
C *                                                          *
C ************************************************************
C
C
C
      SUBROUTINE RADIXC(S,RC,XSEC)

      DIMENSION SAVE(4),FCT(4),A(50),B(50),P(50),SOLT(4)
      XSI=0.01
      CALL FNCT(S,XSI,RC,F1)

      J=1

      DO 50 I=1,100
        XSI=I
        CALL FNCT(S,XSI,RC,F2)
        IF((F1*F2).LT.0.0) GO TO 55
        F1=F2
        GO TO 50

 55               SAVE(J)=I-1
                  FCT(J)=F1
                  SAVE(J+1)=I
                  FCT(J+1)=F2

                  A(1)=SAVE(J)
                  B(1)=SAVE(J+1)
```

```
              P(0)=0.0
        II=0
56      II=II+1
        IF(II.EQ.500) STOP 2222
                P(II)=(A(II)+B(II))/2.0
                CALL FNCT(S,P(II),RC,F)

        IF(ABS(P(II)-P(II-1)).LT.(1.E-6)) GO TO 57
        IF((F*FCT(J)).GT.0.0) GO TO 58

                 A(II+1)=A(II)
                 B(II+1)=P(II)
                 GO TO 56

58               A(II+1)=P(II)
                 B(II+1)=B(II)
                 GO TO 56

57               SOLT(J)=P(II)
        J=J+2
        F1=F2
50      CONTINUE
        IF(SOLT(3).EQ.0.0) GO TO 59
        IF(SOLT(1).GE.SOLT(3)) GO TO 59
                 XSEC=SOLT(3)
                 GO TO 53
59               XSEC=SOLT(1)

53       RETURN
        END
C
C
C
```

```
C
C ************************************************************
C *                                                          *
C *                    SUBROUTINE RADIRC                     *
C *                                                          *
C ************************************************************
C *                                                          *
C * THIS SUBROUTINE SOLVES FOR THE SCALED INNER RADIUS       *
C * "RC" WHICH IS REQUIRED IN ORDER TO SOLVE FOR THE         *
C * CORRESPONDING OUTER TUMOR RADIUS "XSEC". THE NEWTON'S    *
C * ALGORITHM IS USED AS A METHOD OF SOLUTION.               *
C *                                                          *
C ************************************************************
C
C
C
      SUBROUTINE RADIRC(S1,ROC,RC)
      IF(ROC.LE.(1.E-6)) ROC=0.1
      XNEW=ROC
          I=0
60        I=I+1
          IF(I.EQ.500) GO TO 61
               ROC=XNEW
               CALL HYPFCT(ROC,HYPCOT,HYPCSC)
               F=S1-((ROC)*(HYPCSC))
          DF=(-HYPCSC)+((ROC)*(HYPCSC)*(HYPCOT))
          DX=F/DF
                XNEW=ROC-DX
          IF(ABS(XNEW-ROC).GT.(1.E-6)) GO TO 60
                RC=XNEW
61        RETURN
         END
C
C
C
C
```

```
C ***********************************************************
C *                                                         *
C *                    SUBROUTINE SYS                       *
C *                                                         *
C ***********************************************************
C *                                                         *
C * THIS SUBROUTINE SOLVES A NONLINEAR SYSTEM OF            *
C * EQUATIONS FOR THE INNER TUMOR RADII "RO" AND "HTA" .    *
C * THE NEWTON'S ALGORITHM IS USED AS A METHOD              *
C * OF SOLUTION.                                            *
C *                                                         *
C ***********************************************************
C
C
C
      SUBROUTINE SYS(S,SIGMA1,RO,HTA,XSE,RON,HTAN)

      RONEW=RO
      HTANEW=HTA

        I=0
10      I=I+1
        IF(I.EQ.500) STOP 3333

           RO= RONEW
           HTA=HTANEW
           X=RO-HTA

        CALL HYPFCT(X,HYPCOT,HYPCSC)

        F1=1.0+(HTA*HYPCOT)
        F=HYPCSC-(SIGMA1*F1*(1.0/RO))

        DF1=(1.0/RO)+(HTA*(HYPCSC**2))+((HTA*HYPCOT)/RO)
        DF2=HYPCSC*HYPCOT
        DFR=(SIGMA1*(1.0/RO)*DF1)-DF2
        DF3=(HTA*(HYPCSC**2))+(HYPCOT)
        DFH=DF2-(SIGMA1*(1.0/RO)*DF3)

            H1=S-(((XSE**2)-(RO**2))/6.0)
            H2=SIGMA1*RO*(HYPCOT+HTA)
            H3=HYPCSC*(RO+((RO**3)/3.0))
            H4=(XSE-RO)/(RO*XSE)
            H=(HYPCSC*H1)-((H2-H3)*H4)

        DH2=((RO/3.0)*HYPCSC)-(DF2*H1)
        DH3=SIGMA1*(1.0/RO)*(HYPCOT+HTA)
        DH4=(1.0/(RO**2))*H3
        DH5=DH3-DH4
        DH7=SIGMA1*(HYPCOT+HTA)-(SIGMA1*RO*(HYPCSC**2))
        DH8=(HYPCOT*H3)-(HYPCSC*(1.0+(RO**2)))
        DH9=H4*(DH7+DH8)
        DHR=DH2+DH5-DH9
        DH11=SIGMA1*RO*(1.0-(HYPCSC**2))
        DH12=HYPCOT*H3
        DHH=(DF2*H1)-(H4*(DH11-DH12))
```

```
          B1=(DFR*RO)+(DFH*HTA)-F
          B2=(DHR*RO)+(DHH*HTA)-H

          DETR=(DFR*DHH)-(DHR*DFH)

        IF(DETR.EQ.0.0) GO TO 20

          DETRR=(B1*DHH)-(B2*DFH)
          DETRH=(DFR*B2)-(DHR*B1)

          RONEW=DETRR/DETR
          HTANEW=DETRH/DETR

        IF(ABS((RONEW-RO)/RONEW).GT.(1.E-6)) GO TO 10
        IF(ABS((HTANEW-HTA)/HTANEW).GT.(1.E-6)) GO TO 10
        GO TO 30

20      WRITE(*,*) ' NO SOLUTION TO THE SYSTEM '

30              RON=RONEW
                HTAN=HTANEW

         RETURN

        END

C
C
C
C ************************************************************
C *                                                          *
C *                    SUBROUTINE SYST                       *
C *                                                          *
C ************************************************************
C *                                                          *
C * THIS SUBROUTINE SOLVES A NONLINEAR SYSTEM OF             *
C * EQUATIONS FOR THE INNER TUMOR RADII "RO","ZHTA",         *
C * AND "HTA". THE NEWTON'S ALGORITHM IS USED AS A           *
C * METHOD OF SOLUTION.                                      *
C *                                                          *
C ************************************************************
C
C
C
      SUBROUTINE SYST(S,S1,B,Q,DELTA,XSE,RO,HTA,ZHTA,RN,HN,ZN)

            RONEW=RO
            ZNEW=ZHTA
            HTANEW=HTA

         I=0
10       I=I+1
         IF(I.EQ.500) STOP 5555

            ZHTA=ZNEW
            HTA=HTANEW
            RO=RONEW
```

```
        D=SQRT(DELTA)
        X1=RO-ZHTA
        X2=D*(ZHTA-HTA)

CALL HYPFCT(X1,HCOT,HCSC)
CALL HYPFCT(X2,HYPCOT,HYPCSC)
F1=S+(((RO**2)-(XSE**2))/6.0)
F2=((RO-XSE)/XSE)*(1.0+((RO**2)/3.0))
F3=(RO*(RO-XSE)*HCOT)/XSE
F4=(S1*(RO-XSE)*HCSC*(1.0+(HTA*D*HYPCOT)))/(XSE*D)
F=F1-F2+F3-F4

DF1=-((2.0*RO*(RO-XSE))/(3.0*XSE))+(RO/3.0)
DF2=-((1.0+((RO**2)/3.0))*(1.0/XSE))
DF3=-((RO*(RO-XSE)*(HCSC**2))/XSE)
DF10=HCOT*(((2.0*RO)/XSE)-1.0)
DF4=((S1*HCSC)/(XSE*D))-((S1*(RO-XSE)*HCOT*HCSC)/(XSE*D))
DF5=-DF4*(1.0+(HTA*D*HYPCOT))
DFR=DF1+DF2+DF3+DF10+DF5
DF6=DELTA*HTA
DFH=(S1*(RO-XSE)*HCSC*DF6)/(XSE*D)
DF7=(RO*(RO-XSE)*(HCSC**2))/XSE
DF8=(S1*(RO-XSE)*HCSC*((D*HYPCOT)+(HTA*DELTA)))/(XSE*D)
DF9=(S1*(RO-XSE)*HCOT*HCSC*(1.0+(HTA*D*HYPCOT)))/(XSE*D)
DFZ=DF7-DF8-DF9

H1=(B/4.0)-(1.0/3.0)
H2=(1.0/XSE)-(1.0/ZHTA)
H=(Q**2)-((HTA**3)*H1*H2)

DHH=-(3.0*(HTA**2)*H1*H2)
DHZ=-(((HTA**3)/(ZHTA**2))*H1)
DHR=0.0

G1=S1*(1.0/RO)*(HYPCOT+(D*HTA))
G2=1.0+(D*HTA*HYPCOT)
G3=S1*(HCOT/(D*RO))*G2
G=HCSC*HYPCSC-G1-G3

DG1=-(HYPCSC*HCSC*HCOT)
DG2=S1*(1.0/(RO**2))*(HYPCOT+(D*HTA))
DG3=1.0+(D*HTA*HYPCOT)
DG4=S1*(1.0/(D*(RO**2)))*((RO*(HCSC**2))+HCOT)*DG3
DGR=DG1+DG2+DG4
DG5=D*HCSC*HYPCSC*HYPCOT
DG6=S1*(1.0/RO)*((D*(HYPCSC**2))+D)
DG7=(DELTA*HTA*(HYPCSC**2))+(D*HYPCOT)
DG8=S1*(HCOT/(D*RO))*DG7
DGH=DG5-DG6-DG8
DG9=HYPCSC*HCSC*(HCOT-(D*HYPCOT))
DG10=S1*(D/RO)*(HYPCSC**2)
DG11=S1*((DELTA*HTA)/(D*RO))*HCOT*(HYPCSC**2)
DG12=1.0+(D*HTA*HYPCOT)
DG13=S1*(1.0/(D*RO))*(HCSC**2)*DG12
DGZ=DG9+DG10+DG11-DG13

C1=(DFR*RO)+(DFH*HTA)+(DFZ*ZHTA)-F
```

```
      C2=(DHR*RO)+(DHH*HTA)+(DHZ*ZHTA)-H
      C3=(DGR*RO)+(DGH*HTA)+(DGZ*ZHTA)-G

      DET=(DHZ*((DFR*DGH)-(DGR*DFH)))
      DETR=(DHH*((DFR*DGZ)-(DGR*DFZ)))-DET
      DET1=(C1*((DHH*DGZ)-(DGH*DHZ)))-(DFH*((C2*DGZ)-(C3*DHZ)))
      DETRR=DET1+(DFZ*((C2*DGH)-(C3*DHH)))
      DETRZ=(DHH*((DFR*C3)-(DGR*C1)))-(C2*((DFR*DGH)-(DGR*DFH)))
      DETRH=(C2*((DFR*DGZ)-(DGR*DFZ)))-(DHZ*((DFR*C3)-(DGR*C1)))

      IF(DETR.EQ.0.0) GO TO 20

            ZNEW=DETRZ/DETR
            HTANEW=DETRH/DETR
            RONEW=DETRR/DETR

          IF(ABS((RONEW-RO)/RONEW).GT.(1.E-6)) GO TO 10
          IF(ABS((ZNEW-ZHTA)/ZNEW).GT.(1.E-6)) GO TO 10
          IF(ABS((HTANEW-HTA)/HTANEW).GT.(1.E-6)) GO TO 10

          GO TO 30
   20     WRITE(*,*)' NO SOLUTION TO SYST '

   30                          RN=RONEW
                               HN=HTANEW
                               ZN=ZNEW

           RETURN

          END

C
C
C
C ***********************************************************
C *                                                         *
C *                     SUBROUTINE SYS1                     *
C *                                                         *
C ***********************************************************
C *                                                         *
C * THIS SUBROUTINE SOLVES A NONLINEAR SYSTEM OF            *
C * EQUATIONS FOR THE INNER TUMOR RADII "ZHTA" AND "HTA".   *
C * THE NEWTON'S ALGORITHM IS USED AS A METHOD              *
C * OF SOLUTION.                                            *
C *                                                         *
C ***********************************************************
C
C
C
      SUBROUTINE SYS1(SIGMA,S1,B,Q,DELTA,ZHTA,HTA,XSE,ZHTAN,HTAN)

            ZNEW=ZHTA
            HTANEW=HTA

            I=0
   10       I=I+1
            IF(I.EQ.500) STOP 4444
```

```
ZHTA=ZNEW
HTA=HTANEW
D=SQRT(DELTA)
X=D*(ZHTA-HTA)

CALL HYPFCT(X,HCOT,HCSC)
F1=(B/4.0)-(1.0/3.0)
F2=(1.0/XSE)-(1.0/ZHTA)
F=(Q**2)-((HTA**3)*F1*F2)

DFH=-(3.0*(HTA**2)*F1*F2)
DFZ=-(((HTA**3)/(ZHTA**2))*F1)

X1=ZHTA*(XSE-ZHTA)
X2=(ZHTA**2)*(XSE-ZHTA)
H1=((SIGMA*XSE*HCSC)/X1)-((S1*HCOT)/ZHTA)
H2=-((S1*HTA*D)/ZHTA)+(S1*(1.0/(D*(ZHTA**2))))
H3=((S1*HTA*HCOT)/(ZHTA**2))+((ZHTA*HCSC)/3.0)
H4=-(((XSE**3)*HCSC)/(6.0*X1))-((S1*XSE)/(D*X2))
H5=-((S1*HTA*XSE*HCOT)/X2)
H6=(XSE*ZHTA*HCSC)/(6.0*(XSE-ZHTA))
H=H1+H2+H3+H4+H5+H6

DH1=(SIGMA*XSE*D*HCSC*HCOT)/X1
DH2=-((S1*D*(HCSC**2))/ZHTA)-((S1*D)/ZHTA)
DH3=(S1*HTA*D*(HCSC**2))/(ZHTA**2)
DH4=(S1*HCOT)/(ZHTA**2)
DH5=(ZHTA*HCSC*HCOT)/3.0
DH6=-(((XSE**3)*D*HCSC*HCOT)/(6.0*X1))
DH7=-((S1*HTA*XSE*D*(HCSC**2))/X2)
DH8=-((S1*XSE*HCOT)/X2)
DH9=(XSE*ZHTA*D*HCSC*HCOT)/(6.0*(XSE-ZHTA))
DHH=DH1+DH2+DH3+DH4+DH5+DH6+DH7+DH8+DH9
DH10=-((SIGMA*XSE*D*HCSC*HCOT)/X1)

X4=(ZHTA**2)*((XSE-ZHTA)**2)
X5=(ZHTA**3)*((XSE-ZHTA)**2)

DH11=-((SIGMA*XSE*(XSE-(2.0*ZHTA))*HCSC)/X4)
DH12=((S1*D*(HCSC**2))/ZHTA)+((S1*HCOT)/(ZHTA**2))
DH13=((S1*HTA*D)/(ZHTA**2))-((2.0*S1)/(D*(ZHTA**3)))
DH14=-((S1*HTA*D*(HCSC**2))/(ZHTA**2))
DH15=-((S1*2.0*HTA*HCOT)/(ZHTA**3))
DH16=-((D*ZHTA*HCSC*HCOT)/3.0)+(HCSC/3.0)
DH17=((XSE**3)*D*HCSC*HCOT)/(6.0*X1)
DH18=((XSE**3)*(XSE-(2.0*ZHTA))*HCSC)/(6.0*X4)
DH19=(S1*XSE*((2.0*XSE)-(3.0*ZHTA)))/(D*X5)
DH20=(S1*HTA*XSE*D*(HCSC**2))/X2
DH21=(S1*HTA*XSE*((2.0*XSE)-(3.0*ZHTA))*HCOT)/X5
DH22=-((XSE*ZHTA*D*HCSC*HCOT)/(6.0*(XSE-ZHTA)))
DH23=((XSE**2)*HCSC)/(6.0*((XSE-ZHTA)**2))

DZ1=DH10+DH11+DH12+DH13+DH14+DH15+DH16+DH17
DZ2=DH18+DH19+DH20+DH21+DH22+DH23
DHZ=DZ1+DZ2

B1=(DFZ*ZHTA)+(DFH*HTA)-F
```

```
      B2=(DHZ*ZHTA)+(DHH*HTA)-H
      DETR=(DFZ*DHH)-(DFH*DHZ)

      IF(DETR.EQ.0.0) GO TO 20

      DETRZ=(B1*DHH)-(B2*DFH)
      DETRH=(DFZ*B2)-(DHZ*B1)

            ZNEW=DETRZ/DETR
            HTANEW=DETRH/DETR

      IF(ABS((ZNEW-ZHTA)/ZNEW).GT.(1.E-6)) GO TO 10
      IF(ABS((HTANEW-HTA)/HTANEW).GT.(1.E-6)) GO TO 10

      GO TO 30
20    WRITE(*,*)' NO SOLUTION TO SYS1 '

30                  ZHTAN=ZNEW
                    HTAN=HTANEW

      RETURN

      END

C
C
C
C ************************************************************
C *                                                          *
C *                  SUBROUTINE FCTEVL                       *
C *                                                          *
C ************************************************************
C *                                                          *
C * THIS SUBROUTINE EVALUATES THE RIGHT-HAND SIDE OF THE     *
C * GROWTH EQUATION THAT DESCRIBES PHASE-2.                  *
C *                                                          *
C ************************************************************
C
C
C

      SUBROUTINE FCTEVL(S,XSE,RO,F)

        F1=S-((XSE**2)-(RO**2))/6.0

        F2=(RO*XSE)/(XSE-RO)

        F=(XSE/3.0)+((1.0/(XSE**2))*F1*F2)

      RETURN

      END
C
C
C
```

```
C ***********************************************************
C *                                                         *
C *                   SUBROUTINE FUNCTN                     *
C *                                                         *
C ***********************************************************
C *                                                         *
C * THIS SUBROUTINE EVALUATES THE RIGHT-HAND SIDE OF THE    *
C * GROWTH EQUATION THAT DESCRIBES PHASE-3.                 *
C *                                                         *
C ***********************************************************
C
      SUBROUTINE FUNCTN(S,XSE,RO,HTA,GAMA,F)

         F1=S-((XSE**2)-(RO**2))/6.0
         F2=(RO*XSE)/(XSE-RO)
         F3=(1.0/(XSE**2))*GAMA*(HTA**3)

         F=(XSE/3.0)+((1.0/(XSE**2))*F1*F2)-F3

       RETURN

      END


C ***********************************************************
C *                                                         *
C *                   SUBROUTINE FNCT2                      *
C *                                                         *
C ***********************************************************
C *                                                         *
C * THIS SUBROUTINE EVALUATES THE RIGHT-HAND SIDE OF THE    *
C * GROWTH EQUATION THAT DESCRIBES PHASE-4 (CASE-1).        *
C *                                                         *
C ***********************************************************

       SUBROUTINE FNCT2(S1,B1,DELTA,GAMA,XSE,RO,ZHTA,HTA,F)

           D=SQRT(DELTA)
           X=D*(ZHTA-HTA)
           Y=RO-ZHTA
           CALL HYPFCT(Y,HCOT,HCSC)

       F1=(XSE/3.0)-((RO**3)/(3.0*(XSE**2)))
       F2=(((RO**2)*HCOT)/(XSE**2))-(RO/(XSE**2))
       F3=-((RO*ZHTA*HCSC)/(XSE**2))
       F4=-(S1*(1.0/D)*((RO*HCSC*SINH(X))/(XSE**2)))
       F5=S1*(1.0/D)*(ZHTA/(XSE**2))*SINH(X)*HCOT
       F6=S1*(1.0/D)*(SINH(X)/(XSE**2))
       F7=-(S1*((HTA*RO*HCSC*COSH(X))/(XSE**2)))
       F8=S1*((HTA*ZHTA*COSH(X)*HCOT)/(XSE**2))
       F9=S1*((HTA*COSH(X))/(XSE**2))
       F10=(1.0/(XSE**2))*GAMA*(HTA**3)
       F=(F1+F2+F3+F4+F5+F6+F7+F8+F9)-F10

       RETURN

      END
```

```
C ***********************************************************
C *                                                         *
C *                    SUBROUTINE FNCT1                     *
C *                                                         *
C ***********************************************************
C *                                                         *
C * THIS SUBROUTINE EVALUATES THE RIGHT-HAND SIDE OF THE    *
C * GROWTH EQUATION THAT DESCRIBES PHASE-4 (CASE-2).        *
C *                                                         *
C ***********************************************************
C
C
C
      SUBROUTINE FNCT1(DELTA,XSE,ZHTA,HTA,GAMA,F)

           F1=1.0/(XSE**2)
           F2=(((XSE**3)-(ZHTA**3))/(3.0))*F1
           F3=(GAMA*(HTA**3))*F1

           F=F2-F3

        RETURN

       END


C
C
C
C ***********************************************************
C *                                                         *
C *                    SUBROUTINE FNCT                      *
C *                                                         *
C ***********************************************************
C *                                                         *
C * THIS SUBROUTINE EVALUATES, AT THE ENDPOINTS, THE        *
C * FUNTIONS USED BY THE BISCECTION METHOD (IN PHASE-2).    *
C *                                                         *
C ***********************************************************
C
C
C
         SUBROUTINE FNCT(S,XSE,RO,F)

              F1=((XSE**2)-(RO**2))/6.0
              CALL HYPFCT(RO,HYPCOT,HYPCSC)
              F2=RO*((RO*HYPCOT)-1.0)-((RO**3)/3.0)
              F3=(XSE-RO)/(RO*XSE)

              F=S-F1-(F2*F3)

           RETURN

           END
C
C
C
```

```
C ***********************************************************
C *                                                         *
C *                    SUBROUTINE HYPFCT                    *
C *                                                         *
C ***********************************************************
C *                                                         *
C * THIS SUBROUTINE CALCULATES THE HYPERBOLIC COTAGENT      *
C * AND HYPERBOLIC COSECANT OF A GIVEN FUNCTION.            *
C *                                                         *
C ***********************************************************
C
C
C
      SUBROUTINE HYPFCT(A,HCOT,HCSC)

           IF(A.LE.88.0) GO TO 120

         HCOT=1.0
         HCSC=0.0
         GO TO 150

120        IF(A.GE.(-88.0)) GO TO 130
         HCOT=-1.0
         HCSC=0.0
         GO TO 150

130      Z1=EXP(A)
         Z2=EXP(-A)
         HCOT=(Z1+Z2)/(Z1-Z2)
         HCSC=2.0/(Z1-Z2)

150     RETURN

        END
```

Biographical Statement

Sophia Maggelakis was born in the island of Crete in Greece. She received the Bachelor of Science degree in Mathematics with minor in Computer Science from Old Dominion University in May, 1980.

After receiving the Master of Science degree in Computational and Applied Mathematics from Old Dominion University in December, 1982, she worked as a Systems and Scientific Applications Programmer for the City of Virginia Beach Virginia from 1983 to 1985.

In 1985, Ms. Maggelakis enrolled in the Ph.D. program in Computational and Applied Mathematics at Old Dominion University. She is currently a Research Assistant and has been a Teaching Assistant from 1980 to 1982 and from 1985 to 1989. She was awarded for the best student paper presentation at the 13th Annual Southeast Atlantic Section SIAM Meeting held in March, 1989. She is a member of the Society for Mathematical Biology, American Mathematical Society, Mathematical Association of America, and Society for Industrial and Applied Mathematics. During her graduate studies, she served as a Treasurer and Secretary for the SIAM student chapter at Old Dominion University.

Ms. Maggelakis will receive her Doctor of Philosophy degree in Computational and Applied Mathematics in August, 1989. She has planned one year of

Postdoctoral studies at Old Dominion University. Her general area of research is Mathematical Biology. Other interests include Mathematical Modeling, Ordinary and Partial Differential Equations, and Numerical Analysis.